

**EFFECTS OF IONIC LIQUID AND NANOFILLER TO THE
PHYSICOCHEMICAL PROPERTIES OF POLY (ETHYL
METHACRYLATE) BASED POLYMER ELECTROLYTES**

NUR FATINAH MUHAMAD ZAIN

**INSTITUTE OF GRADUATE STUDIES
UNIVERSITY OF MALAYA
KUALA LUMPUR**

2016

**EFFECTS OF IONIC LIQUID AND NANOFILLER TO THE
PHYSICOCHEMICAL PROPERTIES OF POLY (ETHYL
METHACRYLATE) BASED POLYMER ELECTROLYTES**

NUR FATINAH MUHAMAD ZAIN

**DISSERTATION SUBMITTED IN FULFILMENT OF THE
REQUIREMENTS FOR THE DEGREE OF MASTER OF
PHILOSOPHY**

**INSTITUTE OF GRADUATE STUDIES
UNIVERSITY OF MALAYA
KUALA LUMPUR**

2016

DECLARATION

UNIVERSITI MALAYA

ORIGINAL LITERARY WORK DECLARATION

Name of Candidate: **NUR FATINAH BINTI MUHAMAD ZAIN**

Registration/Matric No : **HGA 130013**

Name of Degree : **MASTER OF PHILOSOPHY**

Title of Project Paper/Research Report/Dissertation/Thesis ("this Work"):

EFFECTS OF IONIC LIQUID AND NANOFILLER TO THE PHYSICOCHEMICAL PROPERTIES OF POLY (ETHYL METHACRYLATE) BASED POLYMER ELECTROLYTES

Field of Study : **ADVANCED MATERIALS**

I do solemnly and sincerely declare that:

- (1) I am the sole author/writer of this Work;
- (2) This Work is original;
- (3) Any use of any work in which copyright exists was done by way of fair dealing and for permitted purposes and any excerpt or extract from, or reference to or reproduction of any copyright work has been disclosed expressly and sufficiently and the title of the Work and its authorship have been acknowledged in this Work;
- (4) I do not have any actual knowledge nor do I ought reasonably to know that the making of this work constitutes an infringement of any copyright work;
- (5) I hereby assign all and every rights in the copyright to this Work to the University of Malaya ("UM"), who henceforth shall be owner of the copyright in this Work and that any reproduction or use in any form or by any means whatsoever is prohibited without the written consent of UM having been first had and obtained;
- (6) I am fully aware that if in the course of making this Work I have infringed any copyright whether intentionally or otherwise, I may be subject to legal action or any other action as may be determined by UM.

Candidate's Signature

Date

Subscribed and solemnly declared before,

Witness's Signature

Date

Name:

Designation:

ABSTRACT

Three different series of polymer electrolytes based on poly (ethyl methacrylate) (PEMA) were successfully developed by solution casting technique. Pure PEMA are highly crystalline in nature; exhibiting glass transition temperature (T_g) of ~ 70 °C with low room temperature ionic conductivity of 10^{-11} S cm^{-1} . In order to suppress this crystalline behaviour, the polymers were incorporated with various amounts of room temperature ionic liquid (RTIL), namely 1-ethyl-3-methylimidazolium bis(trifluorosulfonyl) imide (EMITFSI) as a plasticizer. This first series of polymer electrolytes was labeled as System I. The sample containing 40 wt.% EMITFSI showed a maximum room temperature ionic conductivity of 5.41×10^{-7} S cm^{-1} and thermal stability up to 300 °C. System II was prepared by adding both EMITFSI and magnesium triflate (MgTf_2) in the polymer matrix in order to study the effects of addition of both ionic liquid and salt to the properties of PEMA. The interaction between PEMA, EMITFSI and MgTf_2 was confirmed using FTIR by the shifts of significant bands of C=O and C-O-C₂H₅ groups in PEMA that are capable to coordinate with the cation of a salt and ionic liquid. The presence of amorphous phase was observed from SEM analysis for the highest conducting samples for System I and System II. The ionic conductivity obtained was 1.72×10^{-6} S cm^{-1} at room temperature for PEMA-20 wt.% MgTf_2 -30 wt.% EMITFSI electrolyte. However, the composition of PEMA-20 wt.% MgTf_2 -40 wt.% EMITFSI could not produce free-standing film. Nanocomposite polymer electrolytes (NCPEs) (System III) were prepared in order to study the effects of magnesium oxide (MgO) nanofiller to ionic liquid retention properties of polymer-salt-ionic liquid electrolytes. NCPEs were prepared by adding different compositions of nanosized MgO as ceramic nanofiller in PEMA-20 wt.% MgTf_2 -40 wt.% EMITFSI electrolytes. The addition of MgO nanofiller has improved the film stability and ionic liquid retention property of the sample containing 20 wt.% MgTf_2 and 40 wt.%

EMITFSI. The room temperature ionic conductivity was improved up to 10^{-5} S cm⁻¹ by the incorporation of 1 wt.% of MgO nanofiller in the polymer electrolytes film. Temperature-dependence ionic conductivity for all systems showed Arrhenius-like behavior. The highest ionic conductivity was observed for NCPE film with the value of 3.78×10^{-4} S cm⁻¹ at 100 °C. Enhancement of electrochemical potential stability window determined by LSV was observed for System II and System III, due to the impregnation of ionic liquid and ceramic nanofiller. This indicated that NCPE system has the potential for use as an electrolyte in magnesium ion batteries.

University of Malaya

ABSTRAK

Tiga siri elektrolit polimer yang berbeza berdasarkan poly (ethyl methacrylate) (PEMA) telah berjaya dihasilkan melalui teknik penuangan larutan. PEMA yang asli sangat tinggi sifat kekristalannya; ia mempamerkan suhu peralihan kaca (T_g) ~ 70 °C dengan kekonduksian elektrolit yang rendah pada suhu bilik, iaitu 10^{-11} S cm^{-1} . Untuk mengganggu bahagian ini, polimer telah dimasukkan dengan sejumlah cecair ionik pada suhu bilik (RTIL) dikenali sebagai 1-ethyl-3-methylimidazolium bis(trifluorosulfonyl) imide (EMITFSI) sebagai bahan peliat. Bahagian awal penyediaan elektrolit polimer ini telah dilabelkan sebagai Sistem I. Sampel yang mengandungi 40 wt.% EMITFSI menunjukkan kekonduksian ionik suhu bilik maksimum 5.41×10^{-7} S cm^{-1} dan mencapai kestabilan terma sehingga 300 °C. Sistem II telah disediakan dengan memasukkan kedua-dua campuran EMITFSI dan garam magnesium triflat (MgTf_2) ke dalam matriks polimer untuk mengkaji kesan penambahan kedua-duanya sekali ke atas PEMA. Interaksi antara PEMA, MgTf_2 dan EMITFSI telah disahkan menggunakan FTIR melalui perubahan ketara pada jalur kumpulan C=O dan C-O-C₂H₅ dalam PEMA yang mampu untuk bertindakbalas dengan kation daripada garam, dan cecair ionik. Kehadiran fasa amorfus dapat dilihat daripada analisis SEM untuk sampel yang tertinggi kekonduksiannya bagi Sistem I dan Sistem II. Kekonduksian ionik telah sedikit meningkat sehingga 1.72×10^{-6} S cm^{-1} pada suhu bilik untuk elektrolit PEMA-20 wt.% MgTf_2 -30 wt.% EMITFSI. Walaubagaimanapun, komposisi PEMA-20 wt.% MgTf_2 -40 wt.% EMITFSI gagal menghasilkan filem yang dapat berdiri bebas. Elektrolit polimer nanokomposit (NCPEs) (Sistem III) telah disediakan untuk mengkaji kesan magnesium oksida (MgO) pengisi-nano terhadap sifat pengekalan cecair ionik untuk elektrolit polimer-garam-cecair ionik. NCPEs telah disediakan dengan menambah komposisi berbeza MgO saiz-nano sebagai pengisi-nano seramik dalam elektrolit PEMA-20 wt.% MgTf_2 -40 wt.% EMITFSI. Campuran pengisi-nano MgO telah berjaya

meningkatkan kestabilan filem dan sifat pengekalannya cecair ionik bagi sampel yang mengandungi 20 wt.% MgTf_2 dan 40 wt.% EMITFSI. Kekonduksian ionik pada suhu bilik dapat dipertingkatkan lagi sehingga $10^{-5} \text{ S cm}^{-1}$ dengan campuran 1 wt.% pengisi-nano MgO ke dalam elektrolit polimer. Pergantungan-suhu kekonduksian ionik untuk semua sistem menunjukkan kelakuan seperti Arrhenius. Kekonduksian ionik tertinggi diperoleh untuk filem NCPE mempamerkan $3.78 \times 10^{-4} \text{ S cm}^{-1}$ pada suhu $100 \text{ }^\circ\text{C}$. Peningkatan potensi tettingkap kestabilan elektrokimia dari LSV dapat dilihat untuk Sistem II dan Sistem III disebabkan oleh pengisitepuan cecair ionik dan pengisi-nano seramik. Ini menunjukkan bahawa sistem NCPE mempunyai potensi untuk digunakan sebagai elektrolit dalam bateri ion magnesium.

ACKNOWLEDGEMENTS

In the name of Allah Subhanahu Wata'ala, the Most Gracious and the Most Merciful.

Alhamdulillah, a lot of thanks to Allah S.W.T. for His blessings for me to complete this dissertation.

First and foremost, I am obliged to my supervisors Prof. Dr. Nor Sabirin Mohamed and Puan Norazlin Zainal for their continuous guidance and motivation during the entire course of my project, for helping me to complete the writing of this dissertation as well as the challenging research that lies behind it. I really appreciate their enthusiasm, inspiration, and great efforts to explain things concise and precise concerning to my project. Also, throughout my thesis-writing period, they have provided encouragement, sound advice, good teaching, good company, and lots of good ideas. My supervisors have an indispensable role in preparing this thesis by providing lots of sufficient good ideas.

I am indebted to UM as it provided me with instruments, apparatus and facilities, as well as a stimulating and conducive working environment for the completion of my research work. Furthermore, I would like to express my appreciation to all my team mates, laboratory officer and laboratory assistant for assisting me in many different ways. Without the continuous support from them, it will be a hard time for me to complete my research work fruitfully. In addition, I also extend my deepest appreciation to my entire family members for their immense support, love and encouragement to persuade my interest in this research and achieve the fulfillment of the requirements for the Master's degree program.

TABLE OF CONTENTS

DECLARATION	i
ABSTRACT	ii
ACKNOWLEDGEMENTS	vi
LIST OF FIGURES	x
LIST OF TABLES	xii
LIST OF SYMBOLS	xiii
LIST OF ABBREVIATIONS	xiv
1.1 Background	1
1.2 Problem Statement	3
1.3 Objectives of Study	3
1.4 Materials Selection	4
1.5 Thesis Organization	6
2.1 Introduction	7
2.2 Polymer Electrolytes	8
2.2.1 <i>Liquid Polymer Electrolytes</i>	9
2.2.2 <i>Solid Polymer Electrolytes</i>	9
2.2.3 <i>Gel Polymer Electrolytes</i>	10
2.2.4 <i>Nano-Composite Polymer Electrolytes</i>	11
2.3 Transport Mechanisms in Polymer Electrolyte	12
2.4 Poly (ethyl methacrylate)	17

2.5	Ionic Salts	19
2.6	Ionic liquid as plasticizer	20
2.7	Nano-filler as dispersoid	23
3.1	Introduction	25
3.2	Sample Preparation	25
3.3	Sample Characterizations	27
3.3.1.	<i>Fourier Transform Infra-Red Spectroscopy</i>	27
3.3.2.	<i>Electrochemical Impedance Spectroscopy</i>	28
3.3.3.	<i>Transference number measurements</i>	31
3.3.4.	<i>Surface Morphological study</i>	32
3.3.5.	<i>Differential Scanning Calorimetry (DSC)</i>	33
3.3.6.	<i>Thermogravimmetric Analysis</i>	35
3.3.7.	<i>Linear Sweep Voltammetry (LSV)</i>	36
4.1	Introduction	38
4.2	FTIR Results	38
4.3	SEM Analysis	41
4.4	Thermal Analysis	42
4.5	Thermal Analysis	45
4.6	Ionic Conductivity Studies	47
4.7	Electrochemical stability determination	50
4.8	Summary	51
5.1	Introduction	53

5.2	FTIR Results	53
5.3	SEM Analysis	55
5.4	Thermal Analysis (DSC)	56
5.5	Ionic Conductivity Studies	58
5.6	Magnesium Transference Number	60
5.7	Electrochemical stability determination	62
5.8	Summary	63
6.1	Introduction	65
6.2	Retention property of ionic liquid improved by addition of MgO nanofiller	65
6.3	SEM analysis	67
6.4	Thermogravimetric analysis	68
6.5	Room Temperature Ionic Conductivity	70
6.6	Linear Sweep Voltammetric Analysis	73
6.7	Summary	74
7.1	Conclusions	75
7.2	Suggestions for Future Work	77
	REFERENCES	78
	LIST OF PUBLICATIONS AND PAPERS PRESENTED	93

LIST OF FIGURES

Figure 2.1: Cation motion in a polymer electrolyte (a) Intrachain hopping; (b) Interchain hopping; (c) Intrachain hopping via ion cluster; (d) Intercluster hopping (D. H. Gray et al., 1997)	16
Figure 2.2: Structure of PMMA and PEMA	18
Figure 2.3: Structure of EMITFSI	22
Figure 3.1: FTIR spectrum with peaks assignment in the region between 650 and 4000 cm^{-1}	28
Figure 3.2: Nyquist (or Cole-Cole) plot	29
Figure 3.3: DSC thermogram in the heating run from -50 to 350 °C	34
Figure 3.4: TGA thermogram in the heating run up to 800 °C	35
Figure 3.5: Linear sweep voltammogram in the potential range of (-5 to 5) V	36
Figure 4.1: Photograph of PEMA-EMITFSI electrolyte transparent film	38
Figure 4.2: FTIR spectra in the region between 650 and 2150 cm^{-1} for (a) EMITFSI, (b) S_0 , (c) S_1 , (d) S_2 , (e) S_3 and (f) S_4	40
Figure 4.3: FTIR spectra in the region between 1100 and 1200 cm^{-1} , 1400 and 1500 cm^{-1} and 1680 and 1770 cm^{-1} for (a) S_0 , (b) S_1 , (c) S_2 , (d) S_3 and (e) S_4	41
Figure 4.4: SEM micrographs for (a) S_0 , (b) S_2 and (c) S_4	42
Figure 4.5: DSC thermograms in the heating run from 0 to 350 °C	43
Figure 4.6: DSC thermograms in the heating run for (a) S_0 , (b) S_1 , (c) S_2 , (d) S_3 and (e) S_4 samples in selected temperature range	44
Figure 4.7: TGA thermograms in the heating run up to 800 °C for (i) S_0 , (ii) S_2 and (iii) S_4 films	46
Figure 4.8: Cole-cole plots for (a) S_0 and (b) S_4	48
Figure 4.9: Arrhenius plot for films S_1 , S_2 , S_3 and S_4	50

Figure 4.10: Linear sweep voltammogram for sample S ₄	51
Figure 5.1: FTIR spectra in the region between 650 and 4000 cm ⁻¹ for (a) pure PEMA, (b) PEMA-EMITFSI and (c) PEMA-EMITFSI-MgTf ₂	54
Figure 5.2: FTIR spectra in the region between 1100 and 1200 cm ⁻¹ , 1400 and 1500 cm ⁻¹ and 1680 and 1780 cm ⁻¹ for (a) pure PEMA, (b) PEMA-EMITFSI and (c) PEMA-EMITFSI-MgTf ₂	55
Figure 5.3: SEM micrographs for (a) S ₁ (b) S ₂ and (c) S ₃	56
Figure 5.4: DSC thermograms in the temperature range from 50 to 70 °C for (a) S ₁ , (b) S ₂ and (c) S ₃	57
Figure 5.5: Variation of ionic conductivity with content of EMITFSI and MgTf ₂	59
Figure 5.6: Arrhenius plot for films S ₁ , S ₂ and S ₃	60
Figure 5.7: (a) Current-time curve and (b) impedance plots before and after polarization for the Mg S ₂ Mg cell	61
Figure 5.8: Linear sweep voltammogram for (a) PEMA – 20 wt.% MgTf ₂ and (b) S ₂ at room temperature	63
Figure 6.1: SEM micrographs for (a) S ₁ (b) S ₂ and (c) S ₃	68
Figure 6.2: TGA thermograms in the heating run up to 600 °C for (a) S ₁ (b) S ₂ and (c) S ₃	69
Figure 6.3: Arrhenius plot for films S ₁ , S ₂ and S ₃	72
Figure 6.4: Variation of ionic conductivity and activation energy for films S ₁ , S ₂ and S ₃ at 30 °C	73
Figure 6.5: Linear sweep voltammogram for S ₂ at room temperature	74

LIST OF TABLES

Table 3.1: Designations of PEMA-EMITFSI based polymer electrolytes	25
Table 3.2: Designations of PEMA-EMITFSI-MgTf ₂ based polymer electrolytes	26
Table 3.3: Designations of PEMA-EMITFSI-MgTf ₂ based polymer electrolytes	26
Table 4.2: DSC results of PEMA-EMITFSI electrolytes	45
Table 5.2: The value of Mg S ₂ Mg cell during transference number measurement	61
Table 6.2: Film stability of PEMA NCPEs	67
Table 6.3: Development of PEMA NCPEs	70

University of Malaysia

LIST OF SYMBOLS

E_A	-	Activation energy
R_b	-	Bulk resistance
σ	-	Conductivity
T_d	-	Decomposition Temperature
X_c	-	Degree of crystallinity
ϵ_r	-	Dielectric constant
σ_e	-	Electronic conductivity
t_e	-	Electronic transference number
T_g	-	Glass transition temperature
σ_i	-	Ionic conductivity
t_i	-	Ionic transference number
Li^+	-	Lithium ion
Mg^{2+}	-	Magnesium ion
$T_{\text{Mg}^{2+}}$	-	Magnesium transference number
T_m	-	Melting temperature
M_w	-	Molecular weight
R	-	Resistance
t	-	Thickness of sample
σ_T	-	Total conductivity
wt.%	-	Weight percentage

LIST OF ABBREVIATIONS

A	- Area of the disc electrodes in cm^{-2}
CPE	- Composite polymer electrolyte
EMITFSI	- 1-ethyl-3-methylimidazolium bis(trifluorosulfonyl) imide
DSC	- Differential Scanning Calorimetry
EC	- Ethylene carbonate
EIS	- Electrical impedance spectroscopy
FTIR	- Fourier transform infrared
GPE	- Gel polymer electrolyte
LE	- Liquid electrolyte
LiTf	- Lithium triflate
LSV	- Linear sweep voltammetry
MgO	- Magnesium oxide
MgTf ₂	- Magnesium triflate
NCPE	- Nanocomposite polymer electrolyte
PC	- Poly (ethylene carbonate)
PE	- Polymer electrolyte
PEMA	- Poly (ethyl methacrylate)
PEO	- Poly (ethyl oxide)
PMMA	- poly (methyl methacrylate)
SEM	- Scanning electron microscopy
SiO ₂	- Silica dioxide
SPE	- Solid polymer electrolyte
TGA	- Thermogravimmetric analysis
VTF	- Vogel-Tamman-Fulcher

CHAPTER 1

INTRODUCTION TO THE PRESENT WORK

1.1 Background

Magnesium ion-based power storage devices are attracting more attention due to their performance characteristic which is close to that of their lithium counterparts. Furthermore, the magnesium-based electrochemical devices are more attractive from a device fabrication point of view due to their cost effectiveness, low toxicity, and ease of handling and safer. However, the development of magnesium-based devices has yet not accelerated due to irreversibility of the magnesium-based negative electrode and lack of suitable Mg^{2+} conducting electrolytes.

A suitable electrolyte in chemical devices should contain mobile cation which can be transported through the electrolyte layer when contact with the electrodes. To obtain dissociated cation and anion which can contribute to ion conduction, salts like LiClO_4 (Angulakshmi et al., 2011), MgTf_2 (Kumar & Munichandraiah, 2000), etc. were dissolved in low molecular weight organic solvents such as dimethyl sulphoxide (DMSO) (Davey et al., 2000), dimethyl formamide (DMF) (Bishop et al., 1996), diethyl carbonate (DEC) (Moumouzias et al., 2003), ethylene carbonate (EC) (Tobishima et al., 1998) and propylene carbonate (PC) (Kovač et al., 1998). The choice of solvent is based on the viscosity and dielectric constant, ϵ . PC and EC are the most frequently used solvent to prepare gel polymer electrolytes due to its high dielectric constant (ϵ of PC = 64.6, ϵ of EC=89) (Kumar & Sekhon, 2002). In the context of solid state magnesium-based power storage devices, some magnesium-ion conducting polymer electrolytes have been studied (Kumar et al., 2011; Ohba et al., 2004; Pandey et al., 2011; Perera et

al., 2004). However, according to (Kumar et al., 2011) and (Yoshimoto et al., 2003), polymer-magnesium salt complexes offer moderate ionic conductivity. These were attributed to the poor dissociation of magnesium salts in the host polymers due to (i) strong electrostatic interaction between the Mg^{2+} ion and the counterion, (ii) strong electrostatic interaction between the Mg^{2+} with the polar group of the host polymer. Such situation is responsible for the restricted mobility of Mg^{2+} ion in the polymer-salt complexes.

The incorporation of room temperature ionic liquids (RTILs) into polymer electrolytes represents a recent promising approach to obtain highly conducting, thermally and electrochemically stable polymer electrolytes. Other advantages, RTILs are non-flammable and negligible vapour pressure (Armand et al., 2009; Nakajima & Ohno, 2005). Addition of ionic liquids (single or binary) increases ionic conductivity in those complexes as reported by previous works (Shin et al., 2003, 2005; Tominaga et al., 2005). However, high loading of ionic liquid disfavours the mechanical stability of the complex membranes as there is a possibility of leakage of the ionic liquid. In order to enhance ionic liquid retention properties, the use of nanofiller is proposed. As reported by Fedkiw and co-workers, the dispersion of ceramic fillers (fumed silica powders) in low molecular weight poly(ethylene oxide) ethers, resulted in the formation of liquid type, composite polymer electrolytes having stable interfacial properties (Fan & Fedkiw, 1997; Walls et al., 2000).

1.2 Problem Statement

Addition of ionic liquids (single or binary) increases ionic conductivity of polymer electrolytes as reported in literatures. However, high loading of ionic liquid disfavours the mechanical stability of the polymer electrolytes as there is a possibility of leakage of the ionic liquid. In order to enhance ionic liquid retention properties, the use of nanofiller is proposed. The main drawback associated with liquid electrolytes and gel polymer electrolytes is the tendency to flow, which is deleterious in terms of decay in conductivity and, particularly, in battery reliability and safety. In order to overcome this problem, nanofillers may be incorporated into the polymer-magnesium salt-ionic liquid systems to improve the mechanical as well as their electrochemical and ion transport properties.

1.3 Objectives of Study

The objectives of this research work are to study:

1. the effects of ionic liquid to the physicochemical properties of PEMA films.
2. the effects of composition of magnesium salt and ionic liquid to the physicochemical properties of PEMA films.
3. the effects of composition of inorganic nanofillers to the ionic liquid retention and physicochemical properties of polymer-magnesium salt-ionic liquid composites.

1.4 Materials Selection

Substantial effort has been devoted to improve the performance of PEs including the use of variety of host polymers. The methacrylic ester polymers have excellent chemical resistance, high surface resistivity and mechanical properties. The most common polymer in this group is poly (methyl methacrylate) (PMMA), and because of its high resistance, non-tacking characteristics, surface resistance and optical properties; it has been intensively investigated by several researchers (Bohnke et al., 1993; Osman et al., 2014). Besides PMMA, PEMA is also a methacrylic ester polymer. The use of PEMA as a host polymer in electrolyte system has been reported by our group and other research groups (Anuar et al., 2012; Fahmy & Ahmed, 2001; Han et al., 2002; Mohammad et al., 2013; Rudhziah et al., 2011). Recent studies showed that PEMA possesses higher mechanical strength than PMMA (Han et al., 2002). In addition, PEMA shows excellent chemical and high surface resistance and offers high optical transparency (Reiter et al., 2009).

In this study, PEMA was used as a polymer host to be incorporated with ionic liquid. RTILs are molten salts at room temperature which consist of bulky, asymmetric organic cations and inorganic anions. They are non-flammable, non-volatile, having high chemical and thermal stability, and widely used as green organic solvents (Armand et al., 2009), unlike other organic solvent (eg. EC, PC) systems (Jayathilaka et al., 2003; Ma et al., 2014). The physical properties of the RTILs play an important role in modifying the structural and electrical properties of PEs. Apparently, the physicochemical properties of ILs are quite sensitive toward the structure and nature of cations and anions that even a slight variation in their ions that can lead to substantial differences in a mixture (Attri et al., 2014). The lower viscosity leads to enhance the

flexibility in the polymer backbone and hence the segmental motion. In addition, IL functionality may also be incorporated into the polymer itself by the use of suitably derivatized monomers, by a post-polymerization reaction or simply by the formation of a composite comprising (at least) a polymer and an ionic liquid (Winterton, 2006). In this work, EMITFSI was chosen because of its bigger anions that has tendency to free-up the cations from the ether oxygen coordination (Bakker et al., 1995), and the bulky cations (eg. EMI^+) create a free-volume for the ion conduction (Kumar & Hashmi, 2010; Susan et al., 2005). It is also well known that electronic and ionic conductivity properties of conductive PEs are strictly related to morphology (Adebahr et al., 2003; Ding et al., 2002). Although many studies of PEs have been reported, most research focus on Li^+ ion conducting electrolytes (Chattaraj & Basumallick, 1995; Heo et al., 2004; Lian et al., 2014; Nair et al., 2011). Mg^{2+} ion conducting PEs are not widely reported except for a few systems (Asmara et al., 2011; Osman et al., 2014; Pandey et al., 2009). Magnesium salt is attractive to be used as a dopant salt to provide Mg^{2+} ions in PEs due to: (1) magnesium metal is more stable compared to lithium metal; (2) environmentally friendly and easy to handle and (3) the ionic radii of Li^+ (68pm) and Mg^{2+} (65pm) are comparable in magnitude, hence it is possible to replace Li^+ ions with Mg^{2+} ions as the charge carriers in PE systems. Thus, magnesium triflate (MgTf_2) was used as a doping salt in this study. In order to enhance ionic liquid retention properties in PEMA- MgTf_2 system, the technique of addition of nanofillers (i.e. MgO nanofiller) was considered to improve the mechanical as well as their electrochemical and Mg^{2+} transport properties.

1.5 Thesis Organization

This dissertation is divided into seven chapters. An overview of the types of polymer electrolytes and their properties are presented in Chapter 2. This is followed by an overview of the properties of PEMA as polymer host, EMITFSI as plasticizer, MgTf₂ as doping salt and MgO nanofiller to enhance ionic liquid retention properties. The details of the experimental methods which include the sample preparation and characterization techniques employed in this study are described in Chapter 3.

Overall results and discussions for three systems investigated in this work are presented in three chapters. The results of various studies for PEMA-EMITFSI films, PEMA-EMITFSI-MgTf₂ films and PEMA-EMITFSI-MgTf₂-MgO films are presented in Chapter 4, Chapter 5 and Chapter 6, respectively. The conclusion and suggestions for future work are given in Chapter 7.

CHAPTER 2

LITERATURE REVIEW

2.1 Introduction

For the development of science and technology, materials appear as a major role player that can be clearly observed in the field of energy, telecommunication, multimedia, electronics, and construction. Polymers represent a class of materials currently in use in a broad variety of applications. In 1935, Wallace E. Carothers invented nylon (Kauffman, 1988), which quickly found application in fabrics (Stubblefield et al., 1998) tyres (Grigante et al., 2010; Jun-kai & Hai-shan, 1989) and many household items (Hergenrother, 1990; Sharma, 2006). Polymers are also used in dentistry and in a variety of implantable drug-delivery mechanisms.

Polymers also have electrolyte properties for potential applications in electrochemical devices that were first discovered by Wright *et al.*, 1975 (Wright, 1975). The motion of ions in polymeric matrices in the absence of a solvent is a relatively new phenomenon whose existence and importance have been recognised only in the past few decades (Armand, 1986; Bruce, 1995; Gray, 1997; Vincent, 1987; Wright, 1975), and corresponds to a different concept; the macromolecule itself acts as a solvent for a salt which becomes partially dissociated in the matrix, leading to electrolyte behaviour.

Polymers have been tailored as electron or ion conductors; when combined with appropriate salts their conductivity can be put to use as electrolytes. The ionic transport mechanism in polymer electrolyte can be defined as polymer membrane and this has led to the development of new host polymers of various types. In 1978, Armand *et al.*

(Zaghib et al., 1998) proposed the application of solid polymer electrolytes (PEs) to lithium batteries, and research efforts have later been made throughout the world for potential applications in fuel cells, solar cells and supercapacitors.

2.2 Polymer Electrolytes

PEs are materials of interest due to their potential applications in various electrochemical devices. The discovery of ionic conduction in polyethylene oxide (PEO)-alkali metal salt solutions (Lascaud et al., 1994) opened the door to the use of polymer electrolytes in devices such as batteries, supercapacitors, fuel cells and dye sensitized solar cells. As a result, PEs should be able to completely dissolved and dissociated in the nonaqueous media, with high mobility of the solvated ions travelled in the media (Ahmad, 2009). It also has occupied a greater or lesser extent the following properties (Sequeira & Santos, 2010):

- (a) adequate ionic conductivity for practical purposes,
- (b) low electronic conductivity,
- (c) good mechanical properties,
- (d) good chemical, electrochemical and photochemical stability,
- (e) ease of processing.

Interest in solid conducting polymer electrolytes started with a polymer chemist, Peter V. Wright, who first showed that PEO can act as a host for sodium and potassium salts, thus producing a solid electrical conductor polymer/salt complex (Wright, 1975). Since then, a significant amount of work on ionic conducting polymer electrolytes has been reported (Asensio et al., 2004; Wiczorek & Stevens, 1997; Xu et al., 2000; Yates et al., 2002). In general, PEs can exist in a form of liquid (LEs) (Cameron & Ingram, 1989; MacCallum & Vincent, 1989), dry or solid type (SPEs) (Abraham & Alamgir, 1990;

Grigoriev et al., 2015), gelled or plasticized (GPEs) (Dvořák et al., 2014; Kim & Sun, 2001) or as a composite material (CPEs) (Capuano et al., 1991; Malathi et al., 2015).

2.2.1 Liquid Polymer Electrolytes

Liquid polymer electrolytes (LEs) are formed by the dissolution of polymers in proper solvents. LEs are comprised entirely ions and are liquid at room temperature (30 °C). They offer high ionic conductivity (Cameron et al., 1989; MacCallum et al., 1989). However, LEs have leaking problem, gas formation arises from solvent evaporation and have poorer fabrication properties. Therefore, solid polymer electrolytes (SPEs) are more preferred in battery industries because SPEs can be easily manufactured into shapes not available to liquid containing systems, and are safer than LEs.

2.2.2 Solid Polymer Electrolytes

Wright and co-workers (Payne & Wright, 1982) were the first to discover that the PEO-based solid polymer electrolyte was able to dissolve inorganic salts and exhibit ion conduction at room temperature. On the basis of a general survey, on most of SPE systems so far, the ionic conductivity of polymer electrolytes is typically 100 to 1000 times less than that exhibited by a liquid-or ceramic-based electrolyte (Fadzallah et al., 2014; Song et al., 1999; Zalewska et al., 2014). Although higher conductivities are preferable, the suggestions of Armand *et al.* was mainly brought by the following advantages of these type of polymer electrolytes i.e. good mechanical strength and high dimensional stability, no leakage, easy processing, low self-discharge and high energy density. In addition, their properties (particularly conductivity and transport properties), should be sufficiently practical to stimulate their development when compared with other highly conducting solid electrolyte materials.

Considering these critical attributes of their fundamental properties; there has been an enormous amount of research carried out for the development of new generations of polymer electrolyte materials that are commercially more attractive.

2.2.3 Gel Polymer Electrolytes

Gel polymer electrolytes (GPEs) are alternatives to both (SPEs) and (LEs) as potential materials for electrochemical devices. Even though LEs can offer high ionic conductivity, they also bear high risk of leakage and can cause corrosion during packaging, while SPEs conversely, possess no problem with leakage or packaging, but exhibit only low conductivity. The 'dry' SPE is a single phase, containing dissolved salt and where the ions of the salt are mobile. GPEs or plasticised polymers, are single phase and contain organic additives/plasticizers which have the effect of softening the polymer.

According to Gray *et al.* (1997) (Gray et al., 1997), the solid character of polymers is related to the molecular weight of polymer. The polymer can be obtained from liquids to very hard and rigid materials, depends on their molecular weight. Some polymers can organise at the molecular level in such a fashion as to be crystalline. Experiment and detailed mechanistic studies clearly established in 1983 that continuous ionic motion in salt-polymer complexes occurring in the amorphous region of the polymeric material (Minier et al., 1983). Since ionic conductivity comes about through molecular motion in the structure, GPEs have higher ionic conductivity than the SPEs because of greater freedom for molecular motion.

GPE essentially has evolved since 1975 in order to obtain ionic conductivity ranging between 10^{-5} Scm^{-1} to 10^{-3} Scm^{-1} (Watanabe et al., 1982). The ionic conductivity of GPEs depends on the viscosity and the dielectric constant of the plasticizers. Plasticizers such as polyethylene carbonate (PC) and ethylene carbonate (EC) have been much used because of low vapour pressure and high dielectric constant, $\epsilon = 64.92$ and 89.78 , respectively. However, EC and PC are corrosive and flammable. In attempts to emerge concerns with energy and pollution while maintaining the properties of good plasticizers, room temperature ionic liquid (RTIL) has been found to be most potential candidates as plasticizers due to thermally stable at high temperature, can improve electrode-electrolyte interfacial contact and as well as wide electrochemical stability window. In particular, PEMA-based gel polymer electrolytes incorporated with ionic liquid have been found to exhibit high ionic conductivity with high transparency (Anuar et al., 2012; Rudhziah et al., 2013).

2.2.4 Nano-Composite Polymer Electrolytes

It has been observed that the presence of larger amount of liquid electrolyte in polymer matrix gives rise to better ionic conductivity but diminishes the mechanical integrity of GPEs. Therefore, in order to improve the mechanical integrity, GPEs are dispersed with micro- and nano-sized ceramic fillers like SiO_2 , Al_2O_3 , TiO_2 , BaTiO_3 etc. This category of polymer electrolytes is called composite/nanocomposite polymer electrolytes (CPEs/NCPEs). It is found that the dispersion of ceramic fillers not only improves mechanical strength but also improves the electrical conductivity of the GPE systems (Croce et al., 1998; Flora et al., 2014; Pradhan et al., 2008). The dispersion of ceramic fillers has been proven to give favourable effect to ionic conductivity at low temperatures and stability at the interface with electrodes (Kumar et al., 2007). Pioneering research works on the incorporation of inorganic fillers into PEO can be

traced to Weston *et al.* (1982), Stevens *et al.* (1986) and Skaarup *et al.* (1988) (Skaarup *et al.*, 1988; Weston & Steele, 1982; Wieczorek *et al.*, 1995). The conclusions derived from these works were that such addition led to improved ionic conductivity (Skaarup *et al.*, 1988; Weston *et al.*, 1982; Wieczorek *et al.*, 1995).

Numerous research efforts have been carried out later on composite electrolytes using SiO₂, ionic glass and both crystalline and non-crystalline aluminas as the inorganic fillers, which showed improvements in the transport and mechanical properties of the electrolytes (Wieczorek *et al.*, 1991). In addition to this, other researchers also noted that particle size and concentration of the inert solid phases appeared to be critical factors that reduced the degree of crystallinity of polymers resulting in enhanced ionic conductivity (Munichandraiah *et al.*, 1993). In part, because of this idea, NCPEs (Croce *et al.*, 1998) in which nanosized inert solid particles are added to the polymer electrolytes are presently the focus of many studies, both practical and theoretical.

2.3 Transport Mechanisms in Polymer Electrolyte

Ion conduction mechanism is one of the most important studies in PEs. Several models have been proposed to interpret the ion conduction process in polymer electrolytes. The mechanism can be inferred from temperature dependent conductivity studies of the systems. For most PEs, their temperature dependent conductivity exhibits one of the following behaviour (Chandra & Chandra, 1994; Harris *et al.*, 1987):

- (a) Vogel Tamman-Fulcher (VTF) behaviour
- (b) Arrhenius behaviour for low temperature and VTF behaviour at a higher temperature

- (c) Arrhenius behaviour throughout but with different activation energies in different temperature ranges
- (d) VTF behaviour for temperatures slightly greater than T_g but Arrhenius behaviour at high temperatures
- (e) behaviour which neither follows Arrhenius nor VTF behaviour in any temperature range

However, most experimental results show behaviours like (a), (b) and (c). Behaviour (d) can be explained in terms of the free volume theory, whereas behaviour (e) is the most complicated and difficult to understand. One group of PEs obeys Arrhenius type relation, expressed by the following equation:

$$\sigma = \sigma_0 \exp\left(\frac{-E_A}{k_B T}\right) \quad (2.1)$$

where σ_0 is the pre-exponential factor, k_B is the Boltzmann constant, T is the absolute temperature, and E_A is the activation energy that can be calculated from the linear-least-square fit of the data from $\log \sigma$ versus $1000/T$ curve. Arrhenius theory was developed in 1889, by Swedish chemist Svante Arrhenius (Crawford, 1996). It was found to be applicable for liquids and solids electrolytes later. In solids, the ions hop from one vacant site to another by overcoming the energy barrier i.e., activation energy E_A that exists between these (Kumar et al., 2006).

On the other hand, some PEs obey VTF behaviour which was first developed to describe the viscosity of supercooled liquids (Baril et al., 1997; Pas et al., 2005; Vogel, 1921). From a macroscopic point of view, it is well accepted that the variation of ionic conductivity, σ , with temperature for a fully amorphous polymer electrolyte can be

more accurately represented by the Vogel-Tamman-Fulcher (VTF) (Fulcher, 1925; Tamman & Hesse, 1926; Vogel, 1921) equation:

$$\sigma = AT^{-1/2} \exp\left(\frac{-B}{k_B(T-T_0)}\right) \quad (2.2)$$

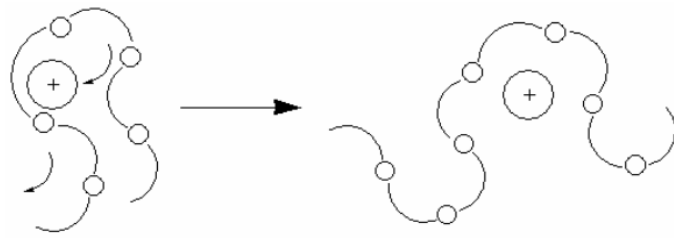
In the above VTF equation, A is the pre-exponential factor, which is related to the number of charge carriers, T is the temperature of measurement, B is the pseudo-activation energy of ion transport and hence relates to the segmental motion of polymer chains (Harris et al., 1987), k_B is the Boltzmann constant, and T_0 is the equilibrium glass transition temperature or the thermodynamic limiting glass transition temperature (T_g) at which the configurational entropy is zero that corresponds to the T_g of the samples. The ionic conductivity σ is usually obtained from AC impedance measurements (Jacobs et al., 1989). The VTF equation can adequately describe the diffusion of uncharged molecules through disordered media such as fluids or polymers. In the case of PEs, the ions are assumed to be transported by the semi-random motion of short polymer segments.

This correlation between ion transport and segmental mobility can be understood by recognizing the free volume model (Uma et al., 2005). As the temperature increases, the polymer can expand easily and produces free volume. Thus, ions, solvated molecules or polymer segments can move into the free volume. Therefore, as the temperature increases, the free volume increases. This leads to an increase in ion mobility and segmental mobility that will assist ion transport.

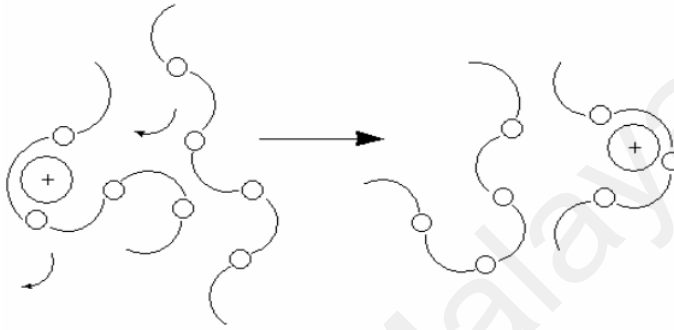
Figure 2.1 shows this type of motion schematically. Figure 2.1(a) shows how a cation could move between coordinating sites on one chain and Figure 2.1(b) shows this

motion between sites on neighboring chains, promoted by the segmental motion of the chain themselves. The model is very much an oversimplification of the real situation as it does not consider effects such as ion-ion interactions. Figure 2.1(c) shows one example of how ion associated species may assist in the conduction mechanism. The extreme example depicted in Figure 2.1(d), shows the polymer chains acting solely as anchor points with conductivity in this case resulting from ions (anions or cations) moving from ionic cluster to ionic cluster. All these mechanisms are feasible and may depend to a large extent on the salt concentration in the matrix.

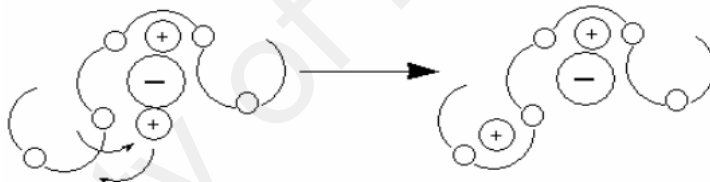
University of Malaya



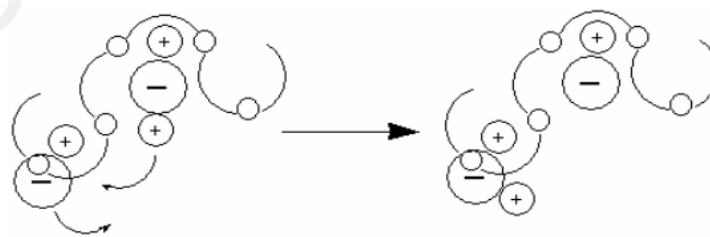
(a) Intrachain Hopping



(b) Interchain Hopping



(c) Intrachain Hopping *via* ion cluster



(d) Intercluster hopping

Figure 2.1: Cation motion in a polymer electrolyte (a) Intrachain hopping; (b) Interchain hopping; (c) Intrachain hopping via ion cluster; (d) Intercluster hopping (D. H. Gray et al., 1997)

2.4 Poly (ethyl methacrylate)

Substantial effort has been devoted to improve the performance of PEs including the use of variety of host polymers. The methacrylic ester polymers have excellent chemical resistance, high surface resistivity and mechanical properties. The most common polymer in this group is poly (methyl methacrylate) (PMMA), and because of its high resistance, non-tacking characteristics, surface resistance and optical properties; it has been intensively investigated by several researchers (Bohnke et al., 1993; Osman et al., 2014). The initial study on methyl acrylate polymer as polymer host was done by Iijima et al. (1985) using poly (methyl methacrylate) (PMMA). Besides PMMA, poly (ethyl methacrylate) (PEMA) is also a methacrylic ester polymer. PEMA is another derivation of methacrylic ester polymers that are currently received much attention in the development of polymer electrolyte membranes. PEMA is reported (Han et al., 2002) to exhibit higher mechanical strength than PMMA. Han *et al.* (2002) reported that the mechanical strength of PVC/poly(ethyl methacrylate) (PEMA) based electrolytes was found to be much higher than that of PVC/PMMA based electrolytes. High transparency, sufficient mechanical strength, elasticity and good adhesion onto substrates (Reiter et al., 2009) make PEMA suitable for use as a host for ionic conduction in electrochromic devices.

In order to develop high conducting polymer electrolytes, a flexible polymer backbone is needed. This requirement attained by PEMA because of its large pendant group compared to PMMA as shown in Figure 2.2. Indeed, the elongation strength of PEMA (7%) is higher and its T_g (336 K) is lower as compared to PMMA.

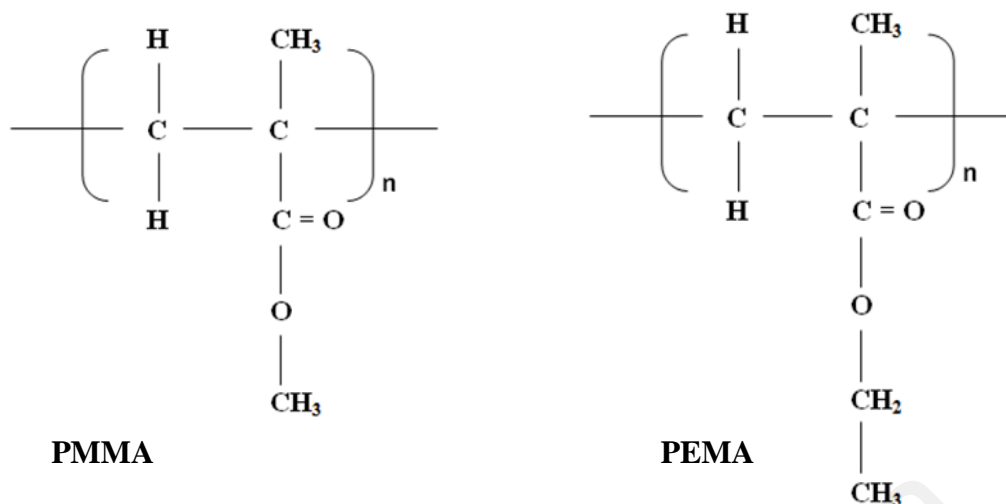


Figure 2.2: Structure of PMMA and PEMA

The polar functional groups in the structure of PEMA exhibit high affinity to cations from inorganic salts, i.e. Li^+ , Mg^{2+} , to form polymer-salt complexes and hence produce ionic conduction. Electron pairs belonging to carbonyl group ($\text{C}=\text{O}$) and ether group ($\text{C}-\text{O}-\text{C}$) in the structure of PEMA are capable to coordinate with the cation of a salt. The use of PEMA as a host polymer was first reported by Han *et al.* (2002) and Fahmy *et al.* (1999). PEMA based polymer electrolytes for electrochromic devices have been reported by Reiter *et al.* (2009) and were found to exhibit good ionic conductivity up to $10^{-4} \text{ S cm}^{-1}$. Our research group previously study of thermal, structural, morphological, composition and temperature dependence ionic conductivity of polymer electrolytes of PEMA doped with ammonium salts (Amir et al., 2013; Rudhziah et al., 2011), and PEMA doped with ammonium salts and ionic liquid (Anuar et al., 2012) and (Mohammad et al., 2013). The highest room temperature ionic conductivity obtained is in the order of 10^{-7} to $10^{-4} \text{ S cm}^{-1}$ for all systems.

2.5 Ionic Salts

Salts are ionic compounds of cations (positively charge ions) and anions (negative ions) that result from the neutralization of an acid and a base. It can be either inorganic such as chloride, or organic such as acetate and monoatomic/polyatomic ions. Gray et al. (1997) stated that the influence of salt on the ionic conductivity of polymer electrolytes depends on several aspects as follows: crystalline complex formation, the intermolecular cross-linking of the polymer chains and the degree of salt dissociation. Salts having low lattice energies and with large anions are generally expected to promote greater dissociation, thus providing higher free ions. The lattice energy gives a rough indication of the solubility of the salt which reflects the energy required to separate the positive and negative ions in a solid ionic compound. According to Gray *et al.* (1991), the lattice energy effects may be compensated by factors such as a low value of cohesive energy density, vacancy formation, favoured by a glass transition temperature, Lewis acid-base interactions between the coordinating sites on the polymer and the ions and long range electrostatic forces such as cation-anion interaction energies.

Although many studies of polymer electrolytes have been reported, most research focus on lithium ion conducting electrolytes which is due to their use as electrolytes in high energy density lithium batteries (Scrosati & Vincent, 2000). However, their commercial success is conditioned by certain drawbacks associated with the high reactivity of this alkaline metal (e.g. dendritic deposition of Li, growth of passive layer on Li surface and safety issues). In view of negligible hazards and enhanced safety, studies on multivalent salt systems like those with Mg^{2+} cations as mobile species in polymer electrolytes may be a good alternative to those with Li^+ . Magnesium ion conducting electrolytes are not

widely reported except for a few systems (Pandey et al., 2009; Piccolo et al., 2013; Tripathi et al., 2012). The high promise of magnesium ion batteries was also highlighted by Aurbach *et al.* (2009) (Levi et al., 2009). Magnesium is an alkaline-earth metal located close to Li in the electrochemical series (electrode potential of -2.37 V vs. SHE) and has good electrochemical performance (high electrochemical equivalence of 2.2 Ahg⁻¹). Unlike Li, Mg is nontoxic, and hence environmentally friendly. It can be handled safely in oxygen and humid atmospheres. Mg raw resources are abundant, and as a consequence it is cheaper than Li. The ionic radii of Li⁺ and Mg²⁺ are comparable in magnitude; hence it is possible to replace Li⁺ ions with Mg²⁺ ions as the charge carrier in polymer electrolytes. Owing to these merits, investigations on electrochemistry of magnesium-based rechargeable battery systems are significantly important.

2.6 Ionic liquid as plasticizer

Plasticizing solvent is a substance, usually a liquid that acts as dissolving agent or an additive to reduce the viscosity of electrolytes. Generally, low molecular weight organic nonaqueous solvents such as ethylene carbonate (EC) and polyethylene carbonate (PC) are used in order to enhance the conductivity by facilitating movement of the ionic charge carriers along the polymer backbone. The main function of plasticizing solvent in the polymer electrolyte is to decrease the glass transition, T_g of the polymer and suppress crystallization of ion-coordinating polymer. However, conventional electrolyte solutions that contains organic solvents, which are both flammable and volatile, posing a safety hazard. As a matter of fact, replacing these solvents with non-volatile, non-flammable plasticizing solvents could lead to the development of devices which are

safer and have greater lifetimes while maintaining high ionic conductivity. For that room temperature ionic liquids (RTILs) are proposed.

RTILs are molten salts at ambient temperature which consist of bulky, asymmetric organic cations and inorganic anions. Since the RTILs are composed of only ions, they are non-flammable with high ionic conductivity, negligible volatility (Forsyth et al., 2004), electrochemically stable (Armand et al., 2009) and high thermal stability (Kosmulski et al., 2004; Paulechka et al., 2005). RTILs have been known since 1914 (Welton, 1999), but the number of publications has exponentially increased only since 2002. Much research has been carried out towards applying RTILs as recyclable solvents in chemical reaction media (Fraga-Dubreuil et al., 2002), alternatives to volatile reaction solvents (Chiappe & Pieraccini, 2005) and catalyst (Dupont et al., 2002). The unique properties of RTILs as non-flammable liquids with high ionic conductivity make them suitable for use as electrolytes in dye sensitized solar cells (Stathatos et al., 2003; Wang et al., 2003), fuel cells (De Souza et al., 2003; Hagiwara et al., 2005), or lithium ion batteries (Ishikawa et al., 2006; Lewandowski & Świdarska-Mocek, 2009; Zhao et al., 2011). Besides, addition of RTILs as plasticizing solvents into polymer electrolytes could lead to the development of devices which are safer and have greater lifetimes while maintaining high ionic conductivity.

One such promising RTILs is 1-ethyl-3-methylimidazolium (bis)trifluoromethanesulfonimide (EMITFSI). The structure of this RTIL is presented in Figure 2.3. EMITFSI is in the liquid state from -15 °C and decomposes above 100 °C (Fredlake et al., 2004; Hapiot & Lagrost, 2008). It has no measurable vapour pressure, immiscible with water and has an electrochemical stability window of ~ 4.5 V on glassy carbon (Watarai et al., 2008). Watanabe *et al.* (Tokuda et al., 2005; Tokuda et al.,

2006) have carried out an empirical study on what effect altering the cation, anion, and alkyl chain organic substitution has on its various properties. When varying anion, TFSI based RTILs exhibit the highest conductivity. When varying alkyl chain length while maintaining the anion and alkylmethylimidazoliumcation ([RMI]), where 'R' is methyl, ethyl, butyl, hexyl, or octyl, abbreviated as [MMI], [EMI], [HMI], and [OMI], the capacity for ion dissociation is observed to remain almost constant from [MMI] to [EMI], then decreases upon increasing the chain length up to [OMI]. The ionic conductivity also follows the same trends, as well as the viscosity. These findings suggest the electrostatic forces dominate at low chain length, and then give way to weak van der Waals interactions as the chain increases (Tokuda et al., 2005; Tokuda et al., 2006). Investigations of the influence of plasticizer in optimizing polymer electrolyte design (Stephan et al., 2000) and on the dependence of ionic conductivity on salt concentration (Stephan et al., 2002) were reported for a PVC/PMMA polymer electrolyte. In the present work, EMITFSI was used as plasticizer to improve properties of PEMA based electrolyte system.

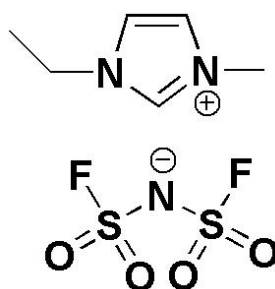


Figure 2.3: Structure of EMITFSI

2.7 Nano-filler as dispersoid

Since amorphous structure of polymers and a fully dissociated ionic salts and RTILs are the two most important factors for high performance PEs, another successful approach to enhance ionic conductivity as well as mechanical stability is to add nanoparticles of passive/active filler materials such as ZrO_2 , TiO_2 , Al_2O_3 , SiO_2 , MgO , etc., in the PE systems, leading to nanocomposite polymer electrolytes (NCPEs).

The addition of inert oxides to the polymer electrolytes has recently become an ever increasing attractive approach, due to the improved mechanical stability and enhanced ionic conductivity and also better electrolyte-electrode interface stability (Nan et al., 2003; Weston et al., 1982). Such polymer-matrix composite electrolytes originate from inorganic-inorganic composite solid electrolytes (Liang, 1973) where the conductivity enhancement is due to the interface (Nan et al., 2003; Zhu, 2006). The increase in ionic conductivity of the composite electrolyte depends on the concentration and particle size of the the inert solid phases (Agrawal & Gupta, 1999; Fan et al., 2003). Generally, the smaller the inert solid particles, the larger the ionic conductivity enhancement. In part, because of this idea, numerous research efforts have been carried out on nanocomposite polymer electrolytes (Croce et al., 1998; Song et al., 2015; Tripathi & Shahi, 2011). Compared with their filler-free counterparts, NCPEs show improved interfacial stability, better cycle ability, comparable or superior ambient-temperature ionic conductivity and good mechanical strength (Hwang & Liu, 2002; Kumar et al., 2014; Tripathi et al., 2011). The nanofiller particles provide almost continuous crystalline domain channels, leading to an increase in free volume, and thus allowing ion migration to take place easily. However, once the optimum conductivity has been achieved, any further additions of nanofiller begin to segregate due to non-complexation in the

polymer salt matrix, and conductivity drops (Pandey et al., 2010). Although the conductivities of nanocomposite electrolytes are significantly improved from those without the nanoparticles, ambient temperature conductivities still remain relatively low for real applications.

Nanomagnesium oxide (nano-MgO) is a versatile material that has been widely used in various areas, such as catalysis, adsorption, oxidation, and sterilization. Notably, nano-MgO exhibits good bactericidal performance in aqueous environments due to the formation of superoxide anions on its surface. In this study, nano MgO was chosen to be added to the PEMA based electrolyte in the hope to improve its ionic liquid retention property.

The choice of MgO as a nanosized ceramic filler in this work is attributed to its abundance in the earth crust, high surface area, and enhanced surface reactivity obtainable from its unusual crystal shapes with a high ratio of coordinative unsaturated edge/corner surface sites as well as defect sites that are inherently more reactive towards incoming adsorbents (Ahmed et al., 2014). In addition to this, the presence of numerous atomic and defective sites on the surface of MgO nanoparticles provide easy diffusion paths for Mg^{2+} ion transport and this will in turn improve ionic conductivity. Furthermore, the MgO may also improve thermal stability and electrochemical stability window of the electrolyte system.

CHAPTER 3

RESEARCH METHODOLOGY

3.1 Introduction

This chapter describes the preparation and characterization methods of SPE films studied in this work. The films were prepared using solution casting technique and characterized using Fourier Transform Infra-Red Spectroscopy (FTIR), Differential Scanning Calorimetry (DSC), Thermogravimmetric Analysis (TGA), Scanning Electron Microscopes (SEM), Electrochemical Impedance Spectroscopy (EIS), Linear Sweep Voltammetry (LSV) and ionic transference number measurement.

3.2 Sample Preparation

Three types of system have been prepared. The systems are:

- (1) polymer-ionic liquid

Table 3.1: Designations of PEMA-EMITFSI based polymer electrolytes

PEMA (g)	EMITFSI (g)	PEMA: EMITFSI (wt. %: wt. %)	Designation
1.0	0	100: 0	S ₀
1.0	0.111	90: 10	S ₁
1.0	0.250	80: 20	S ₂
1.0	0.429	70: 30	S ₃
1.0	0.666	60: 40	S ₄

(2) polymer-ionic liquid-magnesium salt

Table 3.2: Designations of PEMA-EMITFSI-MgTf₂ based polymer electrolytes

PEMA (g)	EMITFSI (g)	MgTf ₂ (g)	PEMA: EMITFSI: MgTf ₂ (wt. %:wt. %: wt. %)	Designation
1.0	0.666	0.111	60: 30: 10	S ₁
1.0	0.666	0.250	50: 30: 20	S ₂
1.0	0.666	0.666	40: 30: 30	S ₃

(3) polymer-ionic liquid-magnesium salt-nanofiller

Table 3.3: Designations of PEMA-EMITFSI-MgTf₂ based polymer electrolytes

PEMA (g)	EMITFSI (g)	MgTf ₂ (g)	MgO (g)	PEMA: EMITFSI: MgTf ₂ : MgO (wt. %: wt. %: wt. %: wt. %)	Designation
1.0	0.666	0.250	0.005	39.5: 40: 20: 0.5	S1
1.0	0.666	0.250	0.01	39: 40: 20: 1.0	S2
1.0	0.666	0.250	0.05	35: 40: 20: 5.0	S3

All the samples for this study were prepared using solution casting method. Various amount of EMITFSI were added into PEMA-THF solutions and stirred thoroughly at 30 °C to produce solid polymer electrolytes (SPEs) with 10 wt.%, 20 wt.%, 30 wt.% and 40 wt.% EMITFSI (System 1). In order to study both composition dependence of magnesium salt and ionic liquid to the properties of PEMA, samples were prepared by dissolving different amount of MgTf₂ and EMITFSI in the PEMA-THF mixture (System 2) at 50 °C for four hours. In order to enhance ionic liquid retention, as well as conductivity and electrochemical stability window, different weight percentages (0.1, 1

and 5) wt.% of nanofillers (i.e. MgO) were then added into the highest conducting PEMA-EMITFSI-MgTf₂ composition and stirred at 55 °C until homogeneous solutions were obtained (System 3). The highest conducting of nanocomposite polymer electrolytes (NCPEs) for PEMA-EMITFSI-MgTf₂-MgO was subjected to electrochemical stability window study at room temperature.

3.3 Sample Characterizations

3.3.1. Fourier Transform Infra-Red Spectroscopy

FTIR is one of efficient tools for materials analysis in the laboratory for over seventy years. In infrared spectroscopy, IR radiation is passed through a sample. Some of the infrared radiation is absorbed by the sample and some of it is passed through (transmitted). The infrared regions of the electromagnetic radiation are from 14000 cm⁻¹ to 10 cm⁻¹. Mid-infrared region which lies in the range from 4000 cm⁻¹ to 400 cm⁻¹ is useful to study organic compounds by analyzing their constituent bonds. An infrared spectrum represents a fingerprint of a sample with absorption peaks corresponding to the frequencies of vibrations of the bonds of the atoms that build up the material. Because each different material is a unique combination of atoms, no two compounds can produce the same infrared spectrum. Therefore, infrared spectroscopy can be promising tool to identify every different kind of organic material. In addition, the size of the peaks in the spectrum represents a direct indication of the amount of material. This makes infrared spectroscopy useful for several types of analysis and with modern software algorithms, infrared is an excellent tool for quantitative analysis.

The sample was directly placed on the UATR top plate mounted in the sample beam of the spectrometer. The measurements were completed within 30 seconds and ATR spectrum was obtained as shown in Figure 3.1. The IR spectrum obtained can be used

for analysis process to gain information about the sample composition in terms of chemical groups present and also to verify the various vibrational modes of a molecule.

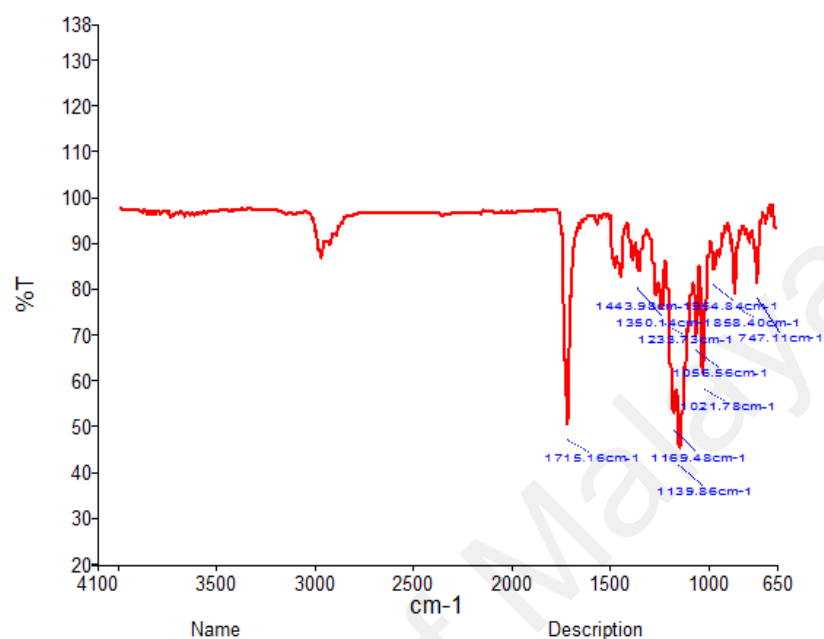


Figure 3.1: FTIR spectrum with peaks assignment in the region between 650 and 4000 cm^{-1}

In this present work, in order to study interactions between the components in the solid polymer electrolytes (i.e. PEMA, EMITFSI, MgTf_2 and MgO), infrared spectra for all SPE films were taken by using Perkin Elmer Frontier FTIR spectrometer in the transmittance mode from 4000 to 600 cm^{-1} with a resolution of 1 cm^{-1} .

3.3.2. Electrochemical Impedance Spectroscopy

EIS is a powerful diagnostic tool for the characterization of many electrical properties of materials and their interfaces with electron conducting electrodes.

EIS is usually measured by applying an AC potential to an electrochemical cell for measuring the current through the cell. Assume that a sinusoidal potential is applied, the

response to this potential is an AC current signal. This current signal can be analyzed as a sum of sinusoidal functions (a Fourier series).

Representation of Impedance Data

EIS data for electrochemical cells such as fuel cells are most often represented in Nyquist (or Cole-Cole) plots as shown in Figure 3.3.

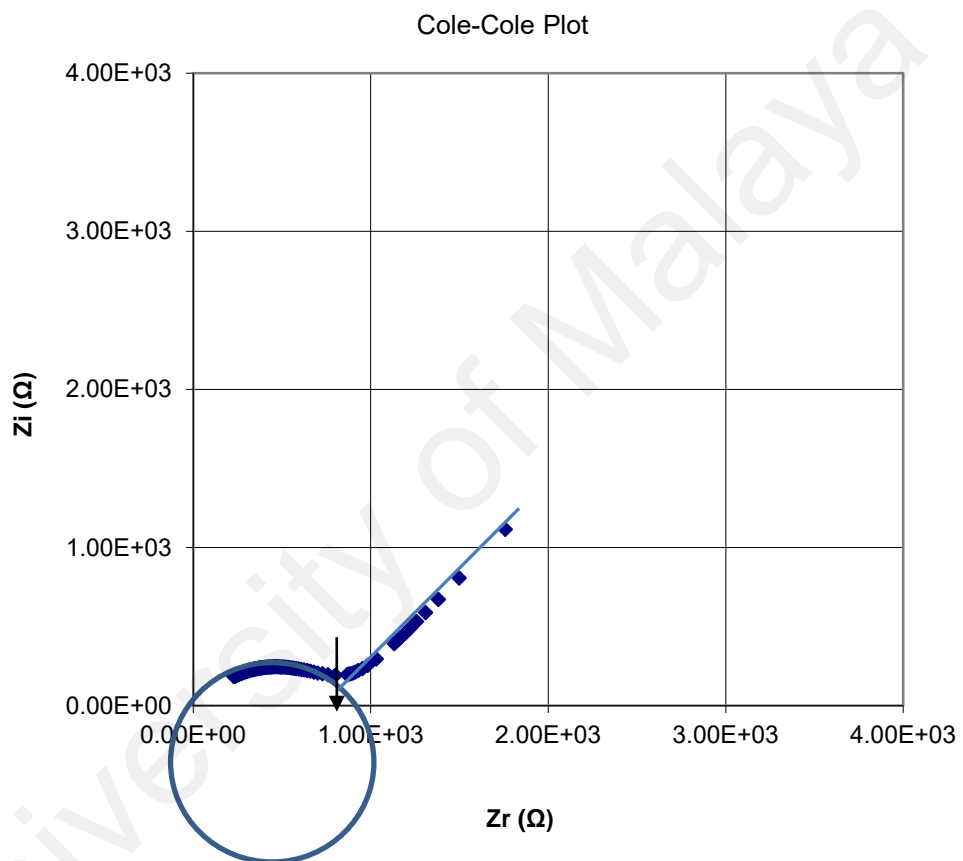


Figure 3.2: Nyquist (or Cole-Cole) plot

A complex plane or Nyquist plot depicts the imaginary impedance, which is indicative of the capacitive and inductive character of the cell, versus the real impedance of the cell. Nyquist plots have the advantage that activation-controlled processes with distinct time-constants show up as unique impedance arcs and the shape of the curve provides insight into possible mechanism or governing phenomena.

From the Cole-Cole plot with the horizontal and vertical axes having the same scale, the bulk resistance, R_b can be obtained from the graph.

Determination of ionic conductivity

The ionic conductivity of the polymer electrolytes (PEs) can be expressed in the equation by the sum of the product of the concentration of ionic charge carriers and their mobility:

$$\sigma = \sum n_i z_i \mu_i \quad (3.10)$$

where n_i is the number of the charge carriers, z_i is the ionic charge and μ_i is the mobility. In this study, the ionic conductivity of the SPE and NCPE films was measured over the frequency range from 100 Hz to 1 MHz using HIOKI 3532-50 LCR Hi-tester with 500 mV voltage amplitude at ambient temperature. The samples were sandwiched between two stainless steel blocking electrodes with diameter of 2 cm under spring pressure. The conductivity, σ of the samples was calculated using the equation:

$$\sigma = \frac{t}{R_b A} \quad (3.11)$$

where R_b is the bulk resistance, A is the electrolyte-electrode contact area and t is the thickness of the sample.

The conductivity-temperature dependence study of the films was carried out in the temperature range between 303 K and 373 K. The conductivity is said to show Arrhenius behavior if it exhibit linear variation of $\log \sigma$ versus $1000/T$. The conductivity thus can be expressed by:

$$\sigma = \sigma_0 \exp\left(\frac{-E_A}{k_B T}\right) \quad (3.12)$$

where σ_0 is a pre-exponential factor, E_A is the activation energy, k_B is Boltzmann constant and T is the absolute temperature in K. The activation energy value can be evaluated from the slope of the Arrhenius plot (Julien & Nazri, 1994).

3.3.3. Transference number measurements

The measurement of ionic transport number was carried out. The transference number or transport number in PEs is due to both ions and electrons. The total conductivity, σ_T of a sample can be obtained from the following equation:

$$\sigma_T = \sigma_i + \sigma_e \quad (3.13)$$

where σ_i and σ_e are the conductivities contributed by ions (cations/anions) and electron/holes, respectively. The fraction of the conductivity due to different charge carriers gives respective transference number given by:

$$\text{Ionic transference number,} \quad t_i = \frac{\sigma_i}{\sigma_T} \quad (3.14)$$

$$\text{Electronic transference number,} \quad t_e = \frac{\sigma_e}{\sigma_T} \quad (3.15)$$

If PEs is purely ionic, then $t_i = 1$ while for an electronic conductor, $t_e = 1$. For mixed conductors, t_i values lie in the range 0 to 1. The transference number of polymer electrolytes can be measured by Wagner's method or also known as direct-current (D.C) polarization method (Pandey et al., 2009). If the electrical conductivity of polymer electrolytes is primarily ionic, the current decreases with time due to the depletion of the ionic species in the electrolytes and become constant in the fully

depleted situation. The curve of polarization current versus time is then plotted and the ionic transference number is evaluated using the following equations:

$$t_e = \frac{\sigma_e}{\sigma_T} = \frac{i_e}{i_T} \quad (3.16)$$

$$t_i = 1 - \frac{i_e}{i_T} = 1 - t_e \quad (3.17)$$

where i_e and i_T are the residual and total current, respectively.

The transport number, t^+ of Mg^{2+} ions in the PE films was evaluated using the Bruce-Vincent method proposed by Evans *et al.* (Bruce *et al.*, 1988) using the combination of A.C impedance spectroscopy and D.C polarization of Mg|film|Mg cell. According to this method, the cells were polarized by applying a constant potential of $\Delta V = 0.07$ V for 8 hours and the current was monitored. The cells were subjected to A.C impedance measurements prior to and after polarization to determine R_0 and R_s from the Cole-Cole plots. The transport number, t^+ values were determined using the equation:

$$t^+ = \frac{I_s(\Delta V - R_0 I_0)}{I_0(\Delta V - R_s I_s)} \quad (3.18)$$

where I_0 and I_s are initial and steady state current, respectively. R_0 and R_s are cell resistances before and after the polarization, respectively.

3.3.4. Surface Morphological study

Scanning Electron Microscopes (SEM) are scientific instruments that use a beam of energetic electrons in the examination of materials on a very fine scale. SEM was developed due to the limitations of light microscopes which are limited by the physics

of light. Invented some 50 years ago, this theoretical limit had been reached and there was a scientific desire to see the fine details of the interior structures of organic cells; with high magnification images and good depth of field, and can also analyze individual crystals or other features which was not possible using current optical microscopes. These advantages make the SEM one of the useful instruments in many research areas because high-resolution SEM image can show detail down to 25 Å, or better. In this work, SPE and NCPE films were analyzed using SEM technique through Zeiss-Evo MA10 Scanning Electron Microscopic system in order to investigate the surface morphology of the samples.

3.3.5. Differential Scanning Calorimetry (DSC)

Differential Scanning Calorimetry (DSC) is the most widely used technique of all the thermal analysis methods. It is a thermoanalytical technique in which the difference in the amount of heat required to increase the temperature of a sample and reference is measured as a function of temperature. From DSC process, thermal analysis (TA) is based upon the detection of changes in the sample that are associated with absorption or evolution of heat cause a change in the differential heat flow which is then recorded as a peak. The area under peak is directly proportional to the enthalpic (heat content) change and its direction indicates whether the thermal process is endothermic or exothermic.

DSC can be used to measure a number of characteristic properties of a sample. It can be used to analyze the chemical reactions that may occur such as heat fusion, oxidation, cross-linking, and crystallization, to study the miscibility of polymers in solid polymer films, and to obtain glass transition temperature, T_g and melting point, T_m of substances. T_g is the phase when the sample turn from the rubbery state to the glassy state and this is due to the sample undergoing an exothermic process. As the temperature of the sample

is increased, the sample eventually reaches its melting temperature, T_m and this process results in an endothermic peak in the DSC curve.

The percentage of crystallinity of the PEs has been estimated using equation,

$$\chi_c = \frac{\Delta H_m}{\Delta H_m^\theta} \times 100\% \quad (3.19)$$

where ΔH_m is the melting heat obtained from DSC results. ΔH_m^θ is the enthalpy melting point of pure 100% crystalline of polymer used in the PEs.

In this work, DSC was employed for characterizing the PE films using Setaram Evo Lab^{sys} differential scanning calorimetry in the temperature range between -50 to 350 °C (as shown in Figure 3.5) in nitrogen atmosphere. Samples were rapidly cooled to -50 °C and heated up to 350 °C at a scan rate of 10 °C min⁻¹. This allows the glass transition temperature, T_g of the amorphous phase and the melting temperature of the crystalline phase of each sample to be determined using the STARe software.

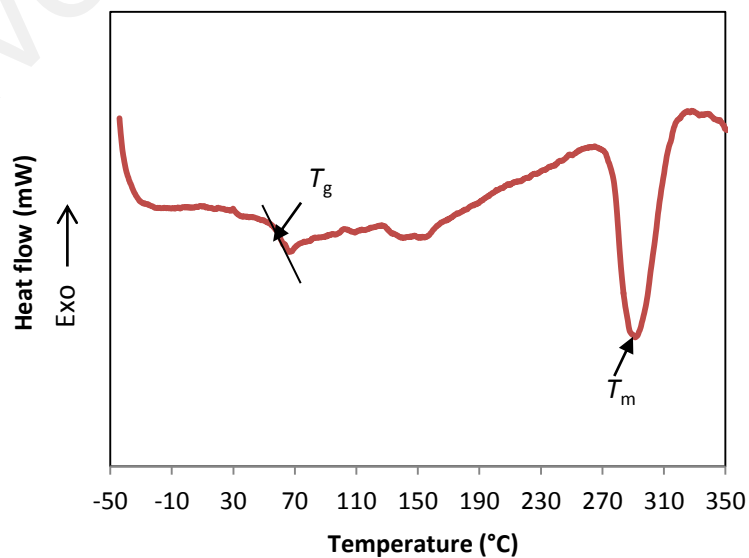


Figure 3.3: DSC thermogram in the heating run from -50 to 350 °C

3.3.6. Thermogravimetric Analysis

Thermal degradation studies of materials are necessary as many applications depend on their thermal stability. Thermogravimetric analysis (TGA) is a common method used to determine the physical and chemical properties of materials measured as a function of increasing temperature (with constant heating rate), or as a function of time (with constant temperature and/or constant mass loss). TGA can provide information about physical and chemical phenomena (i.e. vaporization, sublimation, absorption, desorption and decomposition).

The thermal stability of the PEs was tested using Labsys Evo-Setaram simultaneous thermal analysis Instrument under nitrogen atmosphere from ambient temperature to 800 °C at heating rate of 10 °C min⁻¹. A sample of mass ~ 5 mg in the form of solid films was used. As the temperature increases, various components of the sample are decomposed and the weight percentage of each resulting mass change can be measured. Results are plotted with temperature on the X-axis and mass loss on the Y-axis.

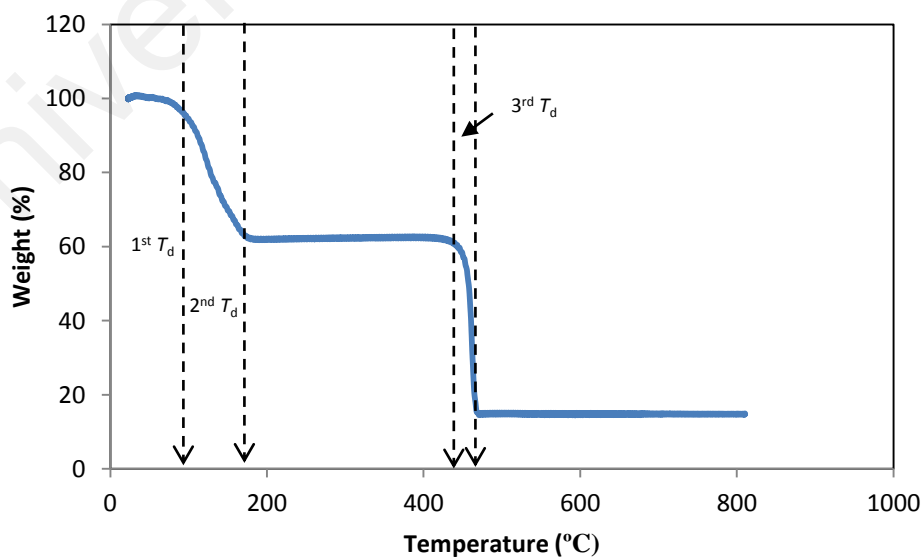


Figure 3.4: TGA thermogram in the heating run up to 800 °C

3.3.7. Linear Sweep Voltammetry (LSV)

In linear sweep voltammetry (LSV) measurements, the voltage is scanned from a lower limit to an upper limit and the current response is plotted as a function of voltage as shown in Figure 3. 7. The scan begins from the left hand side, V_1 of the current/voltage plot where no current flows. However, a current begins to flow as the voltage is swept to the right, V_2 and eventually reaches a peak before dropping. The peak occurs since the surface of the electrode is completely covered in the reactant. This means the diffusion layer has grown sufficiently above the electrode so that the flux of reactant to the electrode is not fast enough.

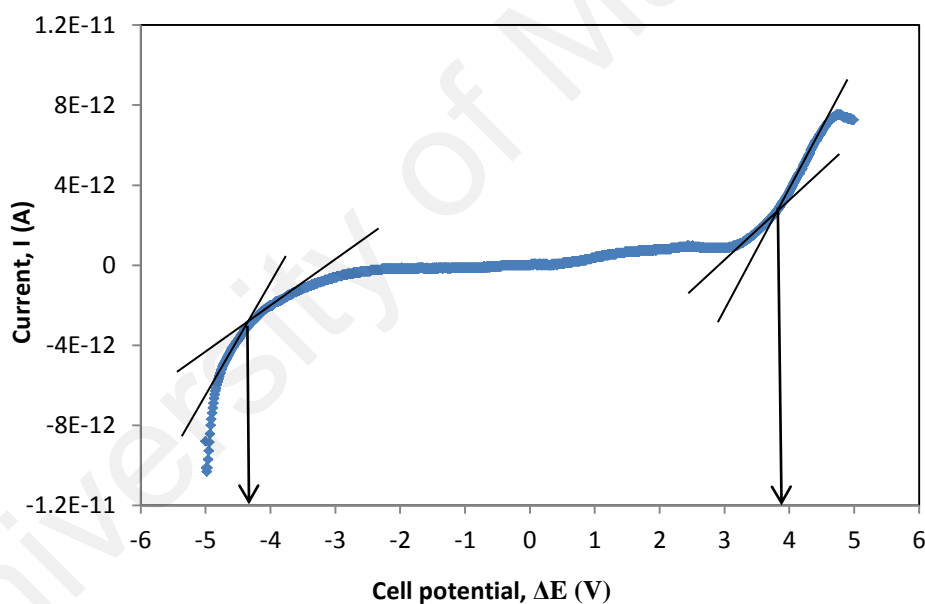


Figure 3.5: Linear sweep voltammogram in the potential range of (-5 to 5) V

The above voltammogram was recorded at a single scan rate. If the scan rate is altered, the current response will also change. Despite each curve from the plot has the same form but it is apparent that total current will decrease with decreasing the scan rate. This again can be rationalized by considering the size of the diffusion layer and the time taken to record the scan. In a slow voltage scan, the diffusion layer will grow much

further from the electrode in comparison to fast scan. Consequently, the flux to the electrode surface is considerably smaller at a slow scan rates than it is at faster rates. As the current is proportional to the flux towards the electrode, the magnitude of the current will be higher at high rates and lower at slow scan rates. A final point to note is the position of the current maximum, the peak is clearly occurs at the same voltage and this is a characteristic of electrode reactions which have rapid electron transfer kinetics. These rapid processes are often referred as reversible electron transfer reactions. In this research work, highest conducting NCPEs film was characterized through LSV technique by using Wonatech ZIVE MP2 multichannel electrochemical workstation at a scan rate of 1 mV s^{-1} in the potential range of (-5 to 5) V.

CHAPTER 4

RESULTS OF PEMA-EMITFSI ELECTROLYTES SYSTEM

4.1 Introduction

In the first part of the present work, the effects of EMITFSI ionic liquid on PEMA were investigated. For this purpose, PEMA was incorporated with different wt.% of EMITFSI. The effects of the ionic liquid on the structural, thermal, morphological, electrical and electrochemical stability properties are presented in the following sections. Table 4.1 lists the composition of polymer electrolyte samples and their designations. The free-standing transparent film obtained has been shown in Figure 4.1.



Figure 4.1: Photograph of PEMA-EMITFSI electrolyte transparent film

4.2 FTIR Results

FTIR spectroscopy was employed to study interactions between the components in the solid polymer electrolytes (i.e. PEMA and EMITFSI). In order to determine the

interaction between PEMA and EMITFSI, the FTIR spectra of PEMA-EMITFSI were recorded and compared with those of pure EMITFSI and PEMA (S₀) samples as shown in Figure 4.2. It could be observed that the bands belonging to PEMA appeared in the spectrum of PEMA-EMITFSI samples: they are the carbonyl stretching $\nu_{(C=O)}$ at 1717-1719 cm^{-1} (Fahmy et al., 2001; Rajendran et al., 2008; Sim et al., 2012), CH₂ scissoring $\delta_{(C-H_2)}$ at 1479 cm^{-1} (Fahmy et al., 2001; Rajendran et al., 2008; Sim et al., 2012), asymmetrical O-C₂H₅ bending $\gamma_{(O-C_2H_5)}$ at 1445-1448 cm^{-1} (Fahmy et al., 2001; Rajendran et al., 2008; Sim et al., 2012), CH₂ twisting $\tau_{(C-H_2)}$ at 1389 cm^{-1} (Sim et al., 2012), $\nu_{(CO)}$ mode of PEMA at 1169-1172 cm^{-1} (Sim et al., 2012), and asymmetric stretching vibration of C-O-C bond $\nu_{a(C-O-C)}$ at 1144 cm^{-1} (Sim et al., 2012). As for pure EMITFSI ionic liquid, the modes of S-O are observed at 1576, 1459, 1350 and 652 cm^{-1} (Kim et al., 2007; Nogami et al., 2012). The bands located at 1351-1057 and 849 cm^{-1} are attributed to the modes of C-F and S-N (Akai et al., 2009; Kim et al., 2007; Nogami et al., 2012), and the bands at 700 and 650 cm^{-1} are assigned to C-S-N bonds (Kim et al., 2007; Nogami et al., 2012).

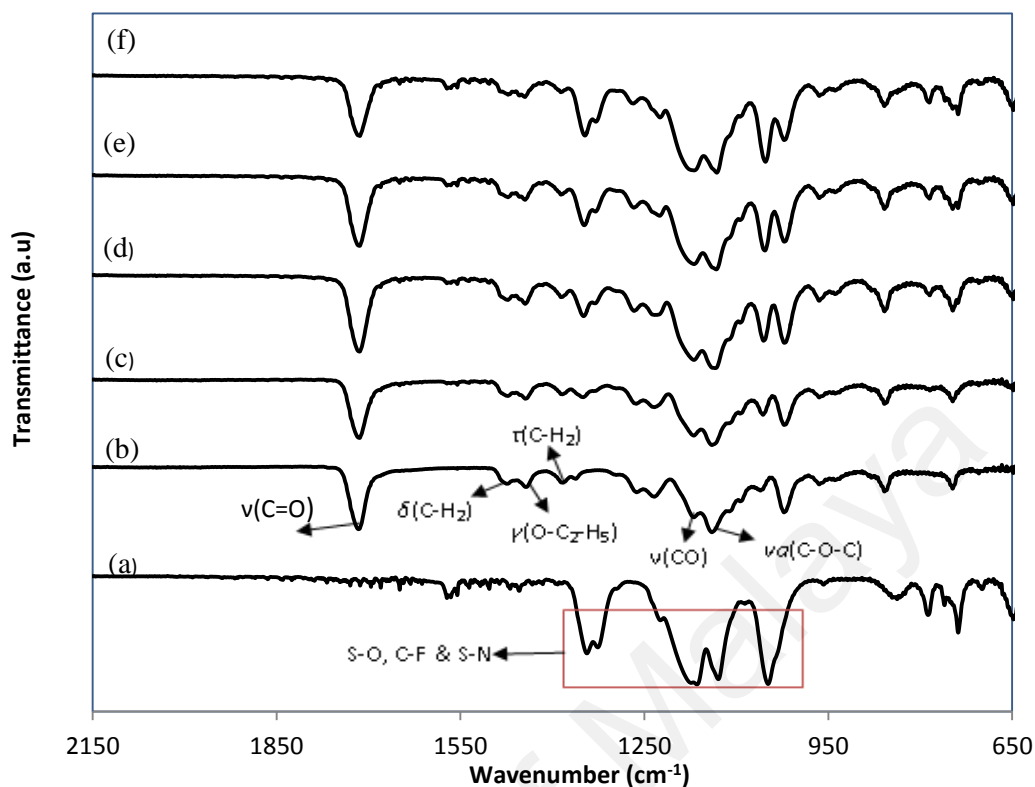


Figure 4.2: FTIR spectra in the region between 650 and 2150 cm^{-1} for (a) EMITFSI, (b) S_0 , (c) S_1 , (d) S_2 , (e) S_3 and (f) S_4

The miscibility of the added EMITFSI in the PEMA solution is the result of their possible interaction. The positively charged EMI^+ from EMITFSI can be electrostatically attracted to the negatively charged lone pair electrons on the oxygen (O) atoms of the carbonyl ($\text{C}=\text{O}$) and $\text{C}-\text{O}-\text{C}_2\text{H}_5$ groups in PEMA. The bands of particular interest in PEMA that can possibly imply interaction between EMITFSI ionic liquid with polymer electrolytes system at room temperature are the carbonyl stretching mode [$\nu_{\text{C}=\text{O}}$], asymmetric $\text{O}-\text{C}_2\text{H}_5$ bending [$\gamma_{\text{OC}_2\text{H}_5}$], and $\text{C}-\text{O}$ stretching [ν_{CO}] of $-\text{OC}_2\text{H}_5$. From Figure 4.3, ν_{CO} mode of PEMA is observed to shift from 1172 cm^{-1} in the pure PEMA to 1169 cm^{-1} in the optimized EMITFSI-containing films. The downshift of the ν_{CO} of PEMA indicates coordination of the ionic liquid with the O atom in the ester group of PEMA. The $\gamma_{\text{OC}_2\text{H}_5}$ mode of PEMA experienced and upshift

from 1445 cm^{-1} in S_0 to 1448 cm^{-1} in S_4 . A similar peak shift trend is observed for all samples for $\nu_{(C=O)}$ mode of PEMA. This reveals that the coordination of EMI^+ ions from EMITFSI onto the oxygen atom of the carbonyl group. The observation shows the presence of interaction between the components of PEMA-EMITFSI electrolyte systems.

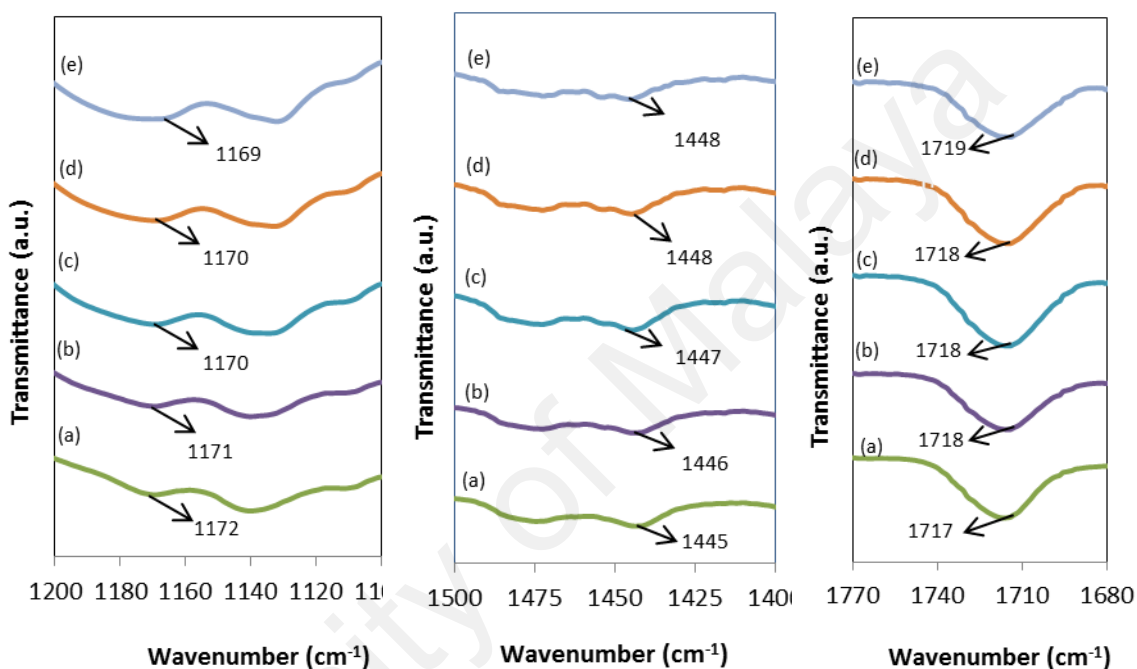


Figure 4.3: FTIR spectra in the region between 1100 and 1200 cm^{-1} , 1400 and 1500 cm^{-1} and 1680 and 1770 cm^{-1} for (a) S_0 , (b) S_1 , (c) S_2 , (d) S_3 and (e) S_4

4.3 SEM Analysis

Figure 4.4 shows SEM images of cross-sectional surface of PEMA with different EMITFSI contents (0, 20 and 40) wt. %, denoted as S_0 , S_2 and S_4 , respectively. It can be seen from Figure 4.4 (a) that the pure PEMA film possessed a rough surface (dark and grey region) with sizes of $1\text{-}10\text{ }\mu\text{m}$ in diameter. When EMITFSI is added to the PEMA system, (Figure 4.4 (b) and (c)), the increase of amorphous region (light grey) is observed as EMITFSI content increases. The smoothness of the surfaces of the sample with 40 wt. % EMITFSI is possibly due to the entrapping of a large amount of ionic

liquid solution (EMITFSI) into the pure PEMA. This could improve the ionic movement of electrolytes which will be discussed later.

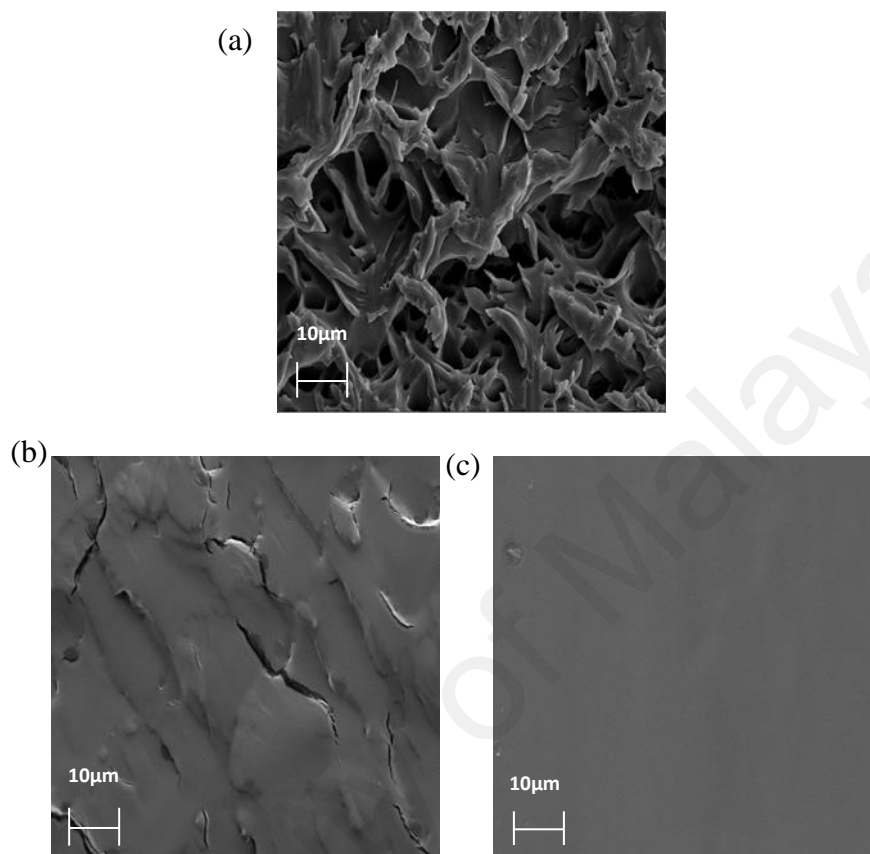


Figure 4.4: SEM micrographs for (a) S_0 , (b) S_2 and (c) S_4

4.4 Thermal Analysis

DSC was used to determine the glass transition temperature, T_g and the melting point, T_m of the solid polymer electrolyte. Figure 4.5 shows the DSC curves of PEMA-EMITFSI electrolytes with varying EMITFSI contents in the range from 0 to 350 °C. Meanwhile, Figure 4.6 presents DSC thermograms in the heating run for all samples in selected temperature range.

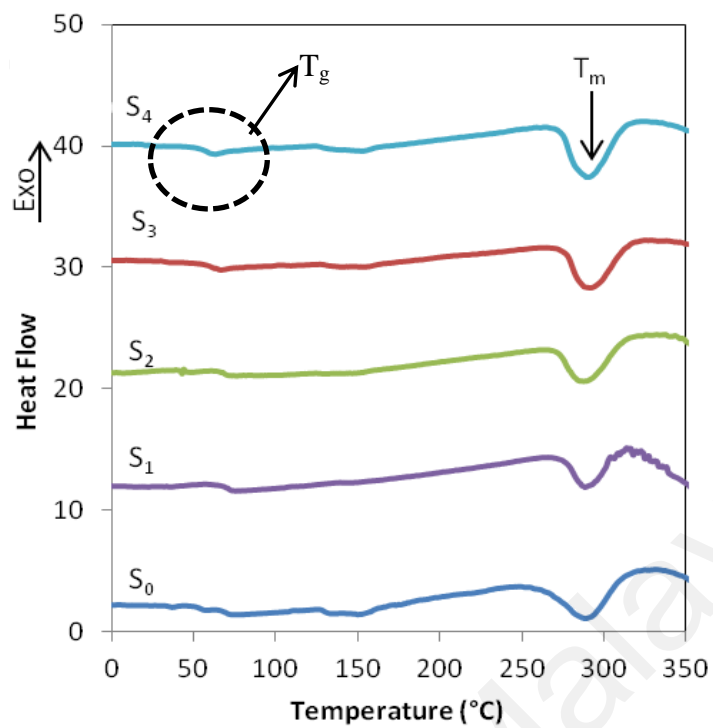


Figure 4.5: DSC thermograms in the heating run from 0 to 350 °C

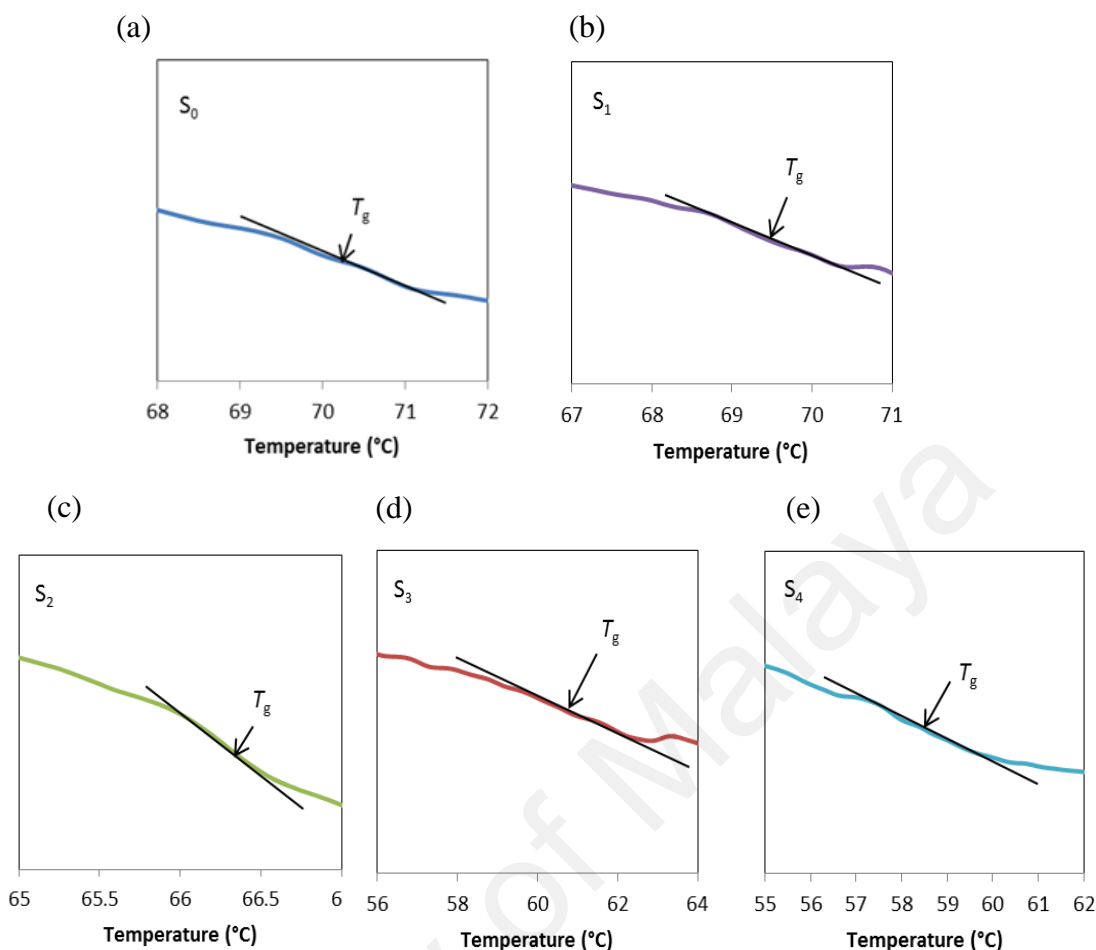


Figure 4.6: DSC thermograms in the heating run for (a) S_0 , (b) S_1 , (c) S_2 , (d) S_3 and (e) S_4 samples in selected temperature range

The values of T_g for all of the PEMA-EMITFSI electrolytes are listed in Table 4.2. The results shown in Table 4.2 indicate that the T_g value decreases with increasing content of EMITFSI. Similar trend could also be observed for melting point values (T_m) and their corresponding heat of fusion (ΔH_m). ΔH_m values were calculated from the area under the melting peak in DSC curves. The decrease in T_g upon addition of ionic liquid is due to dissolved ion accommodated in the PEMA phase (Cai et al., 1992). The enthalpy of polymer electrolytes (ΔH_m) is directly proportional to the degree of crystallinity of all samples. ΔH_m is found to decrease with increasing EMITFSI concentration suggesting that the relative degree of crystallinity, (χ_c) is also decreased. It is believed that IL molecules trapped in PEMA matrix, interrupted polymer-polymer

interaction either by occupying or increasing inter and intra-chain separations, disordered the original polymer crystalline structure and caused reorganization of polymer chains (Bandara et al., 1998). The increase of IL content in PEMA matrix results in greater disordering of crystalline structure and disordering of polymer chains which in turn enhance amorphousness of the PEMA-EMITFSI films. This observation is consistent with that of surface morphological study.

Table 4.1: DSC results of PEMA-EMITFSI electrolytes

Samples	T_g (°C)	T_m (°C)	Heat of fusion of sample, ΔH_m (J g ⁻¹)
S ₀	70	293	131.2
S ₁	69	290	119.1
S ₂	66	289	98.4
S ₃	60	287	53.6
S ₄	58	282	51.5

4.5 Thermal Analysis

Figure 4.7 presents TGA curves of the samples S₀, S₂ and S₄. It can be clearly seen that the samples containing EMITFSI (S₂ and S₄) start complete decomposition at 300 °C. This indicates that the samples are stable up to that temperature. In PEMA (S₀), three decomposition peaks could be observed from the thermogram. For the first stage of decomposition process (1st T_d), PEMA underwent minimal weight loss at lower temperatures (5 %) which is believed to originate from the evaporation of solvent

before showing a drastic weight loss (78 %) at 250 °C (2nd T_d). Above 250 °C, PEMA underwent the second decomposition up to ~ 420 °C, leaving about 18 % of residue. The decomposition that occurred above this temperature is due to the decomposition of polymer backbone (Fares, 2012). According to Fares *et al.*, (Fares, 2012) the decomposition occurred at 230 °C is attributed to elimination of evaporated molecules in the side groups of PEMA, and the decomposition at 230-400 °C is due to quaternized graft chain degradation.

Meanwhile, the weight loss that occurred at 350 °C and 410 °C in the samples containing EMITFSI corresponds to thermal decomposition of EMITFSI (~ 358 °C) (An et al., 2011; Feng et al., 2012). Based on the data mentioned earlier, it can be concluded that the addition of EMITFSI into the PEMA matrix significantly improves the heat-resistivity to make it stable up to 300 °C compared with pure PEMA (S_0) that started to decompose by rapid weight loss at an approximate temperature of ~250 °C.

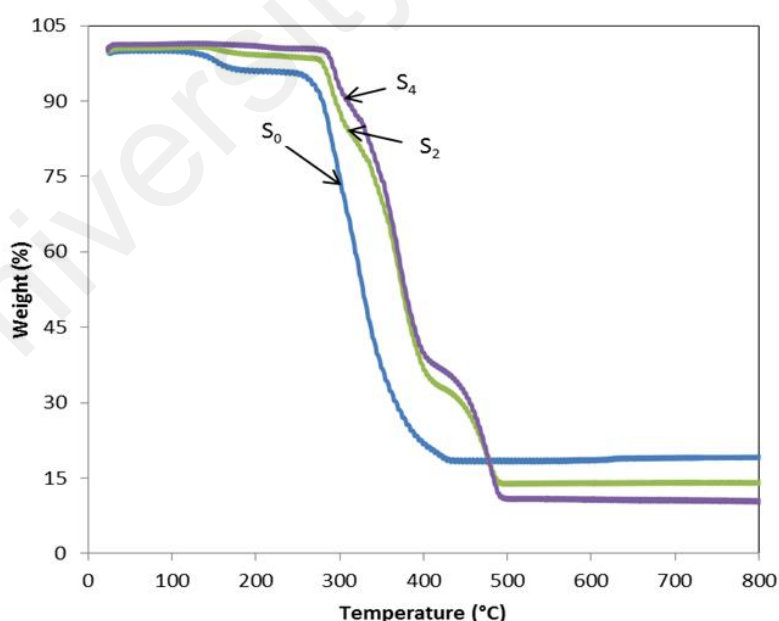


Figure 4.7: TGA thermograms in the heating run up to 800 °C for (i) S_0 , (ii) S_2 and (iii) S_4 films

4.6 Ionic Conductivity Studies

Bulk conductivity (σ) of the samples was evaluated using complex impedance technique. Figure 4.8 displays typical complex impedance spectra for (a) S_0 and (b) S_2 films represented in Nyquist (or Cole-Cole) plot. From the Cole-Cole plot with the horizontal and vertical axes having the same scale, a semicircle corresponding to the bulk resistance, R_b was obtained. The ionic conductivity of PEMA with varying concentrations of EMITFSI, having a thickness in the range 0.1 mm-0.2 mm, are shown in Table 4.3. As the EMITFSI content increases, a dramatic increase in the ionic conductivity is observed. As reported by Chaurasia *et al.*, 2013 (Chaurasia *et al.*, 2014), when IL content increases, the number of charge carriers (n) increases. Furthermore, ionic mobility (μ) is expected to increase due to the enhancement of amorphousness of the sample. As a result, the conductivity ($\sigma = n.e.\mu$) should normally increase with increasing IL content.

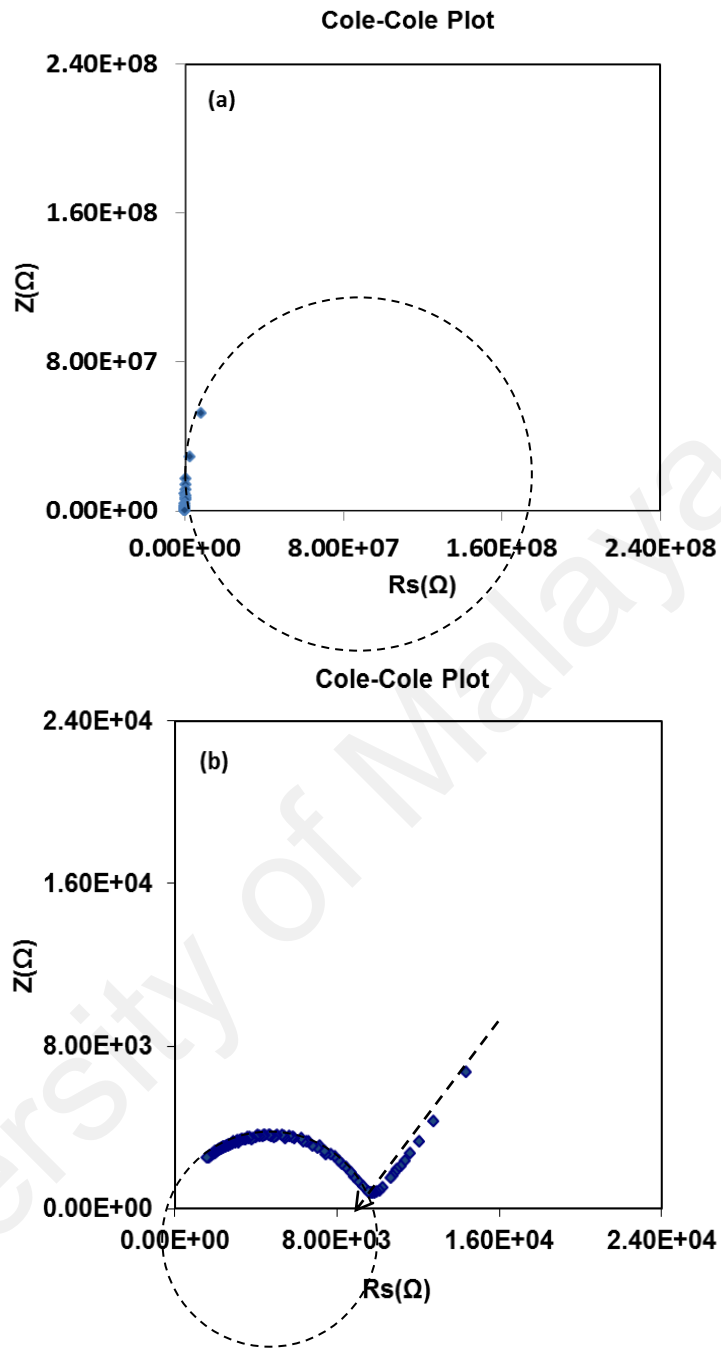


Figure 4.8: Cole-cole plots for (a) S_0 and (b) S_4

Table 4.3: Average conductivity of PEMA incorporated with different compositions of EMITFSI

Samples	Conductivity (S cm ⁻¹)	Standard deviation (S cm ⁻¹)
S ₀	3.75×10^{-11}	7.54×10^{-12}
S ₁	9.23×10^{-11}	2.39×10^{-12}
S ₂	3.00×10^{-10}	9.16×10^{-11}
S ₃	4.74×10^{-9}	2.66×10^{-10}
S ₄	5.41×10^{-7}	7.57×10^{-8}

Figure 4.9 presents the relationship between ionic conductivity of the studied polymer electrolytes as a function of temperature for different contents of ionic liquid over the temperature range from 30 to 100 °C. The Arrhenius natured type of samples underwent enhancement in ionic conductivity with rise in temperature indicating that the ionic transport promoted by the hopping of ionic charge species is predominant. The presence of IL probably promotes a better separation of polymeric chains and consequently, their more pronounced movements (Leones et al., 2012). Activation energies, E_A were calculated using the Arrhenius formula, equation (2.1).

The activation energies, E_A for the set of tested samples were calculated using the slope of the Arrhenius plot with regression value $R^2 \sim 1$. The E_A value increases from 0.24 eV to 0.76 eV for samples containing 10 and 20 wt.% EMITFSI. However, the calculated E_A values are 0.76 eV, 0.74 eV and 0.69 eV for samples S₂, S₃ and S₄, respectively. The decrease of E_A value with IL content is in a good agreement with the fact that the

amount of ions in polymer electrolyte increases, and the energy barrier to the ion transport decreases, leading to a decrease in the activation energy (Leones et al., 2012). The highest conductivity is obtained for sample S₄ with the value $5.41 \times 10^{-7} \text{ S cm}^{-1}$ at 30 °C and $9.75 \times 10^{-5} \text{ S cm}^{-1}$ at 100 °C.

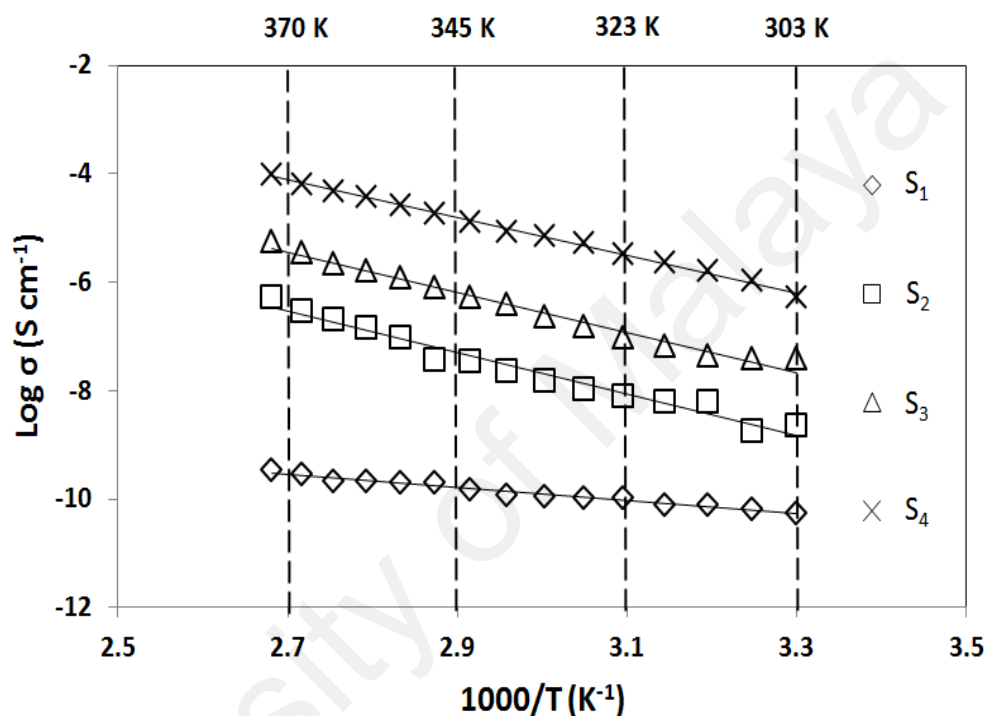


Figure 4.9: Arrhenius plot for films S₁, S₂, S₃ and S₄

4.7 Electrochemical stability determination

Electrochemical stability was investigated for the highest conducting PEMA-EMITFSI electrolyte (S₄). The room temperature electrochemical stability window for the sample was analyzed using the LSV at a scan rate of 1 mV s^{-1} in the potential range of 0 to 5 V. The result is shown in Figure 4.10. From the plot of current versus voltage, current flow is almost constant at low voltage range. The current gradually increases with increasing

applied voltage and reaches a breakdown voltage at 2.8 V. It is evident that PEMA-40 wt. % EMITFSI possessed a reasonable wide electrochemical stability window.

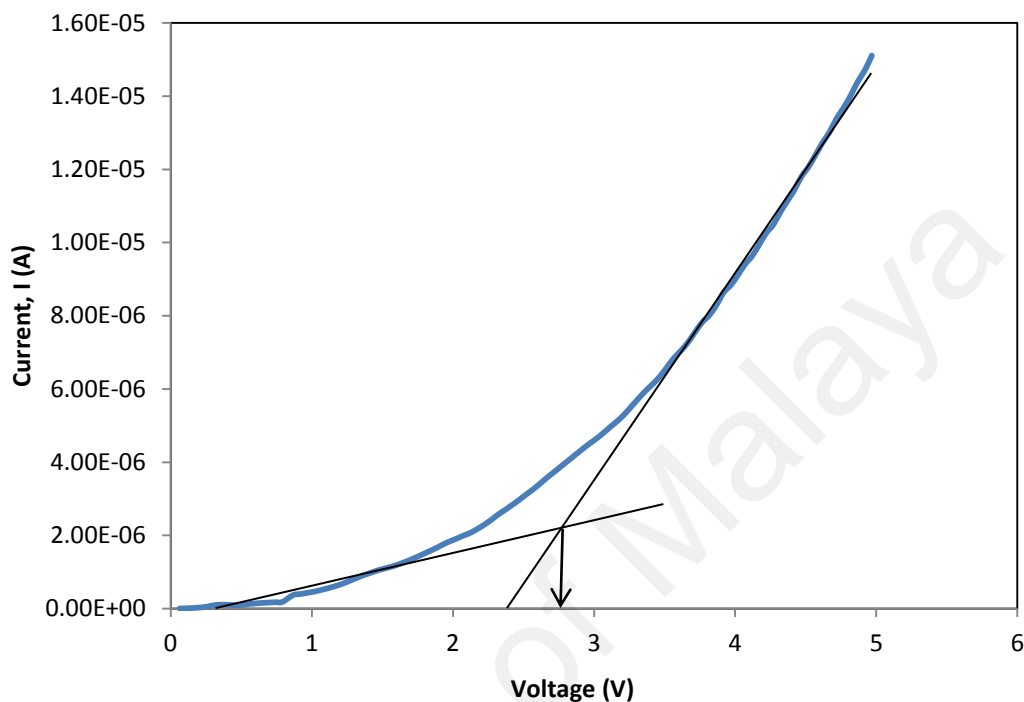


Figure 4.10: Linear sweep voltammogram for sample S₄

4.8 Summary

The effects of EMITFSI ionic liquid on PEMA were investigated. The solid polymer electrolyte films produced were flexible, free standing and transparent. Structural, thermal, morphological, electrical and electrochemical stability studies were performed. FTIR spectroscopic studies showed the interaction between PEMA and EMITFSI, as indicated by significant changes of the bands of all samples. The observed T_g and T_m from DSC were found to decrease as EMITFSI increased. The increase of amorphous fraction upon doping with increasing EMITFSI was clearly seen from SEM images. The addition of EMITFSI in PEMA matrix also improved the thermal stability of the

polymer electrolytes. Room temperature conductivity of the samples was found to increase up to four orders of magnitude when EMITFSI content was increased up to 40 wt.%. Temperature-dependent conductivity demonstrated that all samples obeyed Arrhenius behavior. Electrochemical stability studies using linear sweep voltammetry showed that the highest conducting PEMA-EMITFSI electrolyte exhibited a breakdown voltage at 2.8 V. These results suggested that the incorporation of IL is an alternative way to produce PEMA based polymer electrolytes with reasonably good properties.

University of Malaya

CHAPTER 5

RESULTS OF PEMA-EMITFSI-MgTf₂ ELECTROLYTES SYSTEM

5.1 Introduction

In the second part of the present work, the effects of EMITFSI ionic liquid and MgTf₂ salt on PEMA were investigated. For this purpose, PEMA was incorporated with different wt.% of EMITFSI and MgTf₂. The effects of different amounts of MgTf₂ and EMITFSI on structural, morphological, thermal, conductivity, cationic transport number and electrochemical stability of PEMA-EMITFSI-MgTf₂ complex are presented in the following sections. Table 5.1 lists the composition of polymer electrolyte samples and their designations.

5.2 FTIR Results

FTIR spectroscopic measurements were carried out to investigate the interaction between the constituents in the polymer electrolyte materials. Figure 5.1 presents the FTIR spectra for pure PEMA, PEMA-EMITFSI and PEMA-EMITFSI-MgTf₂. The peak of ~3400 cm⁻¹ of the -OH stretching caused by the absorbed water in air is not observed for all samples meaning that the samples are dried. This property of magnesium ion conducting polymer electrolytes is important to be analyzed in order to ensure the formation anhydrous electrolyte to prevent oxidation and passivation of the Mg anode in magnesium batteries application.

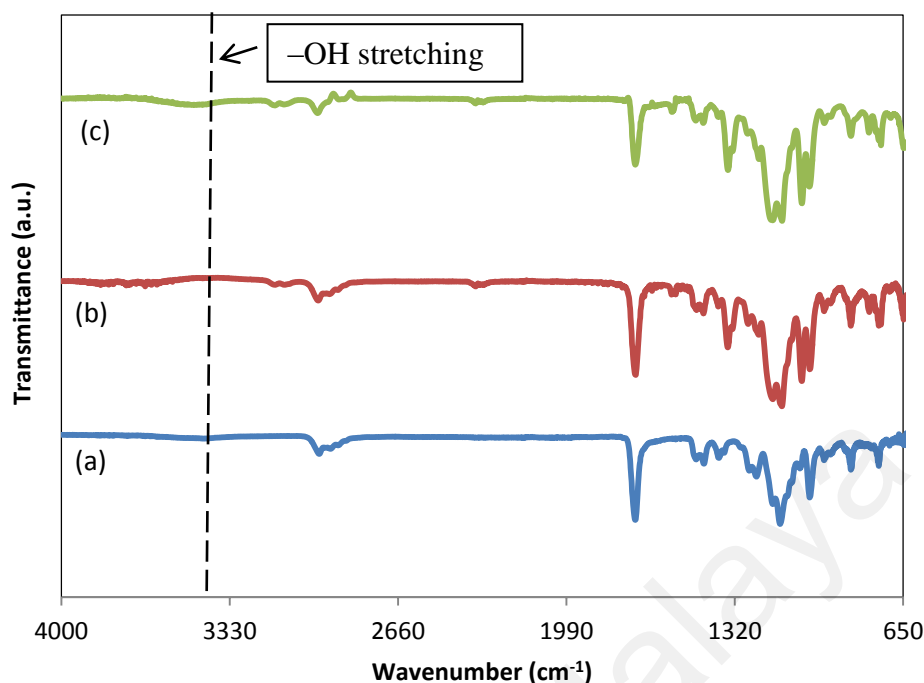


Figure 5.1: FTIR spectra in the region between 650 and 4000 cm^{-1} for (a) pure PEMA, (b) PEMA-EMITFSI and (c) PEMA-EMITFSI-MgTf₂

Figure 5.2 shows the bands of particular interest for PEMA that can possibly imply interaction between EMITFSI and MgTf₂ are: (1) asymmetric stretching vibration of C-O-C bond at 1144 cm^{-1} , (Sim et al., 2012) (2) asymmetrical O-C₂H₅ bending at 1445 cm^{-1} (Fahmy et al., 2001; Rajendran et al., 2008) and (3) the carbonyl stretching at 1720 cm^{-1} (Fahmy et al., 2001; Rajendran et al., 2008) The lone pair electrons on the oxygen atoms in PEMA can be electrostatically attracted to the positively charged (i.e. EMI⁺ and Mg²⁺) from ionic liquid and magnesium salt. The downshift of the bands from 1144 cm^{-1} in pure PEMA to 1135 cm^{-1} in PEMA-EMITFSI-MgTf₂ is due to the coordination of ether oxygen with the cation of the salt and ionic liquid. Furthermore, the upshift trend observed for the band at 1445 cm^{-1} in pure PEMA to 1448 cm^{-1} in PEMA-EMITFSI-MgTf₂ and the decreasing of relative intensity of the band at 1718 cm^{-1} upon addition of MgTf₂ content in PEMA-EMITFSI are other supporting evidences that illustrate the formation of PEMA-EMITFSI-MgTf₂ complexes. However, the shifted

bands are not obviously observed between PEMA-EMITFSI and PEMA-EMITFSI-MgTf₂, compared to pure PEMA with PEMA-EMITFSI. This suggests that the interaction is mainly due to the EMI⁺ (from EMITFSI) with PEMA, not Mg²⁺ (from MgTf₂) with PEMA.

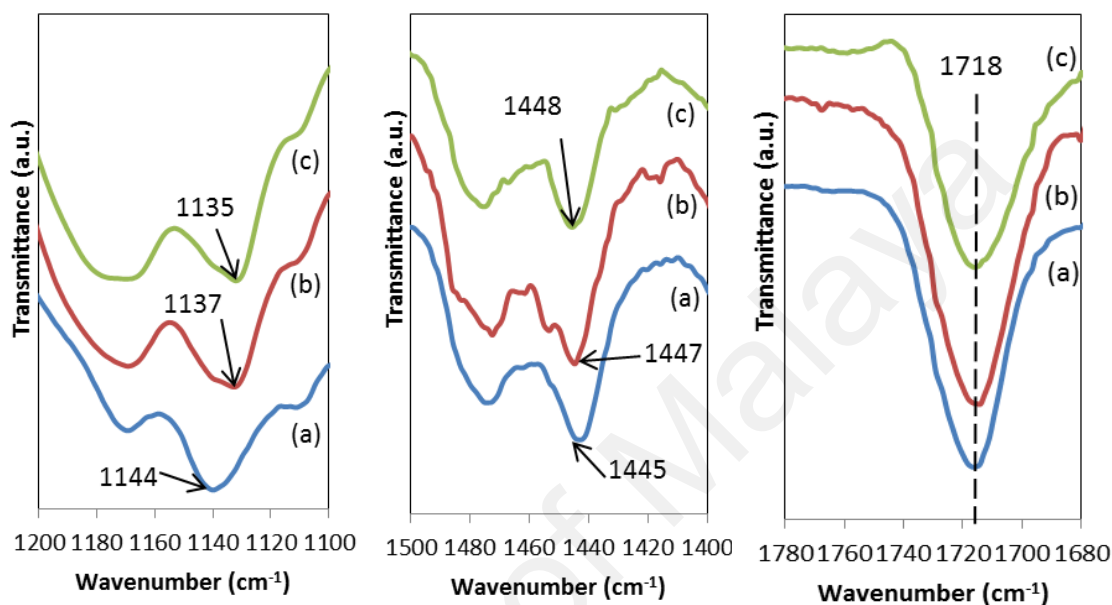


Figure 5.2: FTIR spectra in the region between 1100 and 1200 cm⁻¹, 1400 and 1500 cm⁻¹ and 1680 and 1780 cm⁻¹ for (a) pure PEMA, (b) PEMA-EMITFSI and (c) PEMA-EMITFSI-MgTf₂

5.3 SEM Analysis

To investigate the effect of magnesium salt addition on the PEMA-EMITFSI complex, the morphological studies have been carried out by SEM. Figure 5.3 shows the SEM cross-sectional micrographs of S₁, S₂ and S₃ films. From Figure 5.3 (a), it can be seen that S₁ film possessed a rough surface by the appearance of dark boundaries region. The smoothness of the surfaces for sample S₂ indicates the increase of amorphous fraction of the sample. This can be correlated to the lower glass transition temperature obtained for sample S₂, discussed in the next section. According to Monikowska *et al.*

(Zygadło-Monikowska et al., 2007), the bright region in the SEM image represents the crystalline phase of PEs system. The light grey region observed in S_3 suggests the amorphousness of the sample decreases upon addition $MgTf_2$ content. This observation of the SEM images suggests the existence of intermolecular interactions between the oxygen atom in PEMA with Mg^{2+} and EMI^+ from $MgTf_2$ and EMITFSI. The result is consistent with the result of FTIR study discussed earlier.

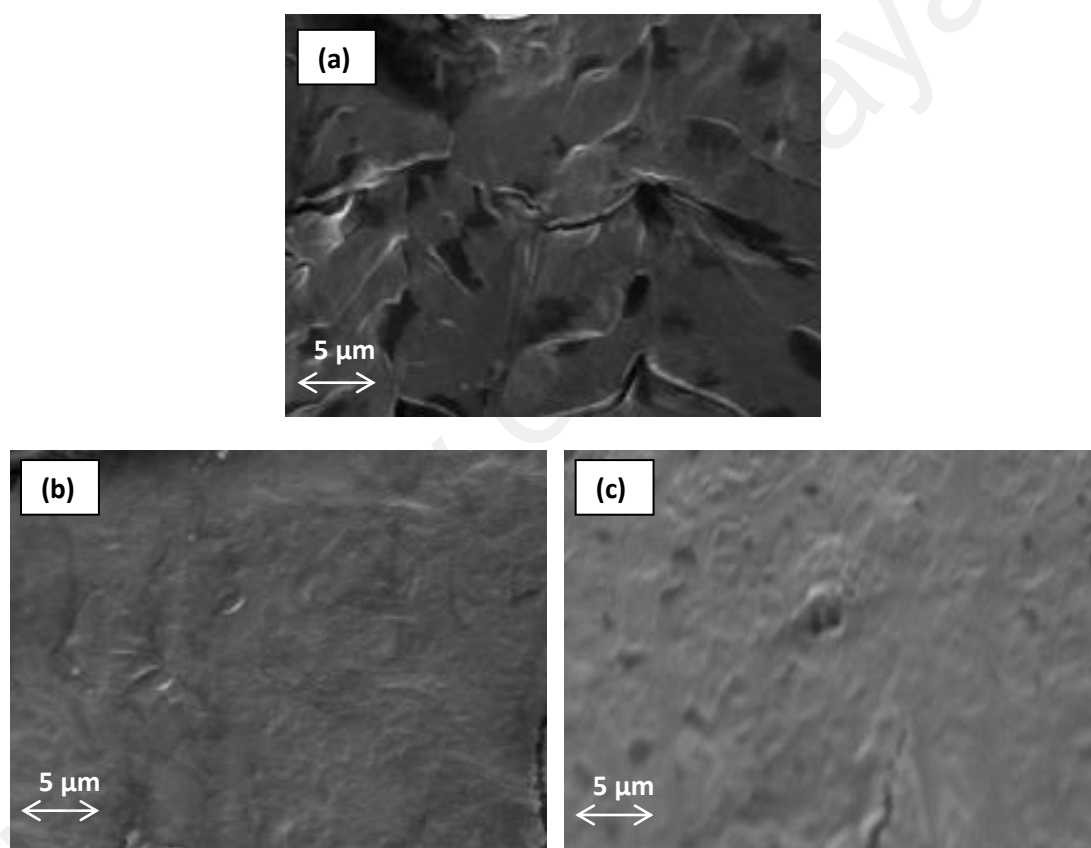


Figure 5.3: SEM micrographs for (a) S_1 (b) S_2 and (c) S_3

5.4 Thermal Analysis (DSC)

DSC has been carried out on the sample S_1 , S_2 and S_3 to determine their T_g . DSC curves of the films are shown in Figure 5.4. From previous work, (Zain et al., 2015) T_g for pure

PEMA and PEMA – 30 wt.% EMITFSI was observed to be 70 °C and 69 °C, respectively. In this work, T_g for S_1 , S_2 and S_3 are observed to be 59 °C, 56 °C and 58 °C, respectively. It can be seen that the T_g shifts to lower temperature upon addition of EMITFSI and MgTf₂. The decrease in T_g upon addition of EMITFSI is due the presence of more ionized [EMI⁺] [TFSI] particles in the matrix which in turn increasingly plasticize the PEMA matrix. Meanwhile, the increasing MgTf₂ doping decreases the T_g values. This may be due to the accommodation of dissolved ion into PEMA (Cai et al., 1992). The lowest T_g is obtained for sample S_2 . The lower the T_g , the higher the flexibility of polymer backbone.

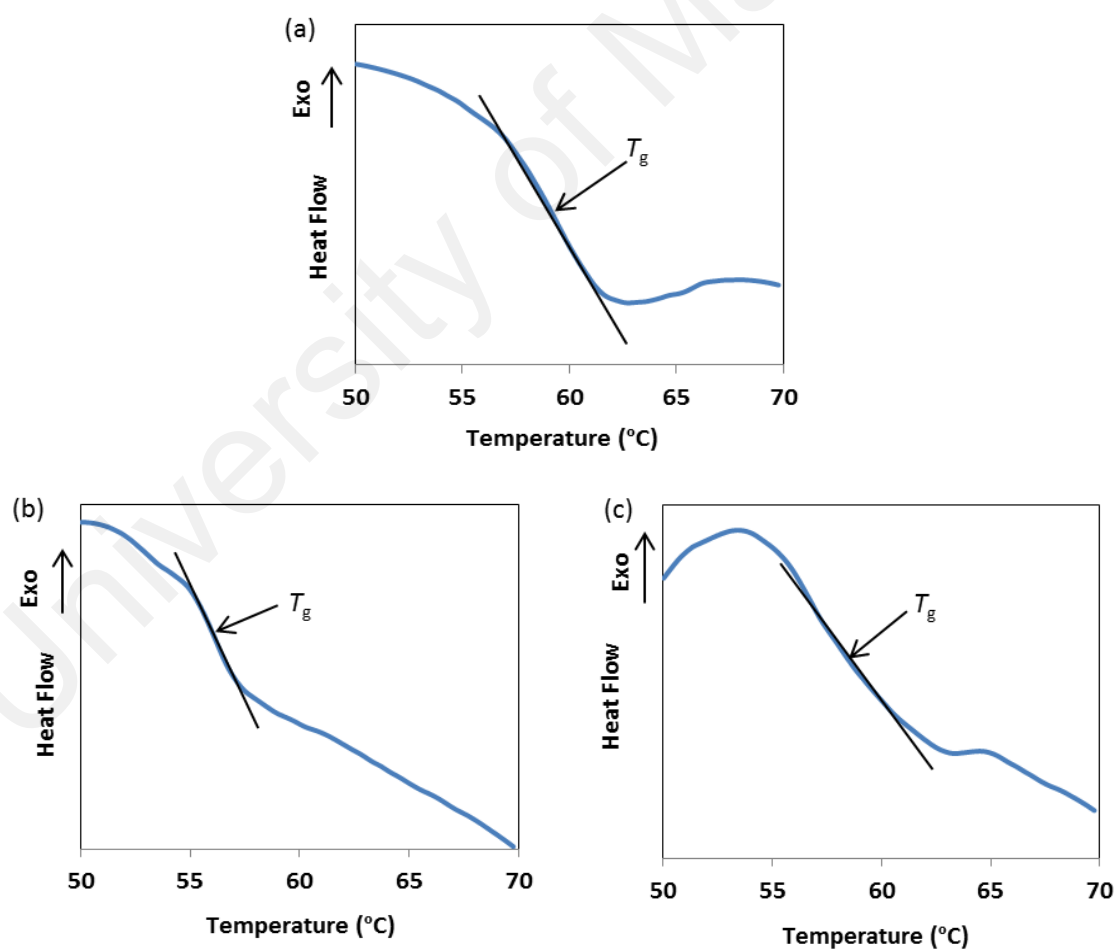


Figure 5.4: DSC thermograms in the temperature range from 50 to 70 °C for (a) S_1 , (b) S_2 and (c) S_3

5.5 Ionic Conductivity Studies

In this research work, in order to study the composition dependence of magnesium salt and the ionic liquid with the ionic conductivity, PEMA-based electrolytes were prepared by varying the amount of MgTf_2 and EMITFSI.

Figure 5.5 depicts the variation of conductivity of PEMA-based electrolytes film as a function of MgTf_2 and EMITFSI concentration. The variation in conductivity with MgTf_2 and EMITFSI content may be attributed to the: (1) concentration of amorphous fraction, (2) concentration of mobile cations and (3) concentration of additional transit sites (Ramesh et al., 2014).

From Figure 5.5, Region 1 shows that the ionic conductivity of all samples dramatically increases as MgTf_2 and EMITFSI content increases. Generally the conductivity enhancement in this region can be rationalized by two reasons: (1) the increase in salt content that increases the number of charge carriers which contributes to ionic conductivity, (2) the increase in ion mobility due to enhanced polymer segmental motion of the host polymer upon addition of EMITFSI as indicated by the decrease of T_g mentioned earlier.

Beyond 20 wt.% of MgTf_2 , Region 2, the ionic conductivity is observed to decrease. For PEMA – 30 wt.% MgTf_2 – 10 wt.% EMITFSI and PEMA – 30 wt.% MgTf_2 – 20 wt.% EMITFSI, the decrease in conductivity is possibly accounted for the low availability of co-ordination sites which slows down Mg^{2+} ions migration. Another reason is due to the presence of neutral ion multiples upon conglomeration of excess ionized EMITFSI particles in PEMA matrix, which block the conducting pathways

(Anantha & Hariharan, 2005; Winie et al., 2009). The blockage is due to the neutral aggregates impose strong repelling force on the mobile Mg^{2+} ions which consequently restricts their transportation and hence reduce the ionic conductivity (Tejedor et al., 2007).

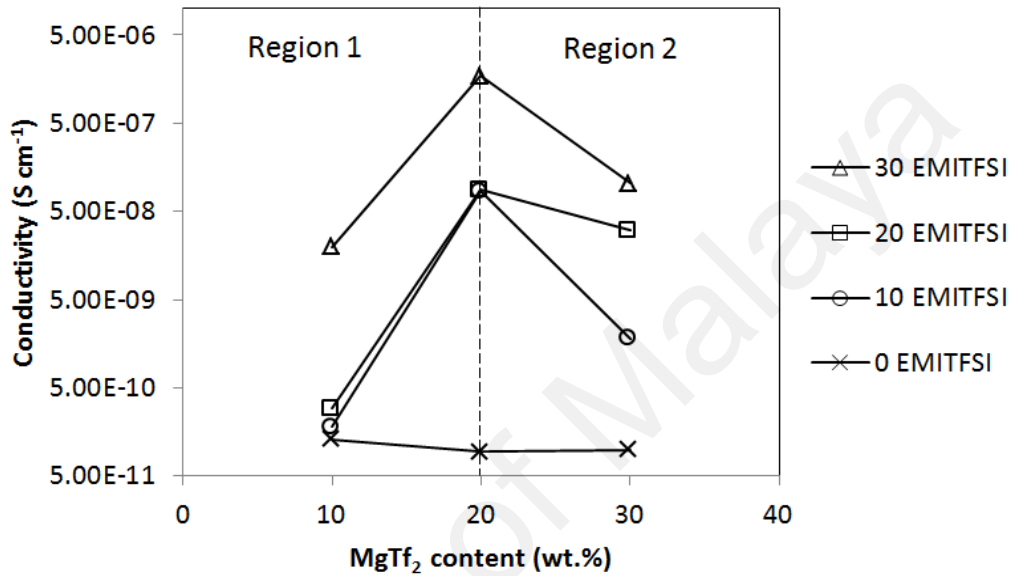


Figure 5.5: Variation of ionic conductivity with content of EMITFSI and MgTf_2

The temperature-dependent plot for sample S1, S2 and S3 as depicted in Figure 5.6 showed that the ionic conductivities increases with temperature from 298 K to 373 K indicating that temperature helps to dissociate salt and produces more free magnesium ions. Sample S1 and S3 show the regression value $R^2 \sim 1$. However, the plot for sample S2 displays two linear sections with regression values, $R^2 \sim 0.96$ below 323 K and $R^2 \sim 0.97$ above 323 K. Activation energies, E_A were calculated from the slope of the Arrhenius plot using the equation (2.1).

The calculated E_A values for sample S1 and S3 are 0.56 eV and 0.49 eV, respectively. For sample S2, the values are 0.86 eV for temperature below 323 K and 0.26 eV for temperature above 323 K. Higher E_A value obtained at temperature 323 K and below indicates that more energy is required to start the hopping mechanism between

coordinating sites available in the polymer matrix (Sim et al., 2012). The change in E_A around 323 K (50 °C) is attributed to a phase transition where the polymer matrix undergoes a phase transition from glassy to rubbery phase. The result is consistent with the DSC.

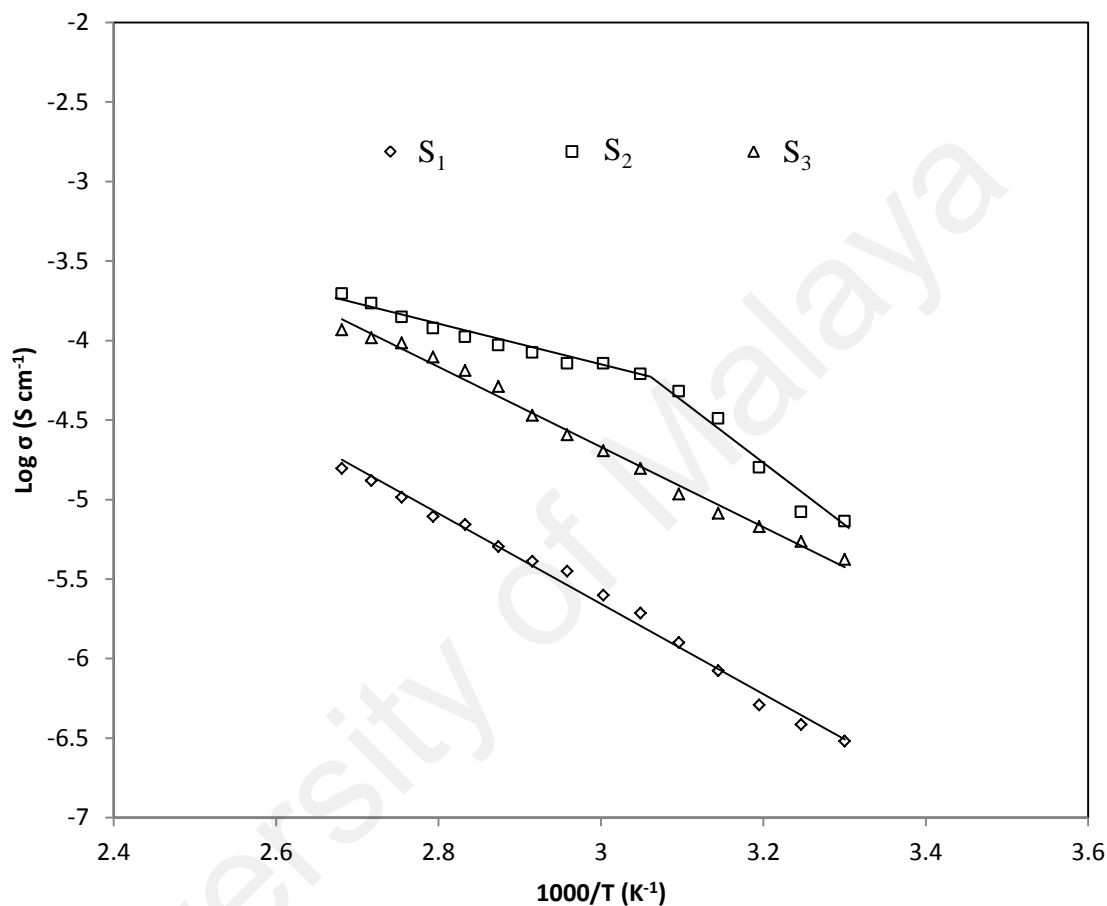


Figure 5.6: Arrhenius plot for films S₁, S₂ and S₃

5.6 Magnesium Transference Number

In the system of ionic liquid and salt incorporated PEMA complexes, four types of charge carriers; namely Mg^{2+} , EMI^+ , Tf^- and $TFSI^-$ are expected to conduct. However, the contribution of each charged specie to the total ionic conductivity is difficult to evaluate. In 1987, Evans *et al.* (Evans et al., 1987) has proposed the combination of a.c

and d.c technique to evaluate cation transport number (T^+). The magnesium-ion transference number ($T_{Mg^{2+}}$) was calculated using Bruce and Vincent method (Bruce & Vincent, 1987) according to the equation (3.18).

Figure 5.7 (a) shows the polarization current graph as a function of time. Figure 5.7 (b) presents the impedance plots before and after polarization for the Mg|electrolyte|Mg cell fabricated using sample S2 and the data derived from the figures are tabulated in Table 5.2.

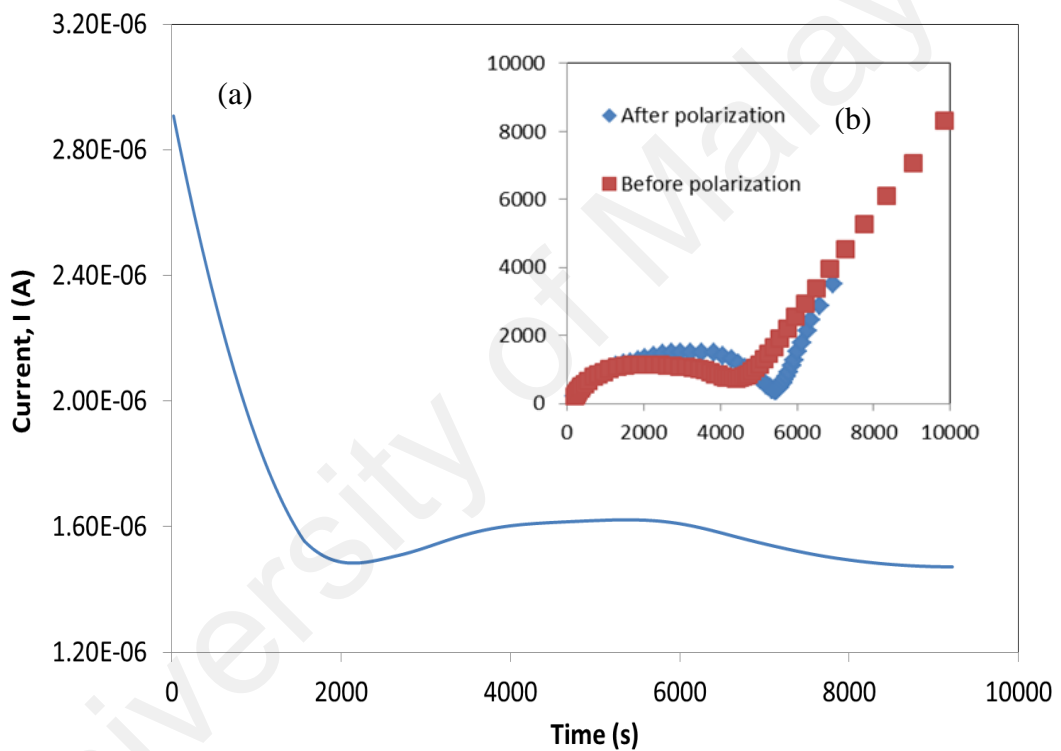


Figure 5.7: (a) Current-time curve and (b) impedance plots before and after polarization for the Mg|S2|Mg cell

Table 5.1: The value of Mg|S2|Mg cell during transference number measurement

Sample	$I_o(A)$	$I_{ss}(A)$	$R_o(\Omega)$	$R_{ss}(\Omega)$	$T_{Mg^{2+}}$
S ₂	3.56×10^{-6}	1.62×10^{-6}	4476	5571	0.40

As seen from Table 5.2, the value of $T_{\text{Mg}^{2+}}$ is found to be 0.40 at room temperature. The value of Mg^{2+} ion transport number in this work was found to be slightly higher than that reported by Asmara *et al.* (Asmara *et al.*, 2011) and Osman *et al.* (Osman *et al.*, 2014) for polymer-based electrolyte containing MgTf_2 . In their work, they obtained Mg^{2+} ion transport number of 0.37 and 0.38, respectively.

5.7 Electrochemical stability determination

The electrochemical stability of the polymer electrolyte was evaluated by LSV. Figure 5.8 (a) and (b) illustrate linear sweep voltammogram of PEMA – 20 wt.% MgTf_2 and PEMA-30 wt.% EMITFSI-20 wt.% MgTf_2 , respectively. The cathodic and anodic decomposition occurred at – 3.03 V and +2.83 V for PEMA – 20 wt.% MgTf_2 and – 4.19 V and +3.74 V for PEMA-30 wt.% EMITFSI-20 wt.% MgTf_2 . This suggests a voltage stability window for PEMA-30 wt.% EMITFSI-20 wt.% MgTf_2 at ambient temperature is up to 3.74 V which is higher than 2.83 V for PEMA – 20 wt.% MgTf_2 . Asmara *et al.* (Asmara *et al.*, 2011) reported a decomposition voltage at 2.42 V for 40 wt.% poly methyl(methacrylate) (PMMA) and 60 wt.% of 0.4 M MgTf_2 in EC:DEC (2:1). PMMA and PEMA are methacrylic ester polymers; thus they exhibit the same dielectric constant values, ($\epsilon_r = 2.6$).^{33, 34} Upon inclusion of EMITFSI into the PEMA- MgTf_2 complexes, the electrolyte film is observed to stable up to 3.74 V. Therefore, it can be concluded that impregnation of ionic liquid enhances the electrochemical potential window.

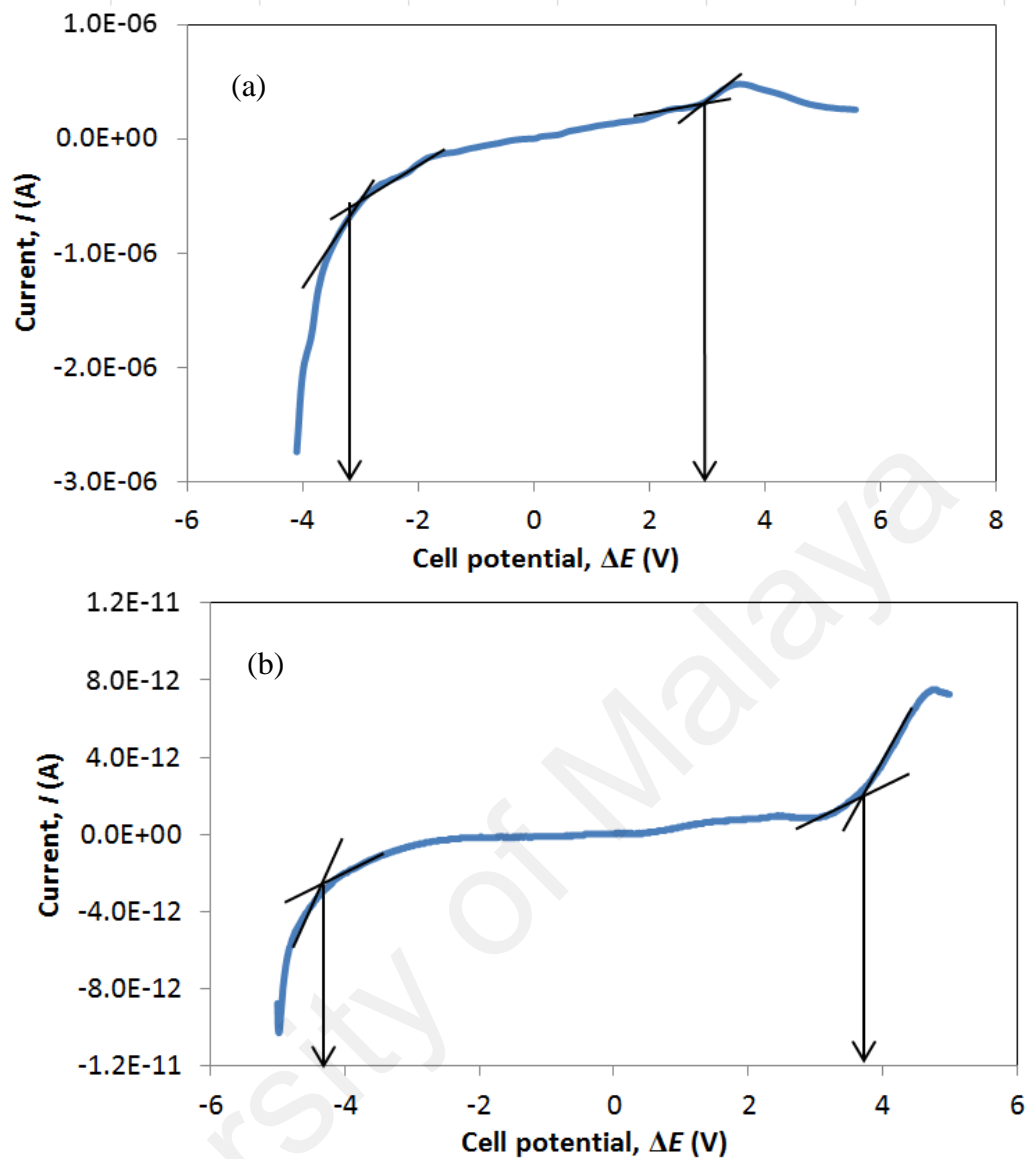


Figure 5.8: Linear sweep voltammogram for (a) PEMA – 20 wt.% MgTf₂ and (b) S₂ at room temperature

5.8 Summary

PEMA based electrolytes have been successfully prepared by incorporation of different amounts of EMITFSI and MgTf₂ using solution casting technique. The interaction between the constituents were confirmed by the shifts and decrease in intensity of significant bands of PEMA based electrolytes. The conductivity behaviour of the

PEMA – EMITFSI – MgTf₂ was attributed to the presence of EMITFSI and MgTf₂ that influenced the number of charge carriers and their mobility. The electrochemical potential window of the electrolytes was also enhanced substantially due to ionic liquid addition.

University of Malaya

CHAPTER 6

RESULTS OF PEMA-EMITFSI-MgTf₂-MgO ELECTROLYTES

SYSTEM

6.1 Introduction

In the previous chapter, PEMA – 30 wt.% EMITFSI – 20 wt.% MgTf₂ is found to exhibit reasonably good ionic conductivity. It is expected that higher ionic conductivity can be achieved if higher amount of EMITFSI is added. However, the addition of 40 wt.% EMITFSI into PEMA – 20wt.% MgTf₂ produced film with poor film stability. Therefore, in order to improve the film stability of this system, we dispersed different amounts of MgO nanopowder and study the film stability and physicochemical properties of the PEMA – EMITFSI – MgTf₂ nanocomposite polymer electrolytes (NCPEs). In the third part of the present work, the effects MgO nanofiller to the physicochemical and ionic liquid retention properties of PEMA – MgTf₂ – EMITFSI NCPEs were investigated. Table 6.1 lists the composition of NCPE samples and their designations.



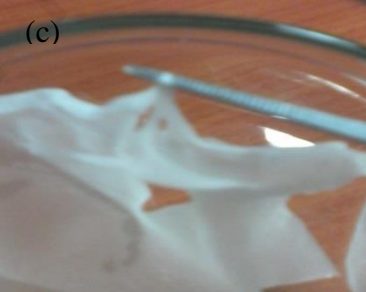
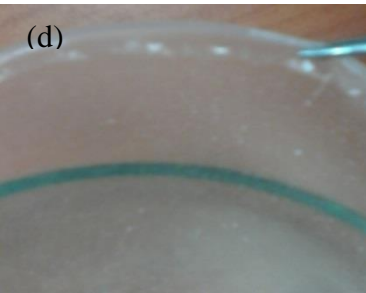
6.2 Retention property of ionic liquid improved by addition of MgO nanofiller

In Chapter 4, we have reported the preparation and characterization of PEMA based electrolytes by varying the amount of EMITFSI from 10 wt.% to 50 wt.%. However, PEMA – 50 wt.% EMITFSI could not produce free standing film due to high loading of ionic liquid in the PEMA system. The highest conducting sample was obtained for PEMA – 40 wt.% EMITFSI. In order to study the effects of both composition of ionic liquid as plasticizer and ionic salt as ion donors, PEMA – MgTf₂ – EMITFSI were

prepared by varying amount of both composition of EMITFSI and MgTf₂. The highest conducting sample was obtained for PEMA – 30 wt.% EMITFSI – 20 wt.% MgTf₂. The addition of more than 30 wt.% EMITFSI into PEMA – MgTf₂ system could not produce free standing film, Table 6.2(c), but is expected to enhance higher ionic conductivity. However, stable films of PEMA – 40 wt.% EMITFSI – 20 wt.% MgTf₂ have been successfully obtained (Figure 6.2(d)) by dispersing small amount of MgO nanofiller into the system which could be correlated to the improvement of ionic liquid retention property of NCPE films.

University of Malaya

Table 6.1: Film stability of PEMA NCPEs

Samples designation	Diagram
PEMA – 40 wt.% EMITFSI	
PEMA – 30 wt.% EMITFSI – 20 wt.% MgTf ₂	
PEMA – 40 wt.% EMITFSI – 20 wt.% MgTf ₂	
PEMA – 40 wt.% EMITFSI – 20 wt.% MgTf ₂ – 1 wt.% MgO	

6.3 SEM analysis

The cross-sectional surface micrographs of NCPE films recorded by SEM are shown in Figure 6.1. In this figure, MgO can be seen as white dots in the microstructure. The surface image for S1 and S2 looks smooth indicating the MgO nanoparticles are

uniformly dispersed in the PEMA matrix. However, it can be seen from Figure 6.1(c), the S3 film possessed a rough surface. White dots associated with the MgO particles are not homogeneously distributed in sample S3 and aggregated MgO nanoparticles can be seen.

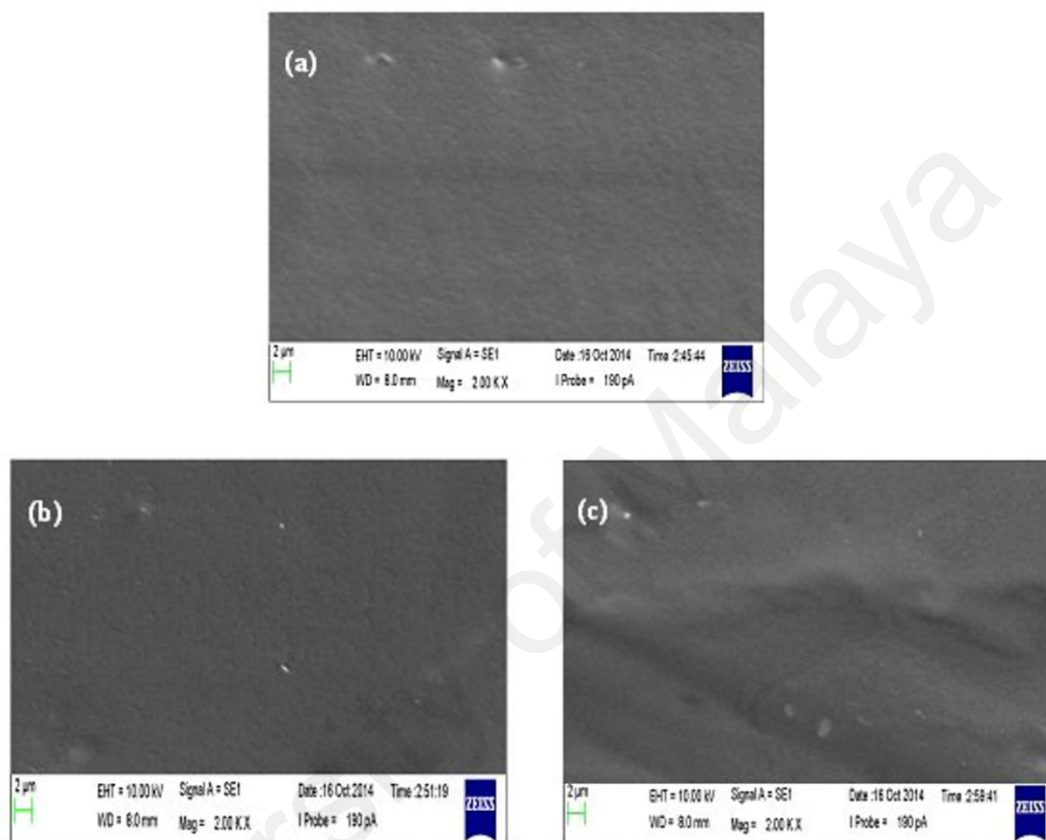


Figure 6.1: SEM micrographs for (a) S1 (b) S2 and (c) S3

6.4 Thermogravimetric analysis

TGA was carried out to investigate the thermal stability of NCPEs. TGA profiles of the sample S1, S2 and S3 are given in Figure 6.2 as a function of the nanofiller concentration. An initial weight loss of 2-7 % observed for all samples in the temperature range 40-140 °C (1^{st} T_d) is presumably due to the evaporation of low molecular weight species such as absorbed moisture, and residual solvent; i.e. THF used

in the electrolyte preparation. In the temperature range between 265-370 °C (2nd T_d) and 370-425 °C (3rd T_d), the samples show a significant weight loss of 45-48 % for S1 and S2 and ~ 40 % for S3 due to the decomposition of PEMA backbone (Fares, 2012). Degradation beyond 425-484 °C is most likely due to the thermal decomposition of EMITFSI (An et al., 2011; Feng et al., 2012). Above 484 °C, the residue (%) obtained from TGA data for the NCPEs follows the order; membrane containing 5 wt.% MgO (~29 %) > 0.5 wt.% and 1 wt.% MgO (~17 %). It can be inferred that the percentage weight loss is minimum for S3 showing that the influences of composition of MgO nanofillers to act as an insulating surface to prevent the heat from expanding quickly; thus, slows down mass loss rate of decomposition products.

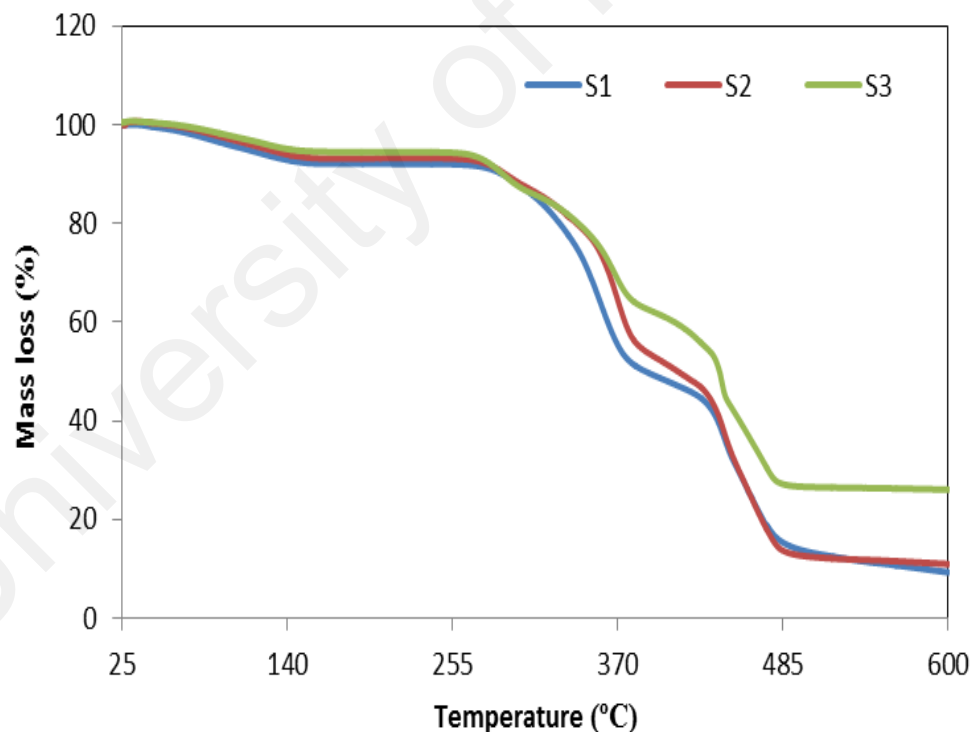


Figure 6.2: TGA thermograms in the heating run up to 600 °C for (a) S1 (b) S2 and (c) S3

6.5 Room Temperature Ionic Conductivity

The types of PEMA based electrolytes and their ambient ionic conductivities are listed in Table 6.3. The ionic conductivity slightly increases to one order of magnitude when 20 wt.% of MgTf₂ was added into PEMA – 30 wt.% EMITFSI system. The results indicate that the type of ion donors (Mg²⁺) has an influence to the ionic conductivity enhancements. Since PEMA – 40 wt.% EMITFSI – 20 wt.% MgTf₂ could not produce free standing film, a different amount of MgO nanofiller was added into the system in prior to improve the retention properties of ionic liquid of the system. The ionic conductivity was enhanced up to two orders of magnitude for PEMA – 40 wt.% EMITFSI – 20 wt.% MgTf₂ – 1 wt.% MgO compared to our previous study (Zain et al., 2015). Interestingly, this observation suggests that the role of nanofiller to the improvement of ionic liquid retention properties as well as ionic conductivity of NCPEs.

Table 6.2: Development of PEMA NCPEs

Samples designation	σ (S cm⁻¹) at ambient temperature	Ref.
PEMA – 40 wt.% EMITFSI	5.41×10^{-7}	(Zain et al., 2015)
PEMA – 30 wt.% EMITFSI – 20 wt.% MgTf ₂	1.72×10^{-6}	previous work
PEMA – 40 wt.% EMITFSI – 20 wt.% MgTf ₂	Could not be determined due to poor film stability	previous work
PEMA – 40 wt.% EMITFSI – 20 wt.% MgTf ₂ – 0.5 wt.% MgO	3.96×10^{-6}	present work

PEMA – 40 wt.% EMITFSI – 20 wt.% MgTf ₂ – 1 wt.% MgO	1.20×10^{-5}	present work
PEMA – 40 wt.% EMITFSI – 20 wt.% MgTf ₂ – 5 wt.% MgO	8.81×10^{-7}	present work

Figure 6.3 shows the dependence of ionic conductivity on temperature for NCPEs. The ionic conductivity increases with an increase in temperature for all samples. The results proved that higher temperature resulted in increasing number of charge carriers and faster ion movement. All curves in Figure 6.3 show regression value of ~ 1 , which indicates that the graphs are linear and conductivity can be said obeying Arrhenius thermal activated model from equation (2.1).

Therefore, the apparent activation energy (eV) for ions transport can be calculated and follows the orders S2 (0.46) < S1 (0.50) < S3 (0.57). The ionic conductivity value at 25 °C ($\times 10^{-5}$ S cm⁻¹) for NCPE follows the order S2 (1.20) > S1 (0.39) > S3 (0.08) as plotted in Figure 6.4.

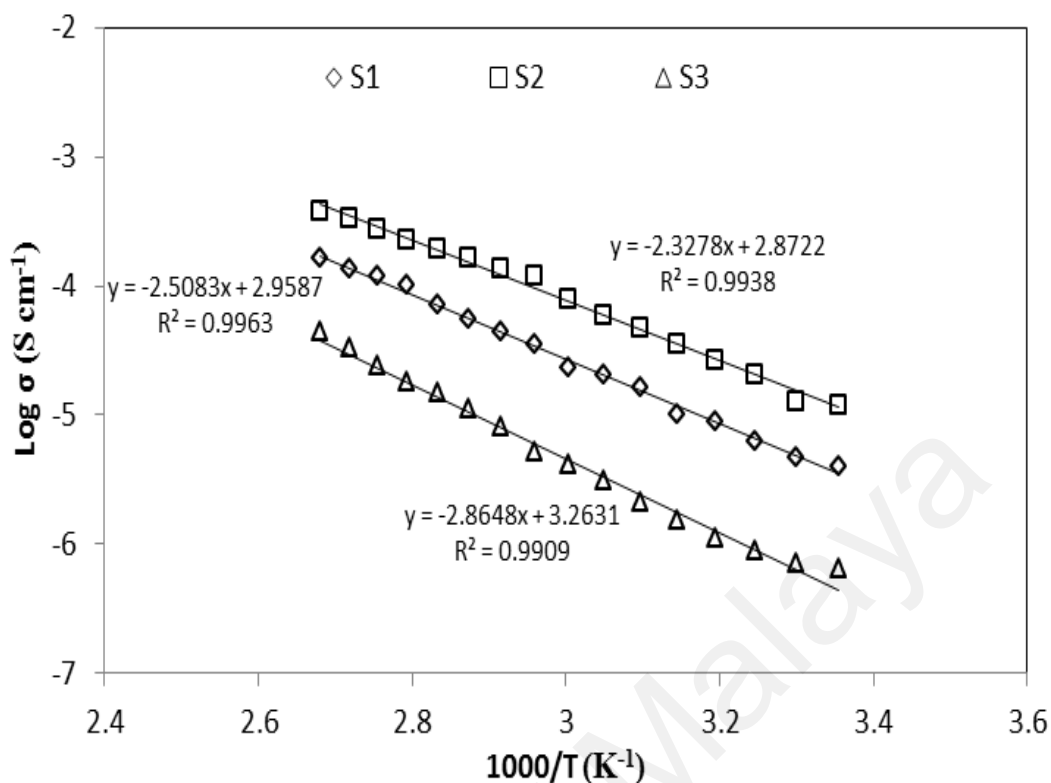


Figure 6.3: Arrhenius plot for films S1, S2 and S3

The ionic conductivity trend increases firstly with the amount of MgO nanopowder, and then decreases at 5 wt.% of MgO content over a wide temperature range even at lower temperatures. The addition of MgO nanofiller to the PEMA matrix creates space charge layer at the filler-polymer interface which assists in ion transport and the particle size of MgO may also influence the kinetics of PEMA chain which promotes localized amorphous regions and thus enhance the Mg^{2+} ions transport in the amorphous polymer electrolyte (Appetecchi et al., 2003; Appetecchi et al., 1999). However, the decrease in room temperature ionic conductivity for S3 probably due to the restriction of ionic motion. The higher filler content (5 wt.% MgO) possibly built up a continuous nonconductive phase and hence this electrically inert filler would blocked magnesium ions transport resulting in increase of total resistance of NCPEs (Kumar et al., 2007).

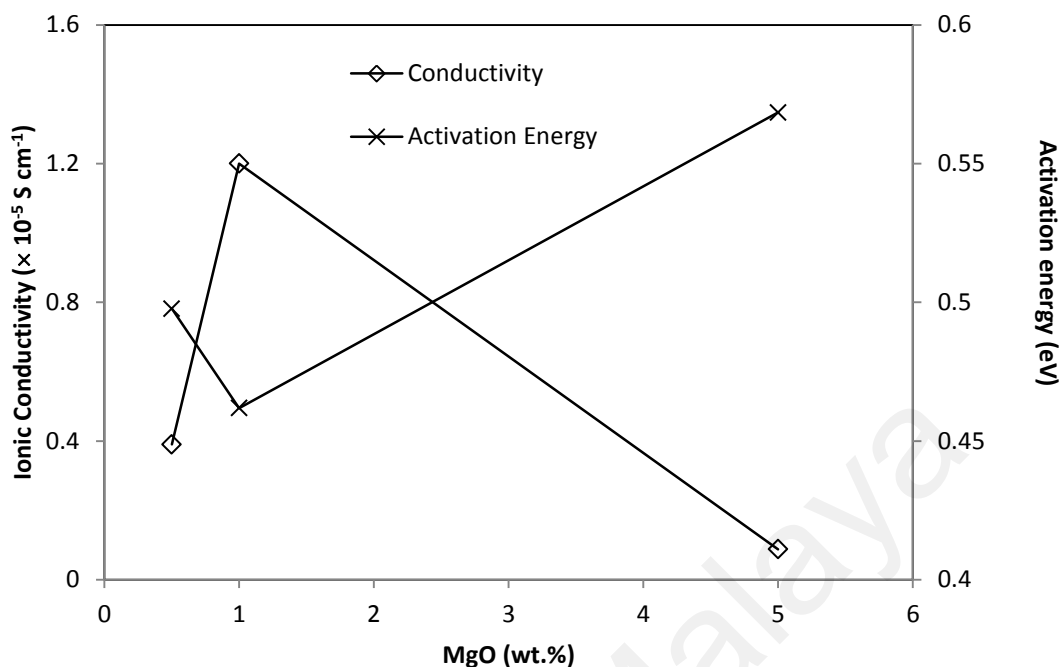


Figure 6.4: Variation of ionic conductivity and activation energy for films S1, S2 and S3 at 30 °C

6.6 Linear Sweep Voltammetric Analysis

According to our previous work (Zain et al., 2015), electrochemical stability window (ESW) obtained for PEMA – 40 wt.% EMITFSI was ~2.8 V. From LSV curve shown in Figure 6.5, the cathodic and anodic decomposition of S2 occurred at – 4.1V and +3.4 V. This suggests a voltage stability window for S2 is up to ~3.4 V which is slightly higher compared to previous system. As reported by Takeshi et al. (Kakibe et al., 2010), the appearance of magnesium deposition/desolution peak in LSV curve demonstrated that magnesium effectively migrating through electrolytes. However, the peaks associated to magnesium are not observed in Figure 6.5. It is presumably the Mg^{2+} was not predominantly factor that contributed to the ionic transport migration in NCPE.

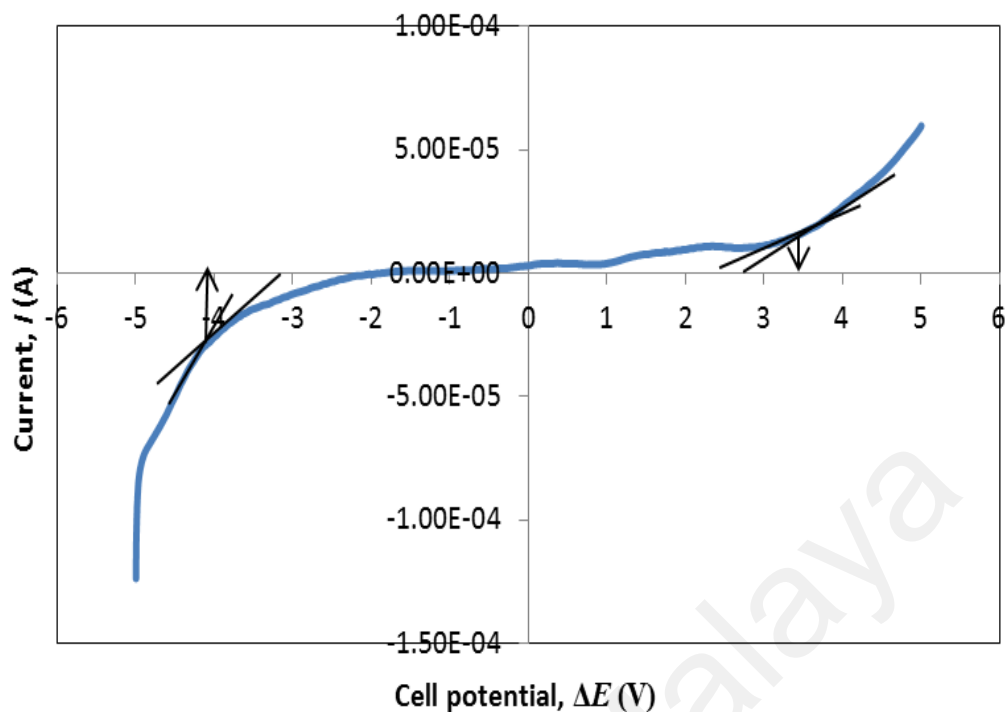


Figure 6.5: Linear sweep voltammogram for S2 at room temperature

6.7 Summary

PEMA based NCPEs have been successfully prepared by incorporation of different amounts of MgO nanofiller into PEMA-40 wt.% EMITFSI-20 wt.% MgTf₂ using solution casting technique. SEM analysis revealed the presence of dispersion of homogeneous nanosized MgO particles was observed in S1 and S2. TGA curves revealed that the larger amount of MgO in NCPE slowed down mass loss rate of decomposition products. The increase in ionic conductivity was consistent with the decreasing of activation energy obtained from Arrhenius-model, as well as retention properties of ionic liquid has been improved. The electrochemical potential window for the highest conducting sample, S2 suggested that magnesium ion was not predominantly factor to the ionic conductivity enhancement of NCPE.

CHAPTER 7

CONCLUSIONS AND SUGGESTIONS FOR FUTURE WORK

7.1 Conclusions

In this study, all objectives have been achieved. Three types of free standing PEMA based electrolyte films which are PEMA-EMITFSI, PEMA-EMITFSI-MgTf₂, and PEMA-EMITFSI-MgTf₂-MgO were successfully prepared using solution casting technique. The physicochemical properties of all samples have been investigated using FTIR, SEM, DSC, TGA, EIS and LSV. The highest conducting sample with the respective composition for all three systems were identified as $9.23 \times 10^{-11} \text{ S cm}^{-1}$ (PEMA – 40 wt.% EMITFSI), $1.72 \times 10^{-6} \text{ S cm}^{-1}$ (PEMA – 30 wt.% EMITFSI – 20 wt.% MgTf₂), and $1.20 \times 10^{-5} \text{ S cm}^{-1}$ (PEMA – 40 wt.% EMITFSI – 20 wt.% MgTf₂ – 1 wt.% MgO), respectively at room temperature.

From the results obtained in this work, it can be concluded that:

The optical properties of PEMA – EMITFSI films using FTIR showed that the interaction between PEMA and EMITFSI by the shifting of particular bands in PEMA with addition of different amount of EMITFSI in PEMA solution. The influences of EMITFSI to the thermal properties of PEMA have also been observed using DSC and TGA. The decrease in T_g , T_m , χ_c from DSC analysis as EMITFSI increased could be correlated with the increase of amorphous fraction that was clearly seen from SEM analysis. The addition of EMITFSI to the PEMA system was found to increase the ionic conductivity at room and elevated temperatures and also showed a reasonably wide electrochemical potential window.

FTIR spectroscopic study confirmed the interactions between the electrolyte constituents (i.e. Mg^{2+} and EMI^+) by the shifts and decrease in intensity of particular bands of PEMA. However, the shifted bands were not obviously observed between PEMA-EMITFSI and PEMA-EMITFSI- MgTf_2 , compared to pure PEMA with PEMA-EMITFSI. This suggested that the interaction was mainly due to the EMI^+ (from EMITFSI) with PEMA, not Mg^{2+} (from MgTf_2) with PEMA. Morphological study suggested that the amorphousness of the samples decreased upon addition MgTf_2 content. The conductivity behavior of the PEMA – EMITFSI – MgTf_2 films was attributed to the presence of both EMITFSI and MgTf_2 that influenced the number of charge carriers and their mobility. The ionic liquid has been found to give slightly higher magnesium transport number compared to other plasticizers. The electrochemical potential window of the electrolytes was also enhanced substantially due to EMITFSI addition into PEMA – 20 wt.% MgTf_2 system.

PEMA based NCPEs have been successfully prepared by incorporation of different amounts of MgO nanofiller into PEMA-40 wt.% EMITFSI-20 wt.% MgTf_2 . In the first system, the highest conducting sample was obtained for PEMA – 40 wt.% EMITFSI. For the second system, we have reported the characterization of PEMA based electrolytes by varying the amount of EMITFSI and MgTf_2 from 10 wt.% to 40 wt.%. However, PEMA – 40 wt.% EMITFSI – 20 wt.% MgTf_2 which has been expected to exhibit higher ionic conductivity could not produce free standing film due to high loading of ionic liquid in the PEMA-salt system. In the third system, stable films of PEMA – 40 wt.% EMITFSI – 20 wt.% MgTf_2 have been successfully obtained by dispersing small amount of MgO nanofiller into the system. This could be correlated to the improvement of ionic liquid retention property of NCPE films. Morphological study from SEM analysis revealed the presence of dispersion of homogeneous nanosized

MgO particles was observed in PEMA – 40 wt.% EMITFSI – 20 wt.% MgTf₂ – 0.5 wt.% MgO and PEMA – 40 wt.% EMITFSI – 20 wt.% MgTf₂ – 1.0 wt.% MgO. TGA curves revealed that the NCPE films were stable up to ~ 300 °C. The increase in ionic conductivity was consistent with the decrease of activation energy obtained from Arrhenius-model. The electrochemical potential window for the highest conducting sample, suggested that magnesium ion was not predominantly factor to the ionic conductivity enhancement of NCPE.

7.2 Suggestions for Future Work

Further work should be carried out in order to enhance the ionic conductivity of PEs.

This can be done by several possible approaches listed below:

- i. Using a combination of binary/tertiary ionic liquid to be added to PEMA based electrolytes system.
- ii. Using the same types of anions of salts and ionic liquid (i.e TFSI) as additives, in order to prevent the system becomes more complicated.
- iii. Using polymer blends (PEMA with highly amorphous polymer) as polymer host in order to improve room temperature ionic conductivity.
- iv. Using different types of active nanofillers rather than passive ceramic nanofillers. The active component materials were expected to participate in conduction process for magnesium ion conducting systems.

REFERENCES

- Abraham, K., & Alamgir, M. (1990). Li⁺-conductive solid polymer electrolytes with liquid-Like conductivity. *Journal of The Electrochemical Society*, 137(5), 1657-1658.
- Adebahr, J., Best, A., Byrne, N., Jacobsson, P., MacFarlane, D., & Forsyth, M. (2003). Ion transport in polymer electrolytes containing nanoparticulate TiO₂: The influence of polymer morphology. *Physical chemistry chemical physics*, 5(4), 720-725.
- Agrawal, R., & Gupta, R. (1999). Superionic solid: composite electrolyte phase—an overview. *Journal of materials science*, 34(6), 1131-1162.
- Ahmad, S. (2009). RETRACTED ARTICLE: Polymer electrolytes: characteristics and peculiarities. *Ionics*, 15(3), 309-321.
- Ahmed, T., Akusu, P., Ismaila, A., & Maryam, A. (2014). Morphology and Transport Properties of Polyethylene Oxide (PEO)-based nanocomposite polymer electrolytes. *International Research Journal of Pure and Applied Chemistry*, 4(2), 170.
- Akai, N., Parazs, D., Kawai, A., & Shibuya, K. (2009). Cryogenic neon matrix-isolation FTIR spectroscopy of evaporated ionic liquids: geometrical structure of cation–anion 1: 1 pair in the gas phase. *The Journal of Physical Chemistry B*, 113(14), 4756-4762.
- Amir, S., Mohamed, N., & Subban, R. (2013). Ionic conductivity studies on PEMA/PVC-NH₄I polymer electrolytes. *International Journal of Materials Engineering Innovation* 2, 4(3-4), 281-290.
- An, Y., Zuo, P., Cheng, X., Liao, L., & Yin, G. (2011). Preparation and properties of ionic-liquid mixed solutions as a safety electrolyte for lithium ion batteries. *Int. J. Electrochem. Sci*, 6(7), 2398.
- Anantha, P., & Hariharan, K. (2005). Physical and ionic transport studies on poly (ethylene oxide)–NaNO₃ polymer electrolyte system. *Solid State Ionics*, 176(1), 155-162.
- Angulakshmi, N., Thomas, S., Nahm, K., Stephan, A. M., & Elizabeth, R. N. (2011). Electrochemical and mechanical properties of nanochitin-incorporated PVDF-HFP-based polymer electrolytes for lithium batteries. *Ionics*, 17(5), 407-414.

- Anuar, N. K., Subban, R. H. Y., & Mohamed, N. S. (2012). Properties of PEMA-NH₄CF₃SO₃ added to BMATSEFI ionic liquid. *Materials*, 5(12), 2609-2620.
- Appetecchi, G., Croce, F., Hassoun, J., Scrosati, B., Salomon, M., & Cassel, F. (2003). Hot-pressed, dry, composite, PEO-based electrolyte membranes: I. Ionic conductivity characterization. *Journal of power sources*, 114(1), 105-112.
- Appetecchi, G. B., Croce, F., Romagnoli, P., Scrosati, B., Heider, U., & Oesten, R. (1999). High-performance gel-type lithium electrolyte membranes. *Electrochemistry Communications*, 1(2), 83-86.
- Armand, M., Endres, F., MacFarlane, D. R., Ohno, H., & Scrosati, B. (2009). Ionic-liquid materials for the electrochemical challenges of the future. *Nature materials*, 8(8), 621-629.
- Armand, M. B. (1986). Polymer electrolytes. *Annual Review of Materials Science*, 16(1), 245-261.
- Asensio, J. A., Borrós, S., & Gómez-Romero, P. (2004). Polymer electrolyte fuel cells based on phosphoric acid-impregnated poly (2, 5-benzimidazole) membranes. *Journal of The Electrochemical Society*, 151(2), A304-A310.
- Asmara, S., Kufian, M., Majid, S., & Arof, A. (2011). Preparation and characterization of magnesium ion gel polymer electrolytes for application in electrical double layer capacitors. *Electrochimica acta*, 57, 91-97.
- Attri, P., Lee, S.-H., Hwang, S. W., Kim, J. I., Jang, W., Kim, Y. B., . . . Kim, I. T. (2014). Effect of temperature on the interactions between low bandgap polymer and ionic liquids. *Thermochimica Acta*, 579, 15-21.
- Bakker, A., Gejji, S., Lindgren, J., Hermansson, K., & Probst, M. M. (1995). Contact ion pair formation and ether oxygen coordination in the polymer electrolytes M [N (CF₃SO₂)₂]₂ PEO_n for M= Mg, Ca, Sr and Ba. *Polymer*, 36(23), 4371-4378.
- Bandara, L. R. A. K., Dissanayake, M. A. K. L., & Mellander, B. E. (1998). Ionic conductivity of plasticized(PEO)-LiCF₃SO₃ electrolytes. *Electrochimica acta*, 43(10-11), 1447-1451.
- Baril, D., Michot, C., & Armand, M. (1997). Electrochemistry of liquids vs. solids: Polymer electrolytes. *Solid State Ionics*, 94(1), 35-47.

- Bishop, A. G., MacFarlane, D. R., McNaughton, D., & Forsyth, M. (1996). FT-IR investigation of ion association in plasticized solid polymer electrolytes. *The Journal of Physical Chemistry*, 100(6), 2237-2243.
- Bohnke, O., Frand, G., Rezrazi, M., Rousselot, C., & Truche, C. (1993). Fast ion transport in new lithium electrolytes gelled with PMMA. 1. Influence of polymer concentration. *Solid State Ionics*, 66(1), 97-104.
- Bruce, P. G. (1995). Structure and electrochemistry of polymer electrolytes. *Electrochimica acta*, 40(13), 2077-2085.
- Bruce, P. G., Evans, J., & Vincent, C. A. (1988). Conductivity and transference number measurements on polymer electrolytes. *Solid State Ionics*, 28, 918-922.
- Bruce, P. G., & Vincent, C. A. (1987). Steady state current flow in solid binary electrolyte cells. *Journal of electroanalytical chemistry and interfacial electrochemistry*, 225(1), 1-17.
- Cai, H., Hu, R., Egami, T., & Farrington, G. (1992). The effect of salt concentration on the local atomic structure and conductivity of PEO-based NiBr₂ electrolytes. *Solid State Ionics*, 52(4), 333-338.
- Cameron, G., & Ingram, M. (1989). Liquid Polymer Electrolytes. *Polymer Electrolyte Reviews*, 2, 157.
- Capuano, F., Croce, F., & Scrosati, B. (1991). Composite polymer electrolytes. *Journal of The Electrochemical Society*, 138(7), 1918-1922.
- Chandra, S., & Chandra, A. (1994). Solid state ionics: Materials aspect. *PROCEEDINGS-NATIONAL ACADEMY OF SCIENCES INDIA SECTION A*, 64, 141-141.
- Chattaraj, A. P., & Basumallick, I. N. (1995). Fabrication and charge/discharge behaviour of some lithium solid polymer electrolyte cells. *Journal of power sources*, 55(1), 123-126.
- Chaurasia, S., Singh, R., & Chandra, S. (2014). Ionic liquid assisted modification in ionic conductivity, phase transition temperature and crystallization kinetics behaviour of polymer poly (ethylene oxide). *Solid State Ionics*, 262, 790-794.
- Chiappe, C., & Pieraccini, D. (2005). Ionic liquids: solvent properties and organic reactivity. *Journal of Physical Organic Chemistry*, 18(4), 275-297.

- Crawford, E. T. (1996). Arrhenius: From ionic theory to the greenhouse effect.
- Croce, F., Appetecchi, G., Persi, L., & Scrosati, B. (1998). Nanocomposite polymer electrolytes for lithium batteries. *Nature*, 394(6692), 456-458.
- Davey, J. M., Too, C. O., Ralph, S. F., Kane-Maguire, L. A., Wallace, G. G., & Partridge, A. C. (2000). Conducting polyaniline/calixarene salts: Synthesis and properties. *Macromolecules*, 33(19), 7044-7050.
- De Souza, R. F., Padilha, J. C., Gonçalves, R. S., & Dupont, J. (2003). Room temperature dialkylimidazolium ionic liquid-based fuel cells. *Electrochemistry Communications*, 5(8), 728-731.
- Ding, J., Chuy, C., & Holdcroft, S. (2002). Enhanced conductivity in morphologically controlled proton exchange membranes: synthesis of macromonomers by SFRP and their incorporation into graft polymers. *Macromolecules*, 35(4), 1348-1355.
- Dupont, J., de Souza, R. F., & Suarez, P. A. (2002). Ionic liquid (molten salt) phase organometallic catalysis. *Chemical reviews*, 102(10), 3667-3692.
- Dvořák, P., Chladil, L., Sedlářková, M., & Vondrák, J. (2014). Gel Polymer Electrolyte. *ECS Transactions*, 63(1), 45-50.
- Evans, J., Vincent, C. A., & Bruce, P. G. (1987). Electrochemical measurement of transference numbers in polymer electrolytes. *Polymer*, 28(13), 2324-2328.
- Fadzallah, I., Majid, S., Careem, M., & Arof, A. (2014). A study on ionic interactions in chitosan-oxalic acid polymer electrolyte membranes. *Journal of Membrane Science*, 463, 65-72.
- Fahmy, T., & Ahmed, M. (2001). Thermal induced structural change investigations in PVC/PEMA polymer blend. *Polymer Testing*, 20(5), 477-484.
- Fan, J., & Fedkiw, P. S. (1997). Composite electrolytes prepared from fumed silica, polyethylene oxide oligomers, and lithium salts. *Journal of The Electrochemical Society*, 144(2), 399-408.
- Fan, L., Nan, C.-W., & Zhao, S. (2003). Effect of modified SiO₂ on the properties of PEO-based polymer electrolytes. *Solid State Ionics*, 164(1), 81-86.
- Fares, S. (2012). Influence of gamma-ray irradiation on optical and thermal degradation of poly (ethyl-methacrylate)(PEMA) polymer. *Natural Science*, 4(07), 499.

- Feng, T., Wu, F., Wu, C., Wang, X., Feng, G., & Yang, H. (2012). A free-standing, self-assembly ternary membrane with high conductivity for lithium-ion batteries. *Solid State Ionics*, 221, 28-34.
- Flora, X. H., Ulaganathan, M., Kesavan, K., & Rajendran, S. (2014). Synthesis of Bendable Plasticized Nanocomposite Polymer Electrolyte Using Poly (Acrylonitrile)/Poly (Methyl Methacrylate) Polymer Blends. *Zeitschrift für Physikalische Chemie*, 228(6-7), 673-684.
- Forsyth, S. A., Pringle, J. M., & MacFarlane, D. R. (2004). Ionic liquids—an overview. *Australian Journal of Chemistry*, 57(2), 113-119.
- Fraga-Dubreuil, J., Bourahla, K., Rahmouni, M., Bazureau, J. P., & Hamelin, J. (2002). Catalysed esterifications in room temperature ionic liquids with acidic counteranion as recyclable reaction media. *Catalysis Communications*, 3(5), 185-190.
- Fredlake, C. P., Crosthwaite, J. M., Hert, D. G., Aki, S. N., & Brennecke, J. F. (2004). Thermophysical properties of imidazolium-based ionic liquids. *Journal of Chemical & Engineering Data*, 49(4), 954-964.
- Fulcher, G. S. (1925). Analysis of recent measurements of the viscosity of glasses. *Journal of the American Ceramic Society*, 8(6), 339-355.
- Gray, D. H., Hu, S., Juuang, E., & Gin, D. L. (1997). Highly ordered polymer–inorganic nanocomposites via monomer self assembly: In situ condensation approach. *Advanced materials*, 9(9), 731-736.
- Gray, F. M. (1997). *Polymer electrolytes*: Royal Society of Chemistry.
- Grigante, M., Ischia, M., Baratieri, M., Dal Maschio, R., & Ragazzi, M. (2010). Pyrolysis analysis and solid residue stabilization of polymers, waste tyres, spruce sawdust and sewage sludge. *Waste and Biomass Valorization*, 1(4), 381-393.
- Grigoriev, S., Kuleshov, N., Grigoriev, A., & Millet, P. (2015). Electrochemical Characterization of a High-Temperature Proton Exchange Membrane Fuel Cell Using Doped-Poly Benzimidazole as Solid Polymer Electrolyte. *Journal of Fuel Cell Science and Technology*, 12(3), 031004.
- Hagiwara, R., Nohira, T., Matsumoto, K., & Tamba, Y. (2005). A fluorohydrogenate ionic liquid fuel cell operating without humidification. *Electrochemical and solid-state letters*, 8(4), A231-A233.

- Han, H.-S., Kang, H.-R., Kim, S.-W., & Kim, H.-T. (2002). Phase-separated polymer electrolyte based on poly (vinyl chloride)/poly (ethyl methacrylate) blend. *Journal of power sources*, 112(2), 461-468.
- Hapiot, P., & Lagrost, C. (2008). Electrochemical reactivity in room-temperature ionic liquids. *Chemical reviews*, 108(7), 2238-2264.
- Harris, C. S., Ratner, M. A., & Shriver, D. F. (1987). Ionic conductivity in branched polyethylenimine-sodium trifluoromethanesulfonate complexes: comparisons to analogous complexes made with linear polyethylenimine. *Macromolecules*, 20(8), 1778-1781.
- Heo, Y., Kang, Y., Han, K., & Lee, C. (2004). Ionic conductivity and lithium ion transport characteristics of gel-type polymer electrolytes using lithium p-[methoxy oligo (ethyleneoxy)] benzenesulfonates. *Electrochimica acta*, 50(2), 345-349.
- Hergenrother, P. M. (1990). Perspectives in the Development of High-Temperature Polymers. *Angewandte Chemie International Edition in English*, 29(11), 1262-1268.
- Hwang, J., & Liu, H. (2002). Influence of organophilic clay on the morphology, plasticizer-maintaining ability, dimensional stability, and electrochemical properties of gel polyacrylonitrile (PAN) nanocomposite electrolytes. *Macromolecules*, 35(19), 7314-7319.
- Ishikawa, M., Sugimoto, T., Kikuta, M., Ishiko, E., & Kono, M. (2006). Pure ionic liquid electrolytes compatible with a graphitized carbon negative electrode in rechargeable lithium-ion batteries. *Journal of power sources*, 162(1), 658-662.
- Jacobs, P., Lorimer, J., Russer, A., & Wasiucioneck, M. (1989). Phase relations and conductivity in the system poly (ethylene oxide) □ LiClO₄. *Journal of power sources*, 26(3), 503-510.
- Jayathilaka, P., Dissanayake, M., Albinsson, I., & Mellander, B.-E. (2003). Dielectric relaxation, ionic conductivity and thermal studies of the gel polymer electrolyte system PAN/EC/PC/LiTFSI. *Solid State Ionics*, 156(1), 179-195.
- Julien, C., & Nazri, G.-A. (1994). Polymer electrolytes *Solid State Batteries: Materials Design and Optimization* (pp. 347-367): Springer.
- Jun-kai, D., & Hai-shan, L. (1989). A study of identification of trace rubber residues in marks from rubber-soled shoes and tyres by Py-GC. *Forensic Science International*, 43(1), 45-50.

- Kakibe, T., Yoshimoto, N., Egashira, M., & Morita, M. (2010). Optimization of cation structure of imidazolium-based ionic liquids as ionic solvents for rechargeable magnesium batteries. *Electrochemistry Communications*, 12(11), 1630-1633.
- Kauffman, G. B. (1988). Wallace Hume Carothers and nylon, the first completely synthetic fiber. *Journal of Chemical Education*, 65(9), 803.
- Kim, D.-W., & Sun, Y.-K. (2001). Electrochemical characterization of gel polymer electrolytes prepared with porous membranes. *Journal of power sources*, 102(1), 41-45.
- Kim, J.-D., Hayashi, S., Mori, T., & Honma, I. (2007). Fast proton conductor under anhydrous condition synthesized from 12-phosphotungstic acid and ionic liquid. *Electrochimica acta*, 53(2), 963-967.
- Kosmulski, M., Gustafsson, J., & Rosenholm, J. B. (2004). Thermal stability of low temperature ionic liquids revisited. *Thermochimica Acta*, 412(1), 47-53.
- Kovač, M., Gaberšček, M., & Grdadolnik, J. (1998). The effect of plasticizer on the microstructural and electrochemical properties of a (PEO)_n LiAl (SO₃ Cl)₄ system. *Electrochimica acta*, 44(5), 863-870.
- Kumar, D., & Hashmi, S. (2010). Ionic liquid based sodium ion conducting gel polymer electrolytes. *Solid State Ionics*, 181(8), 416-423.
- Kumar, G. G., & Munichandraiah, N. (2000). Effect of plasticizers on magnesium-poly (ethyleneoxide) polymer electrolyte. *Journal of Electroanalytical Chemistry*, 495(1), 42-50.
- Kumar, K. S., Nair, C. R., & Ninan, K. (2006). Rheokinetic investigations on the thermal polymerization of benzoxazine monomer. *Thermochimica Acta*, 441(2), 150-155.
- Kumar, M., & Sekhon, S. (2002). Ionic conductance behaviour of plasticized polymer electrolytes containing different plasticizers. *Ionics*, 8(3-4), 223-233.
- Kumar, R., Subramania, A., Sundaram, N. K., Kumar, G. V., & Baskaran, I. (2007). Effect of MgO nanoparticles on ionic conductivity and electrochemical properties of nanocomposite polymer electrolyte. *Journal of Membrane Science*, 300(1), 104-110.
- Kumar, R. S., Raja, M., Kulandainathan, M. A., & Stephan, A. M. (2014). Metal organic framework-laden composite polymer electrolytes for efficient and durable all-solid-state-lithium batteries. *RSC Advances*, 4(50), 26171-26175.

- Kumar, Y., Hashmi, S., & Pandey, G. (2011). Ionic liquid mediated magnesium ion conduction in poly (ethylene oxide) based polymer electrolyte. *Electrochimica acta*, 56(11), 3864-3873.
- Lascaud, S., Perrier, M., Vallee, A., Besner, S., Prud'Homme, J., & Armand, M. (1994). Phase diagrams and conductivity behavior of poly (ethylene oxide)-molten salt rubbery electrolytes. *Macromolecules*, 27(25), 7469-7477.
- Leones, R., Sentanin, F., Rodrigues, L., Marrucho, I., Esperança, J., Pawlicka, A., & Silva, M. (2012). Investigation of polymer electrolytes based on agar and ionic liquids. *eXPRESS Polymer Letters*, 6(12), 1007.
- Levi, E., Gofer, Y., & Aurbach, D. (2009). On the Way to Rechargeable Mg Batteries: The Challenge of New Cathode Materials†. *Chemistry of Materials*, 22(3), 860-868.
- Lewandowski, A., & Świdarska-Mocek, A. (2009). Ionic liquids as electrolytes for Li-ion batteries—an overview of electrochemical studies. *Journal of power sources*, 194(2), 601-609.
- Lian, F., Guan, H.-y., Wen, Y., & Pan, X.-r. (2014). Polyvinyl formal based single-ion conductor membranes as polymer electrolytes for lithium ion batteries. *Journal of Membrane Science*, 469, 67-72.
- Liang, C. (1973). Conduction Characteristics of the Lithium Iodide-Aluminum Oxide Solid Electrolytes. *Journal of The Electrochemical Society*, 120(10), 1289-1292.
- Ma, X., Huang, X., Gao, J., Zhang, S., Deng, Z., & Suo, J. (2014). Compliant gel polymer electrolyte based on poly (methyl acrylate-co-acrylonitrile)/poly (vinyl alcohol) for flexible lithium-ion batteries. *Electrochimica acta*, 115, 216-222.
- MacCallum, J. R., & Vincent, C. A. (1989). *Polymer electrolyte reviews* (Vol. 2): Springer Science & Business Media.
- Malathi, M., Tamilarasan, K., & Ganesan, V. (2015). Role of ceramic reinforcement in composite polymer electrolyte. *Polymer Composites*, 36(1), 42-46.
- Minier, M., Berthier, C., & Gorecki, W. (1983). Differential scanning calorimetry of sodium iodide poly (ethylene oxide) complexes. *Solid State Ionics*, 9, 1125-1127.
- Mohammad, S., Zainal, N., Ibrahim, S., & Mohamed, N. (2013). Conductivity enhancement of (epoxidized natural rubber 50)/poly (ethyl methacrylate)-ionic liquid-ammonium triflate. *Int. J. Electrochem. Sci*, 8, 6145-6153.

- Moumouzias, G., Ritzoulis, G., Siapkis, D., & Terzidis, D. (2003). Comparative study of LiBF₄, LiAsF₆, LiPF₆, and LiClO₄ as electrolytes in propylene carbonate–diethyl carbonate solutions for Li/LiMn₂O₄ cells. *Journal of power sources*, 122(1), 57-66.
- Munichandraiah, N., Scanlon, L., Marsh, R., Kumar, B., & Sirkar, A. (1993). *Studies on the Composite Polymer Electrolyte of Poly (ethylene oxide) and Zeolite*. Paper presented at the Proceedings of the Symposium on Batteries and Fuel Cells for Stationary and Electric Vehicle Applications, Honolulu, USA.
- Nair, J. R., Gerbaldi, C., Destro, M., Bongiovanni, R., & Penazzi, N. (2011). Methacrylic-based solid polymer electrolyte membranes for lithium-based batteries by a rapid UV-curing process. *Reactive and Functional Polymers*, 71(4), 409-416.
- Nakajima, H., & Ohno, H. (2005). Preparation of thermally stable polymer electrolytes from imidazolium-type ionic liquid derivatives. *Polymer*, 46(25), 11499-11504.
- Nan, C.-W., Fan, L., Lin, Y., & Cai, Q. (2003). Enhanced Ionic Conductivity of Polymer Electrolytes Containing Nanocomposite SiO₂ Particles. *Physical review letters*, 91(26), 266104.
- Nogami, M., Kato, A., Nakayama, M., & Lakshminarayana, G. (2012). Proton conduction in ionic liquid-modified P₂O₅–SiO₂ glasses. *Journal of Non-Crystalline Solids*, 358(24), 3495-3500.
- Ohba, N., Miwa, K., Noritake, T., & Fukumoto, A. (2004). First-principles study on thermal vibration effects of MgH₂. *Physical Review B*, 70(3), 035102.
- Osman, Z., Zainol, N., Samin, S., Chong, W., Isa, K. M., Othman, L., . . . Sonsudin, F. (2014). Electrochemical impedance spectroscopy studies of magnesium-based polymethylmethacrylate gel polymer electrolytes. *Electrochimica acta*, 131, 148-153.
- Pandey, G., Agrawal, R., & Hashmi, S. (2009). Magnesium ion-conducting gel polymer electrolytes dispersed with nanosized magnesium oxide. *Journal of power sources*, 190(2), 563-572.
- Pandey, G., Kumar, Y., & Hashmi, S. (2011). Ionic liquid incorporated PEO based polymer electrolyte for electrical double layer capacitors: a comparative study with lithium and magnesium systems. *Solid State Ionics*, 190(1), 93-98.

- Pandey, K., Dwivedi, M. M., Das, I., Singh, M., & Agrawal, S. L. (2010). Ion transport studies on Al–Zn ferrite dispersed nano-composite polymer electrolyte. *Journal of electroceramics*, 25(2-4), 99-107.
- Pas, S. J., Ingram, M. D., Funke, K., & Hill, A. J. (2005). Free volume and conductivity in polymer electrolytes. *Electrochimica acta*, 50(19), 3955-3962.
- Paulechka, Y., Zaitsau, D. H., Kabo, G., & Strechan, A. (2005). Vapor pressure and thermal stability of ionic liquid 1-butyl-3-methylimidazolium Bis (trifluoromethylsulfonyl) amide. *Thermochimica Acta*, 439(1), 158-160.
- Payne, D., & Wright, P. (1982). Morphology and ionic conductivity of some lithium ion complexes with poly (ethylene oxide). *Polymer*, 23(5), 690-693.
- Perera, K., Dissanayake, M., & Bandaranayake, P. (2004). Ionic conductivity of a gel polymer electrolyte based on Mg (ClO₄)₂ and polyacrylonitrile (PAN). *Materials research bulletin*, 39(11), 1745-1751.
- Piccolo, M., Giffin, G. A., Vezzù, K., Bertasi, F., Alotto, P., Guarnieri, M., & Di Noto, V. (2013). Molecular relaxations in magnesium polymer electrolytes via GHz broadband electrical spectroscopy. *ChemSusChem*, 6(11), 2157-2160.
- Pradhan, D. K., Choudhary, R., & Samantaray, B. (2008). Studies of dielectric relaxation and AC conductivity behavior of plasticized polymer nanocomposite electrolytes. *International Journal of Electrochemical Science*, 3(5), 597-608.
- Rajendran, S., Prabhu, M. R., & Rani, M. U. (2008). Ionic conduction in poly (vinyl chloride)/poly (ethyl methacrylate)-based polymer blend electrolytes complexed with different lithium salts. *Journal of power sources*, 180(2), 880-883.
- Ramesh, S., Uma, O., Shanti, R., Yi, L. J., & Ramesh, K. (2014). Preparation and characterization of poly (ethyl methacrylate) based polymer electrolytes doped with 1-butyl-3-methylimidazolium trifluoromethanesulfonate. *Measurement*, 48, 263-273.
- Reiter, J., Krejza, O., & Sedlářiková, M. (2009). Electrochromic devices employing methacrylate-based polymer electrolytes. *Solar Energy Materials and Solar Cells*, 93(2), 249-255.
- Rudhziah, S., Ibrahim, S., & Nor Sabirin, M. (2011). *Polymer Electrolyte of PVDF-HFP/PEMA-NH₄CF₃So₃-TiO₂ and its Application in Proton Batteries*. Paper presented at the Advanced Materials Research.

- Rudhziah, S., Mohamed, N., & Ahmad, A. (2013). Conductivity and Structural Studies of Poly (vinylidene fluoride co-hexafluoropropylene)/Polyethyl methacrylate Blend Doped with Ammonium Triflate. *Int. J. Electrochem. Sci*, 8, 421-434.
- Scrosati, B., & Vincent, C. A. (2000). Polymer electrolytes: the key to lithium polymer batteries. *Mrs Bulletin*, 25(03), 28-30.
- Sequeira, C., & Santos, D. (2010). *Polymer electrolytes: fundamentals and applications*: Elsevier.
- Sharma, K. R. (2006). *Continuous Polymerization Process: Some Scale-Up Issues*. Paper presented at the AIChE Spring National Meeting.
- Shin, J.-H., Henderson, W. A., & Passerini, S. (2003). Ionic liquids to the rescue? Overcoming the ionic conductivity limitations of polymer electrolytes. *Electrochemistry Communications*, 5(12), 1016-1020.
- Shin, J.-H., Henderson, W. A., & Passerini, S. (2005). PEO-based polymer electrolytes with ionic liquids and their use in lithium metal-polymer electrolyte batteries. *Journal of The Electrochemical Society*, 152(5), A978-A983.
- Sim, L., Majid, S., & Arof, A. (2012). FTIR studies of PEMA/PVdF-HFP blend polymer electrolyte system incorporated with LiCF₃SO₃ salt. *Vibrational Spectroscopy*, 58, 57-66.
- Skaarup, S., West, K., & Zachau-Christiansen, B. (1988). Mixed phase solid electrolytes. *Solid State Ionics*, 28, 975-978.
- Song, H., Zhao, N., Qin, W., Duan, B., Ding, X., Wen, X., . . . Ba, X. (2015). High-performance ionic liquid-based nanocomposite polymer electrolytes with anisotropic ionic conductivity prepared by coupling liquid crystal self-templating with unidirectional freezing. *Journal of Materials Chemistry A*, 3(5), 2128-2134.
- Song, J., Wang, Y., & Wan, C. (1999). Review of gel-type polymer electrolytes for lithium-ion batteries. *Journal of power sources*, 77(2), 183-197.
- Stathatos, E., Lianos, P., Zakeeruddin, S., Liska, P., & Grätzel, M. (2003). A quasi-solid-state dye-sensitized solar cell based on a sol-gel nanocomposite electrolyte containing ionic liquid. *Chemistry of Materials*, 15(9), 1825-1829.
- Stephan, A. M., Kumar, T. P., Renganathan, N., Pitchumani, S., Thirunakaran, R., & Muniyandi, N. (2000). Ionic conductivity and FT-IR studies on plasticized

PVC/PMMA blend polymer electrolytes. *Journal of power sources*, 89(1), 80-87.

Stephan, A. M., Saito, Y., Muniyandi, N., Renganathan, N., Kalyanasundaram, S., & Elizabeth, R. N. (2002). Preparation and characterization of PVC/PMMA blend polymer electrolytes complexed with LiN (CF₃SO₂)₂. *Solid State Ionics*, 148(3), 467-473.

Stubblefield, M. A., Yang, C., Pang, S. S., & Lea, R. H. (1998). Development of heat-activated joining technology for composite-to-composite pipe using prepreg fabric. *Polymer Engineering & Science*, 38(1), 143-149.

Susan, M. A. B. H., Kaneko, T., Noda, A., & Watanabe, M. (2005). Ion gels prepared by in situ radical polymerization of vinyl monomers in an ionic liquid and their characterization as polymer electrolytes. *Journal of the American Chemical Society*, 127(13), 4976-4983.

Tamman, G., & Hesse, W. (1926). 2. *Anorg. Chem.*, 1926, 149, 21.

Tejedor, J. G., Acosta, T. R., Ribelles, J. G., Polizos, G., & Pissis, P. (2007). Poly (ethyl methacrylate-co-hydroxyethyl acrylate) random co-polymers: Dielectric and dynamic-mechanical characterization. *Journal of Non-Crystalline Solids*, 353(3), 276-285.

Tobishima, S.-I., Hayashi, K., Nemoto, Y., & Yamaki, J.-I. (1998). Multi-component nonaqueous electrolytes for rechargeable lithium cells. *Electrochimica acta*, 43(8), 925-933.

Tokuda, H., Hayamizu, K., Ishii, K., Susan, M. A. B. H., & Watanabe, M. (2005). Physicochemical properties and structures of room temperature ionic liquids. 2. Variation of alkyl chain length in imidazolium cation. *The Journal of Physical Chemistry B*, 109(13), 6103-6110.

Tokuda, H., Ishii, K., Susan, M. A. B. H., Tsuzuki, S., Hayamizu, K., & Watanabe, M. (2006). Physicochemical properties and structures of room-temperature ionic liquids. 3. Variation of cationic structures. *The Journal of Physical Chemistry B*, 110(6), 2833-2839.

Tominaga, Y., Asai, S., Sumita, M., Panero, S., & Scrosati, B. (2005). Fast ionic conduction in PEO-based composite electrolyte filled with ionic liquid-modified mesoporous silica. *Electrochemical and solid-state letters*, 8(1), A22-A25.

- Tripathi, B. P., & Shahi, V. K. (2011). Organic–inorganic nanocomposite polymer electrolyte membranes for fuel cell applications. *Progress in Polymer Science*, 36(7), 945-979.
- Tripathi, S., Jain, A., Gupta, A., & Mishra, M. (2012). Electrical and electrochemical studies on magnesium ion-based polymer gel electrolytes. *Journal of Solid State Electrochemistry*, 16(5), 1799-1806.
- Uma, T., Mahalingam, T., & Stimming, U. (2005). Conductivity studies on poly (methyl methacrylate)–Li₂SO₄ polymer electrolyte systems. *Materials chemistry and physics*, 90(2), 245-249.
- Vincent, C. A. (1987). Polymer electrolytes. *Progress in solid state chemistry*, 17(3), 145-261.
- Vogel, H. (1921). The law of the relation between the viscosity of liquids and the temperature. *Phys. Z*, 22, 645-646.
- Walls, H., Zhou, J., Yerian, J. A., Fedkiw, P. S., Khan, S. A., Stowe, M. K., & Baker, G. L. (2000). Fumed silica-based composite polymer electrolytes: synthesis, rheology, and electrochemistry. *Journal of power sources*, 89(2), 156-162.
- Wang, P., Zakeeruddin, S. M., Comte, P., Exnar, I., & Grätzel, M. (2003). Gelation of ionic liquid-based electrolytes with silica nanoparticles for quasi-solid-state dye-sensitized solar cells. *Journal of the American Chemical Society*, 125(5), 1166-1167.
- Watanabe, M., Nagaoka, K., Kanba, M., & Shinohara, I. (1982). Ionic conductivity of polymeric solid electrolytes based on poly (propylene oxide) or poly (tetramethylene oxide). *Polymer Journal*, 14(11), 877-886.
- Watarai, A., Kubota, K., Yamagata, M., Goto, T., Nohira, T., Hagiwara, R., . . . Kumagai, N. (2008). A rechargeable lithium metal battery operating at intermediate temperatures using molten alkali bis (trifluoromethylsulfonyl) amide mixture as an electrolyte. *Journal of power sources*, 183(2), 724-729.
- Welton, T. (1999). Room-temperature ionic liquids. Solvents for synthesis and catalysis. *Chemical reviews*, 99(8), 2071-2084.
- Weston, J., & Steele, B. (1982). Effects of inert fillers on the mechanical and electrochemical properties of lithium salt-poly (ethylene oxide) polymer electrolytes. *Solid State Ionics*, 7(1), 75-79.

- Wieczorek, W., Florjanczyk, Z., & Stevens, J. (1995). Composite polyether based solid electrolytes. *Electrochimica acta*, 40(13), 2251-2258.
- Wieczorek, W., & Stevens, J. (1997). Impedance spectroscopy and phase structure of polyether-poly (methyl methacrylate)-LiCF₃SO₃ blend-based electrolytes. *The Journal of Physical Chemistry B*, 101(9), 1529-1534.
- Wieczorek, W., Such, K., Przyłuski, J., & Floriańczyk, Z. (1991). Blend-based and composite polymer solid electrolytes. *Synthetic metals*, 45(3), 373-383.
- Winie, T., Ramesh, S., & Arof, A. (2009). Studies on the structure and transport properties of hexanoyl chitosan-based polymer electrolytes. *Physica B: Condensed Matter*, 404(21), 4308-4311.
- Winterton, N. (2006). Solubilization of polymers by ionic liquids. *Journal of Materials Chemistry*, 16(44), 4281-4293.
- Wright, P. V. (1975). Electrical conductivity in ionic complexes of poly(ethylene oxide). *British Polymer Journal*, 7(5), 319-327. doi: 10.1002/pi.4980070505
- Xu, Q., Xu, C., Wang, Y., Zhang, W., Jin, L., Tanaka, K., . . . Itoh, A. (2000). Amperometric detection studies of poly-o-phenylenediamine film for the determination of electroinactive anions in ion-exclusion chromatography. *Analyst*, 125(8), 1453-1457.
- Yates, B. J., Temsamani, K. R., Ceylan, Ö., Öztemiz, S., Gbatu, T. P., LaRue, R. A., . . . Mark, H. B. (2002). Electrochemical control of solid phase micro-extraction: conducting polymer coated film material applicable for preconcentration/analysis of neutral species. *Talanta*, 58(4), 739-745.
- Yoshimoto, N., Yakushiji, S., Ishikawa, M., & Morita, M. (2003). Rechargeable magnesium batteries with polymeric gel electrolytes containing magnesium salts. *Electrochimica acta*, 48(14), 2317-2322.
- Zaghib, K., Armand, M., & Gauthier, M. (1998). Electrochemistry of anodes in solid-state Li-ion polymer batteries. *Journal of The Electrochemical Society*, 145(9), 3135-3140.
- Zain, N., Zainal, N., & Mohamed, N. (2015). The influences of ionic liquid to the properties of poly (ethylmethacrylate) based electrolyte. *Physica Scripta*, 90(1), 015702.
- Zalewska, A., Dumińska, J., Langwald, N., Syzdek, J., & Zawadzki, M. (2014). Preparation and performance of gel polymer electrolytes doped with ionic

liquids and surface-modified inorganic fillers. *Electrochimica acta*, 121, 337-344.

Zhao, L., Hu, Y. S., Li, H., Wang, Z., & Chen, L. (2011). Porous Li₄Ti₅O₁₂ Coated with N-Doped Carbon from Ionic Liquids for Li-Ion Batteries. *Advanced materials*, 23(11), 1385-1388.

Zhu, B. (2006). Next generation fuel cell R&D. *International journal of energy research*, 30(11), 895-903.

Zygadło-Monikowska, E., Florjańczyk, Z., Rogalska-Jońska, E., Werbanowska, A., Tomaszewska, A., Langwald, N., . . . Chung, S. (2007). Lithium ion transport of solid electrolytes based on PEO/CF₃SO₃Li and aluminum carboxylate. *Journal of power sources*, 173(2), 734-742.

University of Malaysia

LIST OF PUBLICATIONS AND PAPERS PRESENTED

Papers published/sent for publication in journals

1. Zain, N.F., Zainal N. and Mohamed, N.S. (2015), The influences of ionic liquid to the properties of poly(ethylmethacrylate) based electrolyte, *Physica Scripta* (90) 015702-015709.
2. Zain, N.F., Zainal N. and Mohamed, N.S., Physicochemical properties of PEMA-MgTf₂-EMITFSI polymer electrolytes. Has been accepted for publication in *Science of Advanced Materials* (ISI journal).
3. Zain, N.F., Zainal N. and Mohamed, N.S., The effects of MgO nanofiller to the physicochemical and ionic liquid retention properties of PEMA-MgTf₂-EMITFSI nanocomposite polymer electrolytes. Submitted to *Polymer Composites* (ISI journal).
Status: under review.

Presentation in conference:

1. Zain, N.F., Zainal N. and Mohamed, N.S. (2014), The Effect of Magnesium Salt and Ionic Liquid Composition on Poly(Ethyl Methacrylate) Based Polymer Electrolytes, presented at XIV International Symposium on Polymer Electrolytes 2014 (ISPE14), Geelong, Australia, held 24th – Friday 29th August 2014.